STUDIES ON SYNTHESIS AND ASSEMBLY OF METAL NANOPARTICLES

THESIS SUBMITTED TO THE UNIVERSITY OF PUNE

FOR THE DEGREE OF
DOCTOR OF PHILOSOPHY
IN
PHYSICS

BY
DEEPTI S. SIDHAYE

UNDER THE GUIDANCE OF
DR. B. L. V. PRASAD

**PHYSICAL AND MATERIALS CHEMISTRY DIVISION
NATIONAL CHEMICAL LABORATORY
PUNE – 411008, INDIA**

DECEMBER 2009

STUDIES ON SYNTHESIS AND ASSEMBLY OF METAL NANOPARTICLES

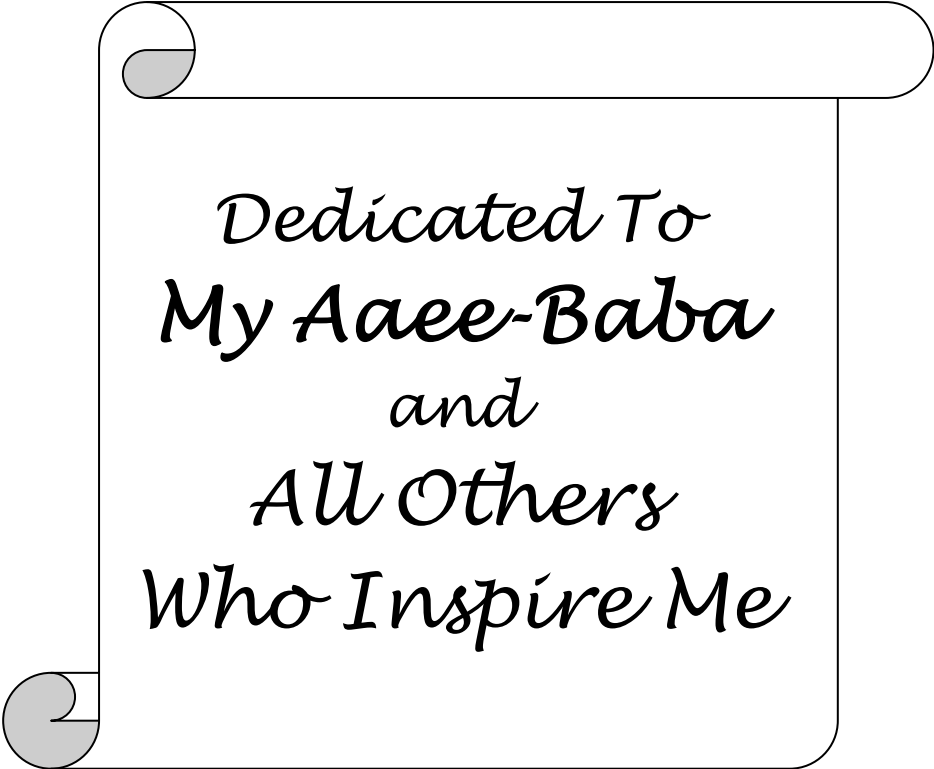**THESIS SUBMITTED TO THE UNIVERSITY OF PUNE**

FOR THE DEGREE OF
DOCTOR OF PHILOSOPHY
IN
PHYSICS

BY
DEEPTI S. SIDHAYE

UNDER THE GUIDANCE OF
DR. B. L. V. PRASAD

**PHYSICAL AND MATERIALS CHEMISTRY DIVISION
NATIONAL CHEMICAL LABORATORY
PUNE – 411008, INDIA**

DECEMBER 2009

Dedicated To
My Aaee-Baba
and
All Others
Who Inspire Me

CERTIFICATE

This is to certify that the work incorporated in the thesis entitled **"STUDIES ON SYNTHESIS AND ASSEMBLY OF METAL NANOPARTICLES"** by **DEEPTI S. SIDHAYE**, submitted to the University of Pune for the degree *Doctor of Philosophy in Physics* was carried out under my supervision at the Physical and Materials Chemistry Division of National Chemical Laboratory, Pune. Such material as has been obtained by other sources has been duly acknowledged in this thesis. To the best of my knowledge, the present work or any part thereof has not been submitted to any other University for the award of any other degree or diploma.

Date: **Dr. B. L. V. Prasad**

Place: Pune   (Research Guide)

DECLARATION

I hereby declare that the work described in the thesis entitled **"STUDIES ON SYNTHESIS AND ASSEMBLY OF METAL NANOPARTICLES"** submitted for the degree of *Doctor of Philosophy in Physics* to the University of Pune, has been carried out by me at the Physical and Materials Chemistry Division of National Chemical Laboratory, Pune under the supervision of Dr. B. L. V. Prasad. Such material as has been obtained by other sources has been duly acknowledged in this thesis. The work is original and has not been submitted in part or full by me for any other degree or diploma to other University.

Date: **Deepti S. Sidhaye**

Place: Pune   (Research Student)

ACKNOWLEDGEMENT

"If I have seen further, it is by standing on the shoulders of giants"
-Issac Newton

"Where Nature finishes producing its own species, man begins, using natural things and with the help of this nature, to create an infinity of species"
-Leonardo da Vinci

"The role of infinitely small is infinitely large"
-Luis Pasteur

"What I want to talk about is the problem of manipulating and controlling things on a small scale."
-Richard Feynmann

"The grand aim of all science is to cover the greatest number of empirical facts by logical deduction from the smallest possible number of hypotheses or axioms."
-Albert Einstein

"A scientist in his laboratory is not a mere technician: he is also a child confronting natural phenomena that impresses him as though they were fairy tales"
-Marie Curie

"Science is a perception of the world around us."
- S. Chandrasekhar

"No law of nature, however general, has been established all at once; its recognition has always been preceded by many presentiments."
Dmitri Mendeleev

" Vidya naam narasya rupamadhikam, prachchannaguptam dhanam Vidya bhogakari, yashas-sukhakari, vidya gurunaam guru…"
-Sanskrit Subhashitam describing Vidya (knowledge)

Table of Contents

Chapter III: Role of alkanethiol in the formation of organized assemblies of gold nanoparticles

Chapter IV: Photo-responsive assemblies of gold nanoparticles

Chapter V: Conclusions

Chapter I

Introduction

Why nano "matters"?

This chapter serves as a preamble to the thesis. It brings out the importance of nanomaterials with an emphasis on the unique properties of metal nanoparticles followed by portrayal of applications based on them. The chapter then describes two key aspects essential to reach the stage of applications – the synthesis and assembly of nanoparticles. Accordingly, a brief literature survey of the prominent synthesis protocols and assembly methods of metal nanoparticles is presented. Finally, the chapter summarizes the outline of the thesis - the chapter wise division of the work and its salient features.

1.1 Preamble

Interdisciplinary Science is the mantra of today's age. An enormous amount of research is now devoted to fields situated at the interfaces of conventional branches of science. Investigations based on nanomaterials constitute one such field [1,2] as illustrated by cartoon shown in Fig. 1.1A.
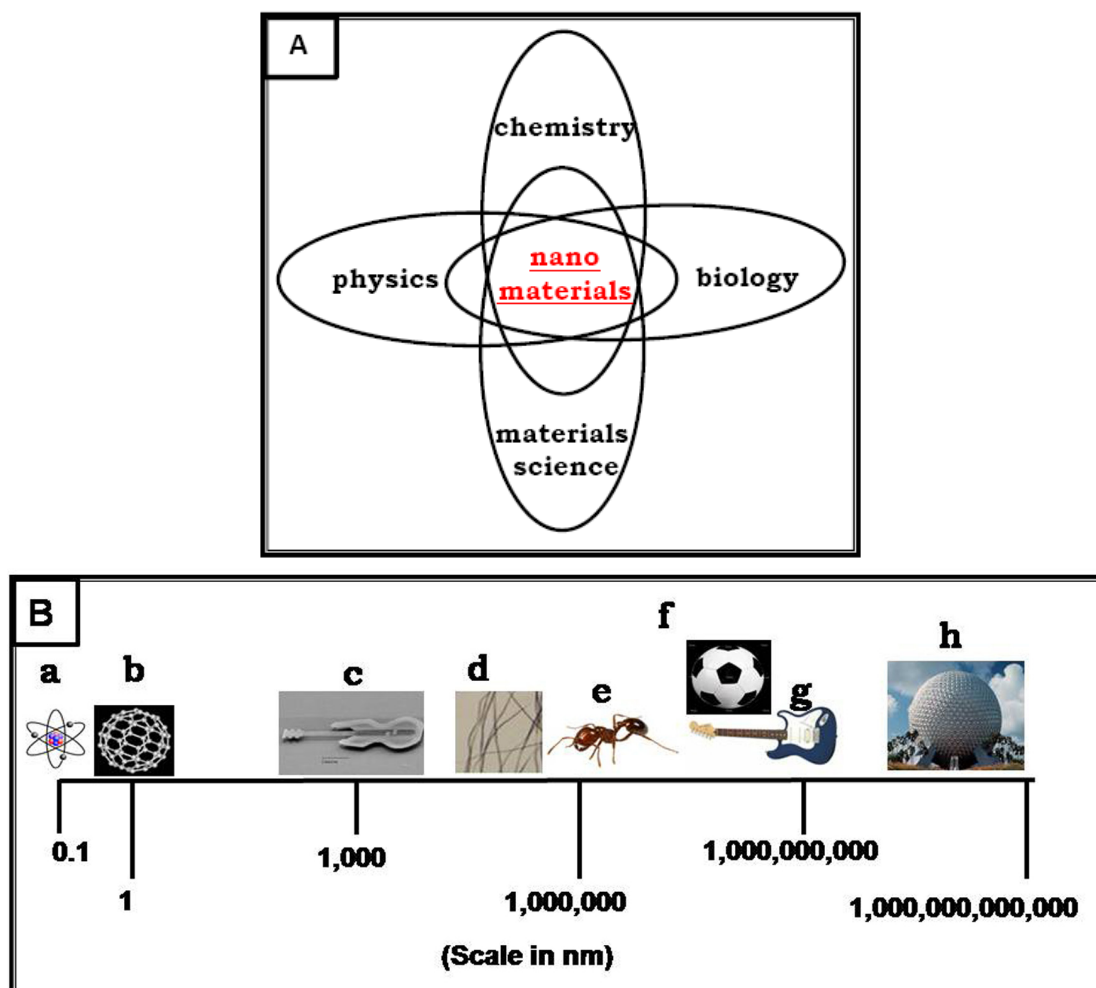
Fig. 1.1 A) *Schematic illustrating the interdisciplinary nature of nanoscience and nanotechnology.* **B)** *Comparative sizes of different objects on nanoscale (a) an atom (b) fullerene or bucky ball (c) guitar fabricated from crystalline silicon with length = 10 μm (d) hair (e) an ant (f) football (g) conventional guitar (h) geodesic dome- football-like architecture originally designed by the architect Buckminster Fuller and inspiration for the name fullerene-* [**images courtesy-** *a, b, d, e, f, g: various sources at* <u>*images.google.com*</u>*; c:* <u>*www.news.cornell.edu*</u>*; h:* <u>*www.essential-architecture.com*</u>]

Nanoscience encompasses the study of phenomena and manipulation of materials of the order of nanometer i.e. 10^{-9} m or a billionth of a meter (nano = Greek word for 'dwarf'). It involves design, synthesis and characterization of nanomaterials. Application of nanoscience is essentially called nanotechnology. To put things into perspective, comparative length-scales for objects of different sizes have been shown in Fig. 1.1B.

The 'nano' length-scale is not just about making materials of that dimension. Its importance comes from interesting properties evolving due to this size-scale. These properties also act as the driving forces for the research in this field. Illustration of these features can be seen in Fig. 1.2 and they can be described as follows:

1) At nano-scale, the properties of matter differ significantly from those of their bulk counterparts as well as from single atoms or molecules [3-5]. Further, these properties can be tuned by varying parameters like size, shape, composition of their constituent nanoparticles [6]. As can be seen from Fig.1.2 A, gold in bulk form retains its colour irrespective of change in its size or shape but when it become nanostructured, its colour is tunable. Such tunability gives rise to 'designer' applications. So, these unique properties are hugely responsible for making 'nanomaterials' an alluring option for researchers.

2) The quest in electronics for miniaturization of circuits but with larger number of components has been proceeding in accordance with the Moore's law illustrated in Fig.1.2 B. It shows the increase in the number of transistors with respect to the higher versions of Intel processors – the number roughly doubling every year. It has now been postulated that the current technologies being practised may not allow any further growth in this direction and a new technology is needed for it. Many look forward to nanotechnology in this context [7]. In semiconductor industry, MicroElectroMechanical Systems (MEMS) and NanoElectroMechanical Systems (NEMS) are being constructed (Inset, Fig. 1.2 B). These are very small devices incorporating a mechanical element sensitive to force whereby mechanical energy will be converted into an electrical or optical signal.
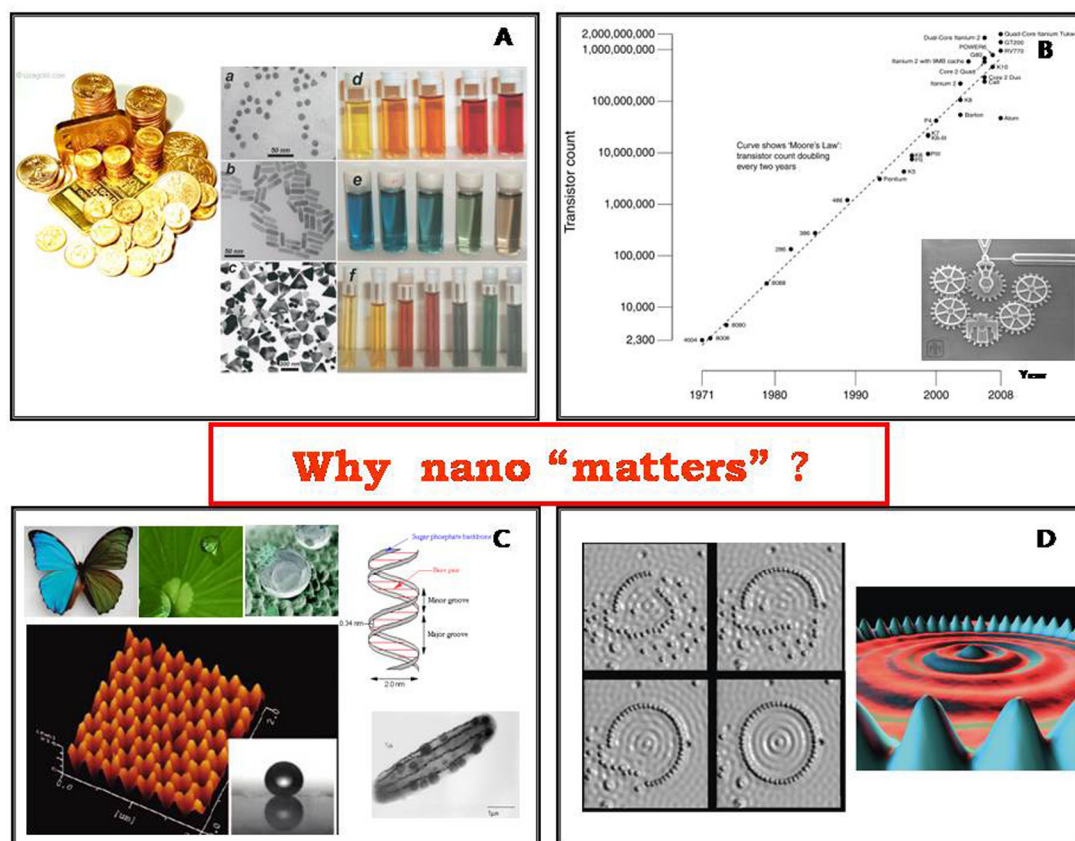
Fig. 1.2 *Pictures showing the driving forces for the research in nanoscience A) Tunability of optical properties of gold nanomaterials (colours) as against bulk gold B) Illustration of Moore's law with the images of Micro-Electro-Mechanical Systems (MEMS) as an inset. C) Butterfly wing and lotus leaf are the inspiration for films showing colour modulation and superhydrophobicity; DNA molecule with size-scale in nanometers; magnetotatctic bacterium containing iron oxide colloid. D) Construction of a quantum corral from single Fe atoms on a Cu (111) surface. Evaporated Fe atoms have been dragged across the surface by STM tip. The ripples inside the ring of Fe atoms are due to charge-density waves of electrons confined to the corral.*

*(**Images courtesy** - gold nanomaterials [8], MEMs: sandia labs, butterfly wing, film [9] , quantum corral [10]. Images of bulk gold, graphic of Moore's law, DNA, lotus leaf and magnetotactic bacteria: have been taken from various sources at images.google.com.)*

3) Nature is the main inspiration for nanoscience research in many ways. The researchers are trying to mimic some of the distinguishing phenomena occurring in nature by synthesis of nanomaterials [11-13]. For example, natural objects like a lotus leaf and wing of the 'morpho' butterfly have been the inspiration for preparation of colloidal films using photoresponsive azobenzene derivatives showing properties like superhydrophobicity and photonic bandgap (Fig.1.2 C). One of the best examples of naturally occurring nanomaterials can be seen in the form of magnetite colloids within the magnetotactic bacteria [14,15]. These colloids are used by the bacteria as a compass, to orient themselves along the magnetic field of earth for their movement.

   Natural building blocks like DNA are a few nanometer in size while microbes are a few hundred nanometer in size (see Fig. 1.2 C). Due to this 'right' size [16], not only can such biological entities be utilized in nanoscience, but also, the nanomaterials prepared can have biological applications such as drug delivery. Hence, nanomaterials can contribute to the advancement of basic understanding of biological systems as well as have applications in biomedical arena [17-22].

4) Simultaneous progress in instrumentation techniques: Development of tools like high resolution electron microscopes and scanning probe microscopes have enabled visualization and imaging at atomic level resolution (See Fig. 1.2 D) [23]. The techniques used for analyzing and measuring properties of nanomaterials are undergoing rapid advancement these days [24]. Nanomaterials can be interrogated and/or manipulated using such tools hence research on the nanomaterials has been accelerated [25-28].

Due to such reasons, nanoparticles are being touted as key materials and building blocks in the 21st century. But they have been present for the past few centuries in natural and man-made forms. For example, nanopaticle solutions are manifestation of age-old colloidal solutions. They were prepared and used for some specific purposes. However, for want of technology, the fine grain-size was predicted and not visible. But along with the advancement of technology, the research in nanoscience emerged as a distinguished branch of science. Some milestones in the progress of nanoscience have been listed in Table 1.1.

Table 1.1 S*ome prominent milestones in the development of nanoscience*

Time period	Description
5th century BC onwards	Gold colloids used for medicinal and aesthetic purposes [29-31].
1857	Michael Faraday synthesized gold nanoparticles by reduction of an aqueous solution of chloroaurate ions (AuCl$_4$)$^-$ using phosphorus in CS$_2$ (a two-phase system) and elucidated his findings in the lecture "Experimental Relations of Gold (and other Metals) to Light" [32,33].
1861	The term "colloid" coined by Graham [34].
1895-1925	Pioneering work in colloidal chemistry by Zsigmondy [35].
1930-40	Initial development of electron microscopes [36].
1959	Seminal lecture "There's Plenty of Room at the Bottom"[37] , given by physicist Richard Feynman at Caltech on December 29, 1959.
1965	Moore's Law: prediction by Gordon Moore: founder, Intel Corporation (Fig. 1.2 C).
1974	Taniguchi coined the term 'nanotechnology' [38].
1980-87	Advent of scanning probe microscopy [39,40].
1980s	Invention of quantum dots [41].
1985	Discovery of C$_{60}$ Buckminsterfullerene [42] which was followed by other nanomaterials of carbon like carbon nanotube [43] and graphene [44,45].

Metal nanoparticles:

Nanomaterials such as carbon nanotubes, quantum dots, ceramics like titanium dioxide (TiO_2) and zinc oxide (ZnO) have attracted researchers due to the large number of applications they offer [46-49]. Apart from these, metal nanoparticles are being studied extensively. Metal nanostructures could be zero-dimensional (e.g. nanoparticles), one-dimensional (e.g. nanorods, nanotubes and nanowires), two-dimensional (thin films or arrays of nanoparticles) or three-dimensional (superstructures). The work in this thesis deals exclusively with metal nanoparticles, specifically gold, cobalt and nickel and their assembled structures. Hence, an overview of properties, applications, synthesis protocols and assembly methods of metal nanoparticles has been presented here with prominence given to gold, nickel and cobalt nanoparticles.

1.2 Properties of metal nanoparticles

1.2.1 Surface effects

The surface atoms of a particle have fewer adjacent coordinating atoms as compared to the core atoms. So, the surface atoms are more active than the core atoms. Due to this, surface of a material determines the material characteristics like light emission, solubility etc. As the size of the particle decreases, a larger number of its constituent atoms occupy the surface. The reason behind this can be understood from a simple calculation given below.

Consider a spherical particle of radius "r",

Surface area of the particle $= S$ $= 4\pi r^2$
Volume of the particle $= V$ $= (4/3)\,\pi\,r^3$
So, the surface to volume ratio $= (S/V) = (3/r)$

As can be seen, the surface to volume ratio is inversely proportional to 'r'. So, as the size of the particle decreases, the surface effects become more prominent.

1.2.2 Electronic properties

Electronic structures of nanoparticles are very different from their bulk form as illustrated in Fig. 1.3. Electrical conductivity is the most significant property of metals since electrons are free to move even at low temperature in their half-filled

conduction band [51]. When a metal is divided finely, the continuum of the electronic states breaks down. The discreteness of the energy levels can be measured in terms of average spacing between the successive quantum levels namely Kubo gap. Such changes come under the so-called quantum size effects [52,53]. As the size of metal nanocrystals is reduced, they can show insulating behaviour due to the changes in the electronic structure. This transition is called the size-induced metal–insulator transition.
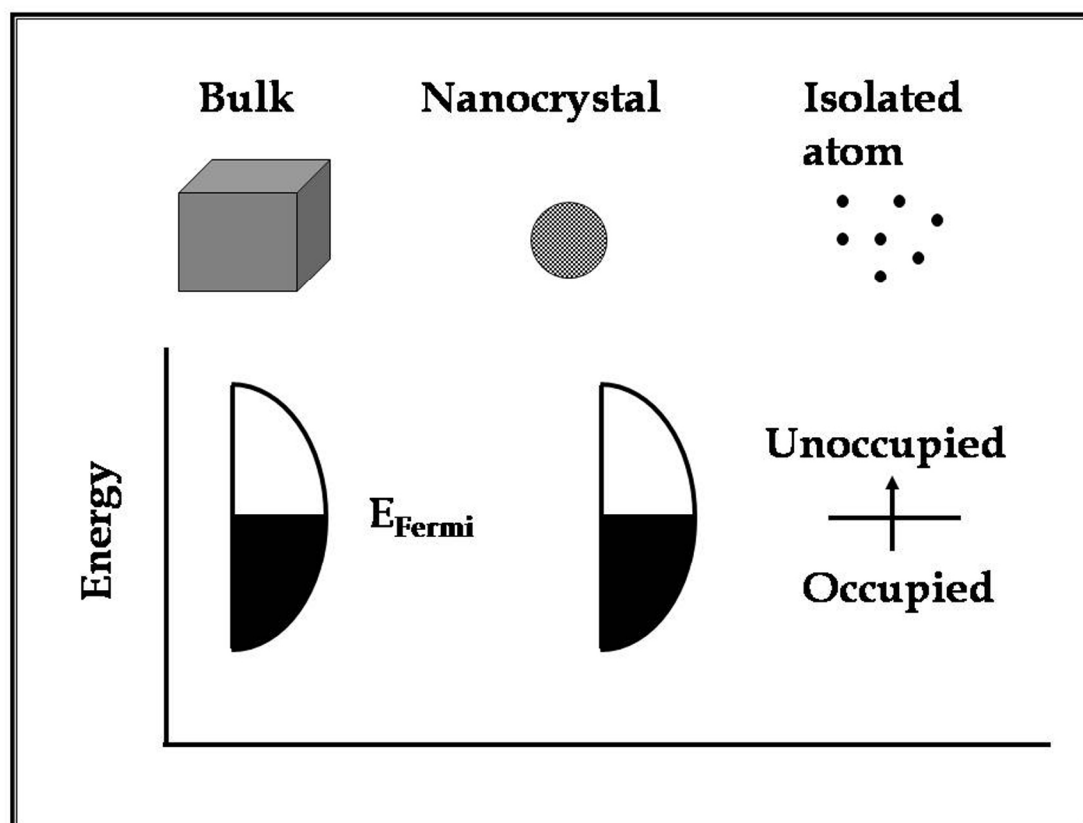
Fig. 1.3 *Comparative electronic structures of metals in bulk form, nano form and isolated atoms (adapted from [50]).*

In bulk metals, the motion of electrons is in accordance with Ohm's law i.e. linear relation V = IR between applied voltage V and induced current I. But as the size of the metal approaches the nanometer scale, Ohm's law may not be obeyed. I-V characteristic of such metal nanoparticles can be measured by placing them between the tip of the electrodes. In this case, the electrical charge transport would depend upon the charging energy which is determined by the capacitance of the particle. Here, the charging of capacitor is discrete. Typically, I-V characteristics show no current upto $V_{coulumb}$ where $V_{coulumb} = \pm$ e/2C (For a current to flow through a

nanocrystal, an external voltage greater than e/2C is required). This phenomenon is called 'coulomb blockade'. So, when one electron is transferred to the particle, its Coulomb energy will increase by $e^2/2C$. Further, injection of an additional electric charge into an already charged nanoparticle is prevented by coulombic repulsion. When the Coulomb blockade barrier is broken by applying sufficient voltage, electrons tunnel into the nanocrystal. The electrons may reside long enough to provide a voltage feedback preventing an additional electron from tunnelling in simultaneously. A continuous one electron current *I,* given by *I = e/2RC* flows through the circuit. To place an additional electron on the nanocrystal, a full *e/2C* increase in voltage is required. Thus, steps called a Coulomb staircase become visible in the I-V spectra of nanocrystals. This has made the realization of single electron devices at room temperature possible.

1.2.3 Optical properties

Optical properties of nanoparticles have been studied comprehensively [54-60]. Optical properties are most significant for noble metal nanoparticles like gold and silver as displayed by the beautiful colours of the nanoparticle dispersions [61]. When light is incident on bulk gold, absorption occurs at wavelength corresponding to blue colour hence bulk gold displays complementary colour yellow. On the other hand, at the nanoscale, gold shows different colours depending on parameters like size, shape, surroundings etc. of the nanoparticles [62, 63] and this is credited to the surface plasmon resonance (SPR) as seen in Fig.1.4.

Qualitatively speaking, free electrons and the positively charged metal ion cores in a bulk metal form a plasma state. Surface plasmons are modes of oscillation comprising an electromagnetic field coupled with the oscillations of conduction electrons. They arise because electromagnetic surface waves can propagate along the interface between conducting materials and a dielectric over a range of frequencies. Due to the surface plasmons, an enhanced field is observed at the interface of the conducting materials and dielectric. Since the order of penetration depth of electromagnetic waves in metals falls in the nanometer range, it polarizes or displaces the surface electrons from its equilibrium position.
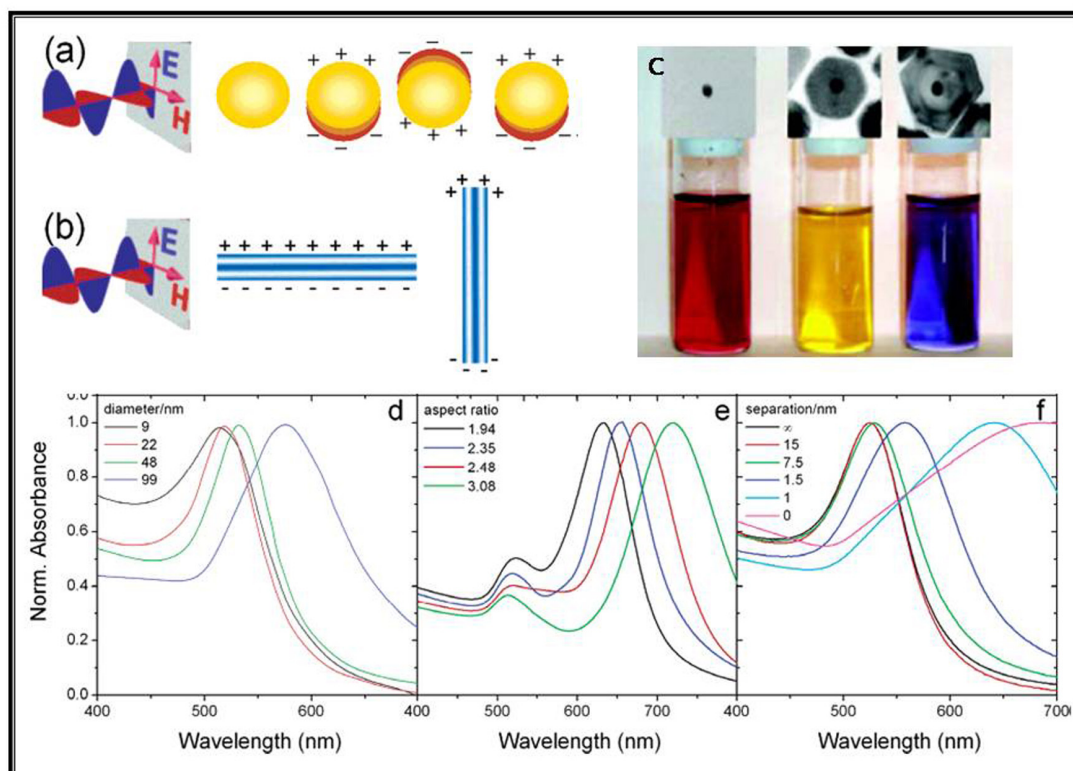
Fig. 1.4 A) *Phenomenon of surface plasmon resonance in spherical nanoparticles.* **B)** *Phenomenon of surface plasmon resonance in anisotropic nanostructure like nanorods.* **C)** *Nanoparticle solutions demonstrating the variation of optical properties i.e. colour with respect to change in composition.* **D)** *UV-visible absorbance spectra for nanoparticles of varying sizes.* **E)** *UV-visible absorbance spectra for anisotropic nanostructures with different aspect ratios.* **F)** *UV-visible absorbance spectra for nanoparticles of varying interparticle distance [64].*

Therefore, when the size of the conductor approaches nanodimensions, the boundary and surface effects become significant. This means that surface plasmons are also present in the bulk matter but their effect is manifold for nanoparticles. In nanoparticles, the electric field of incident electromagnetic radiation induces collective coherent excitation of conduction electrons relative to the cationic lattice. Then, the coulombic attraction between the cationic lattice and electrons acts as restoring force to bring back the electron cloud to the equilibrium position. In this manner, a dipolar oscillation of electrons is created (called plasma oscillation) with a characteristic frequency called plasmon frequency. Thus, the electron density within the surface layer undergoes collective oscillations whereas; the density in the interior

of the particle remains constant. Therefore, any change in the electron density of this surface layer will lead to changes in the plasmon absorption.

If the frequency of the excitation light field is in resonance with the frequency of this collective oscillation, even a small exciting field leads to a strong oscillation. The resonance frequency is mainly determined by the strength of the restoring force. The force depends on the separation of surface charges i.e. the particle size, and the polarizability of the medium and the polarizability of the core electrons. In case of metals like Pb and Cd, the resonating (plasma) frequency corresponds to the ultra-violet region of the electromagnetic spectrum. But in case of noble metals like Au, Ag and Cu, due to d-d transitions, the frequency corresponds to the visible part of the spectrum. This results in spectacular colours of the nanoparticle solutions where the colour is determined by the resonant frequency. In case of anisotropic nanoparticles (Fig. 1.4 b), this frequency depends on the orientation of the electric field relative to the particle. Hence, there can be more than one peak in the UV-visible absorbance spectrum of anisotropic, noble metallic structures; for example in gold nanorods, there are two peaks- namely, high energy band corresponding to out of plane transverse plasmon resonance and low energy band corresponding to the in-plane longitudinal plasmon resonance along the axis of the nanorods (Fig. 1.4 e).

Quantitatively, the optical properties can be explained by theories like Mie theory [65] for the absorption and scattering of electromagnetic radiation by small spheres and discrete dipole approximation.

$$C_{ext} = \frac{24\pi^2 R^3 \varepsilon_m^{3/2}}{\lambda} \frac{\varepsilon_2}{(\varepsilon_1 + 2\varepsilon_m)^2 + \varepsilon_2^2}$$

Given here, is the expression for the extinction cross section of a single particle C_{ext} according to Mie theory. This expression is for a spherical particles of radius R with a frequency dependent dielectric function ($\varepsilon_1 + i \varepsilon_2$), present in a dilute nanoparticle dispersion medium of dielectric function ε_m, where λ is the wave-length. The resonance is said to occur when $\varepsilon_1 (\lambda) = -2\varepsilon_m$.

In case of nanogold, the position and shape of a plasmon peak is found to be a function of several parameters like the size, shape, composition (doping, alloying), surrounding medium (its dielectric constant and refractive index), interparticle

distance, surface modification (functionalizing ligand or shell) etc (Fig. 1.4 c-f)
[57,66-68].

1.2.4 Melting point

As nanoparticles have a larger surface to volume ratio, the number of defects
is higher which could result in change in their mechanical properties with respect to
their bulk counterparts. Change in specific heat, hardness, mechanical strength and
melting point could be some salient examples of this property.
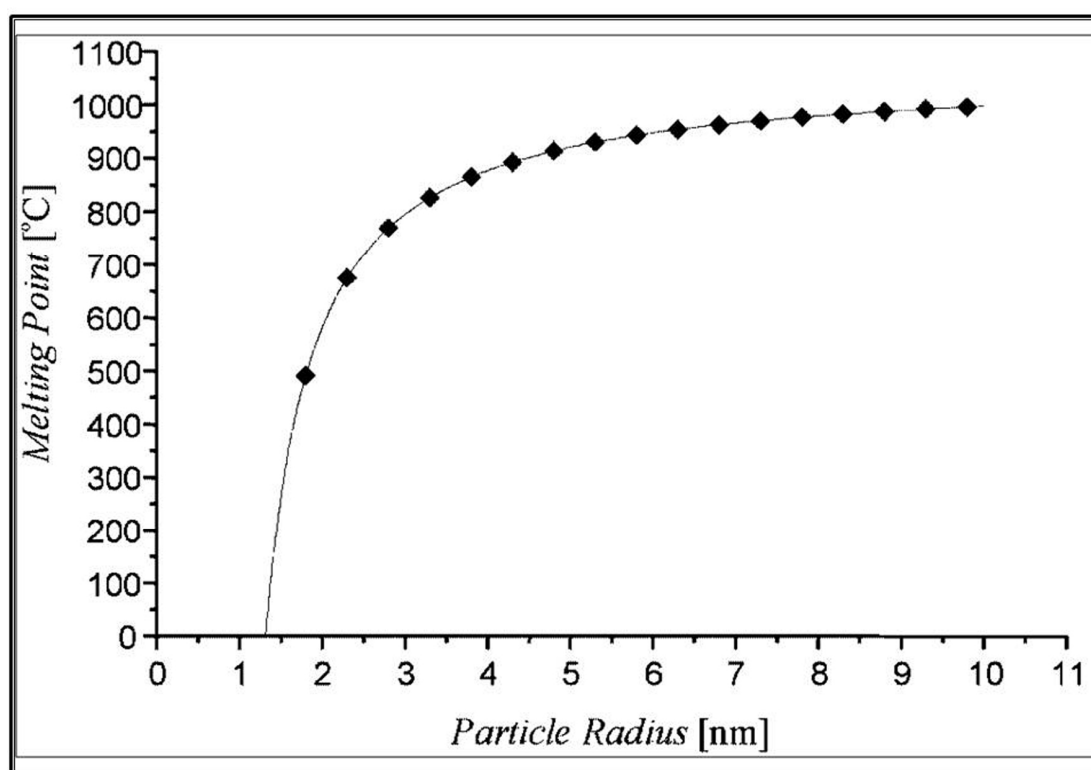
Figure 1.5 *Variation of melting point of gold nanoparticles with respect to their size* [69]

The melting point of the nanocrystals is seen to decrease with the decrease in
the size [70]. This is a consequence of the presence of a higher number of surface
atoms in a smaller particle. It is supposed that the surface atoms are more susceptible
to thermal displacement and initiate the melting process due to the lower
coordination. Such a surface melting process is thought to be the major cause for the
lowering of melting points.

1.2.5 Magnetic Properties
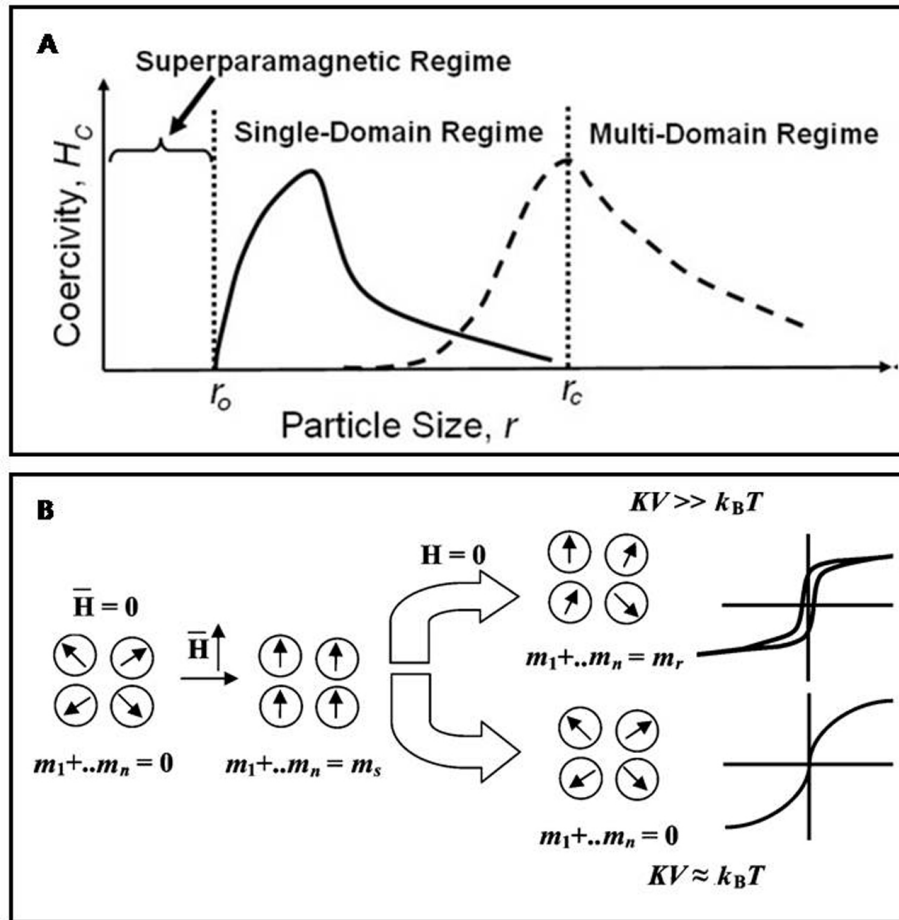
Fig. 1.6 A) *Schematic showing the change in the coercivity of a ferromagnetic particle with the diameter in the superparamagnetic, single-domain and multi-domain regions [71].*
B) *Illustration of superparamagnetism [72].*

Nanomaterials show novel magnetic properties [73-75]. As seen in Fig. 1.6, magnetic nanoparticle, below a critical size r_c, can contain only a single magnetic domain which means that all the spins of the particle are coupled in the same direction, and the particle behaves as a single magnetic dipole. Hence, to change the magnetization, the domain needs to be rotated instead of moving the domain wall. For a particle size smaller than the single domain size, the spins can be easily affected by the thermal fluctuations and the originally ferromagnetic material shows superparamagnetic nature [76]. This can be understood from the equation $KV = 25$ $k_\beta T_B$ where V, k_β and T_B are the volume of a single particle, Boltzmann constant and blocking temperature respectively [77].

From this equation, it can be seen that as the particle size decreases, the magnetic anisotropy energy KV (the energy difference involved in changing the magnetization direction from a low-energy direction or easy axis to a high energy direction or hard axis) also decreases. For a given particle, K, V and k_β would be constant and the thermal energy would be a function of the blocking temperature. Above the blocking temperature, the thermal energy is sufficient to flip the spins in the magnetic material, hence the material will not show any hysteresis loop. Consequently, for superparamagnetic materials, a hysteresis loop is obtained only below its blocking temperature. In case of superparamagnetic materials, a plot of the magnetization (*M*) and the ratio of the magnetic field and the temperature (*H/T*) produces a universal curve for all temperatures above T_B. Superparamagnetism is also related to the relaxation rate and is sensitive to the characteristic time scale of measurement.

1.3 Applications of metal nanoparticals

As evident from the above discussion, the properties of metal nanoparticles are distinguishable and tunable with respect to various parameters. Due to their tunability, the properties of metal nanoparticles can lead to a large number of applications in diverse fields [78]. Some of the prominent applications would be described in this section.

1.3.1 Catalysis

Metal containing catalysts can be of three types - heterogeneous catalysts, enzyme catalysts and homogeneous catalysts. Most of the industrial and lab scale synthesis involves metal based catalysts due to increase in the turnover, conversion and selectivity of the product formation. Nanoparticles of metal could be the potential alternatives for these bulk metal catalysts due to the following advantages:

1) They have a much larger total surface area per unit weight than the materials currently used, thus allowing more effective utilization of the expensive transition metal as a result of dispersion.

2) Metals like gold are inert in their bulk state but nanoparticles of such metals display catalytic activity.

3) Adsorption of the reactant can be specific to certain crystalline faces of the catalyst and it is possible to design nanoparticles of different shapes to have those surfaces for the selective binding of that reactant. Catalytic activity can also be enhanced by changing the shape of the nanostructure or by functionalizing it [79].

4) When nanomaterials are used as catalysts, they can also be separated easily and hence can be reused [80].

Owing to such reasons, nanoparticles are being used as catalysts. The pioneering work of Haruta demonstrated the usage of gold nanoparticles as catalyst. There, oxide supported gold nanoparticles were shown to catalyze CO oxidation by O_2 at low temperatures [81]. After the initial breakthroughs, catalytic properties of metal nanoparticles are being widely studied [82-87]. Nanoparticles are now being used to catalyze many reactions like cross-coupling [88], electron transfer [89], hydrogenation [90], oxidation [91] etc. Gold nanoparticles [92-99] and transition metal nanoparticles [100-108] [109] are some of the most widely used nanocatalysts. Metal nanoparticles are also being used as catalysts to prepare one–dimensional structures like carbon nanotubes, zinc oxide nanowires etc.[110]

1.3.2 Bio-medical applications

Nanoparticles can be utilized for biological applications [111-115] because

1) Their size is comparable to biomolecules like nucleic acids

2) They can be functionalized with biocompatible moieties.

3) They show properties such as fluorescence and magnetic behavior which can be utilized for imaging, drug delivery etc.

The medical applications can be classified as diagnostic, therapeutic, imaging and drug-delivery while other biological applications include biosensing [116,117] and bioseparation [118]. The conjugation of nanoparticles with biomolecules can be done by direct covalent linkage or using non-covalent interactions [119].

Nanoparticles can be used for biodignostics or to detect biomolecules. This is based on the principle that when a nanoparticle label or probe binds to the target biomolecule, a measurable signal characteristic of the target biomolecules will be produced or a change in the property will be observed as a result of binding. Since the optical properties of gold nanoparticles (the position and shape of SPR band) are known to be sensitive to the surrounding environment, binding etc., they can be used as biosensors. For example, if the Au nanoparticles bind with biomolecules, their

interparticle distance will change. When this distance decreases, the SPR band shifts to longer wavelength and hence they show a colour change from red to blue while the increase in interparticle distance causes a concomitant colour change towards the shorter wavelength (colour change from blue to red). Gold nanoparticles are being used for sensing biological entities like viruses etc. [120,121].

Mirkin *et al.* have worked extensively to develop highly sensitive colorimetric sensors for oligonucleotides based on the oligonucleotide-mediated nanoparticle aggregation [122-124]. Willner *et al.* reported several systems using nanoparticle–enzyme hybrids as electrochemical sensors by using the conductivity properties of gold nanoparticles [125]. Bicompatibility [126] and possibility of versatile functionalization of gold nanoparticles make them important candidates for biomedical applications.

In therapies like cancer chemotherapy, both malignant and normal cells are damaged alike. To avoid this, a drug delivery strategy that selectively targets the malignant tumour can be used. Nanoparticles can act as carriers for biomolecules and drugs, protecting them from degradation and transporting them across the cell-membrane barrier. Hence, gold nanoparticles as well as magnetic nanoparticles can be used for gene-delivery [127] and drug delivery [128-131]. The transport of the molecules could be under the external force like magnetic field.

Fluorescent or luminescent nanoparticles can be used for optical imaging while magnetic nanoparticles can be utilized for magnetic resonance imaging [132]. Due to the ability of gold nanoparticles to scatter light, they can be used for cellular imaging [133] and cell labelling [134].

Gold nanostructures can be bioconjugated with antibodies for selective targeting of cancer cells which can then be subjected to photo-thermal therapy [135]. When light is irradiated on these nanostructures, the energy collected by the nanoparticle could excite the phonons, resulting in a temperature increase in the close proximity of the particles. Heat dissipation from the hot particles can then selectively kill the targeted cancer cells. Magnetic nanoparticles can also be used for hyperthermia where they could selectively cause damage to the tumour cells [136,137]. Magnetic nanoparticles can also act as contrast enhancing agents [138].

Silver nanoparticles are known to be highly toxic and show antimicrobial activity and hence can be employed for biomedical applications like reducing infections, preventing bacteria colonization on medical equipments as well as skin etc [139-141].

1.3.3 Ions and gas sensors

A sensor contains two parts-a recognition element for target binding and a transduction element for signaling. Application of gold nanoparticles as biological sensors has been described earlier. Using similar principles, gold nanoparticles can also be used to sense metal ions, organic vapours and toxic elements in the environment [142-151].

1.3.4 Optoelectronic applications

The optoelctronic applications are mainly demonstrated by the nobel metal nanoparticles [152]. Apart from applications like sensing and imaging, these nanoparticles can also be utilized for plasmonics, optical waveguides, surface-enhanced Raman scattering (SERS) and photovoltaic devices [153,154].

SERS is a Raman spectroscopic technique that provides greatly enhanced signal from Raman-active analyte molecules that have been adsorbed onto certain specially prepared metal surfaces. Metal nanoparticles, especially silver nanoparticles, can enhance the efficiencies of surface-enhanced Raman scattering (SERS) signal by as much as 10^{14}–10^{15} fold and this tremendous enhancement allows spectroscopic detection and identification of even a single molecule under appropriate conditions [155-162]. SERS is highly sensitive as well as surface selective.

Metal nanoparticles like gold and silver demonstrate noticeable photoactivity under UV-visible irradiation and hence can be used for optoelectronic applications [163]. The strong interaction of individual metal nanoparticles with light can be exploited to fabricate waveguides, to transfer energy through nanoparticles. Plasmon waveguides can be used to build nanoscale optical devices [164-166].

1.3.5 Ultra-high density storage and magnetic recording

Single domain magnetic nanoparticles can be utilized for magnetic recording [167]. Magnetic recording media are of two types 1) Particulate – flexible storage media area (tape and floppy disks). They contain distinct particles of magnetic oxides

or metals with an organic binder coated on a flexible polymer substrate. 2) Thin film type – rigid disk media. These consist of thin film media of magnetic oxides or metals deposited by sputtering or thermal evaporation on rigid disk substrate or a flexible polymer substrate. Recording media can be defined as thin magnetic layer supported by a rigid or flexible substrate which can be magnetized by a rigid magnetic field and which retains its magnetization even after removal of the field. Information is recorded in the form of oppositely magnetized regions in the surface layer of the medium, utilizing fringing field of the inductive transducer. This information is then read by such an inductive transducer or magneto-resistive sensor.

Ferromagnetic nanoparticles allow writing and storing magnetic transitions at high densities, with each recording bit containing hundreds of nanoparticles [168]. Advanced ultra-high density recording media require uniform particles with room temperature coercivity Hc of ~3000 to 5000 Oe. Nanomaterials like FePt or CoPt are expected to have coercivity values in that range [169]. This, apart from other properties like large uniaxial anisotropy and chemical stability make CoPt and FePt magnetic alloys suitable candidates for the permanent magnetic applications. Self-assembled ferromagnetic FePt and CoPt nanoparticle arrays can be used in ultra-high density recording devices [170]. FeCo nanoparticles are a 'soft 'magnetic material since they quickly switch the magnetization direction once the external magnetic field is reversed. So, they can be utilized in high-frequency electric circuits like mobile phones [171].

1.3.6 Other applications

Mg, Al, and Zn nanostructures have been reported to be useful for batteries [172]. Platinum nanostructures have been studied for applications in fuel cells [173]. Metal nanoparticles like cobalt and nickel can act as nucleators for the growth of high apect-ratio nanomaterials [174] and also for magnetocaloric applications [175].

In fact, what has been listed can only be termed as the 'tip of the iceberg' and many new applications are being perceived and reported daily. For want of brevity, it is not possible to list all these here. Similarly, the next sections dealing with methods of synthesis and assembly of nanoparticles also contain the description of a few of the available methods.

1.4 Synthesis of metal nanoparticles

The two approaches used for the synthesis of nanomaterials [176] are shown in fig.1.7.
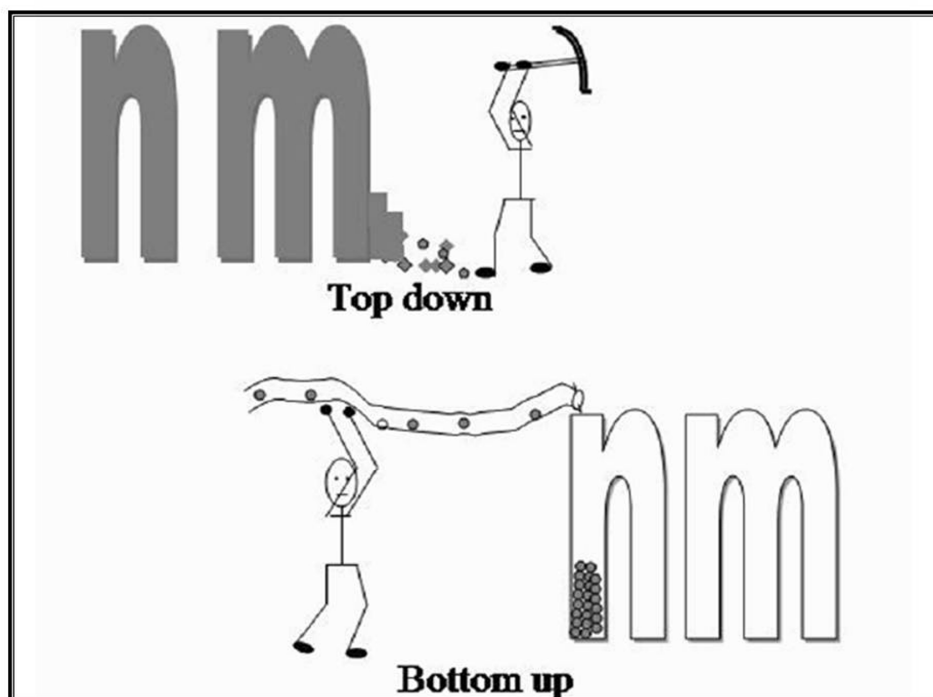
Fig. 1.7 *Cartoon showing the two pathways of synthesis of nanoparticles- top-down and bottom up approach. (Image courtesy : "Nanochemistry" by G. A. Ozin and Arsenault)*

The top–down approach involves mainly physical methods where a bulk material is sliced into pieces till the desired size is achieved. Lithographic techniques, LASER induced chemical etching and ball milling fall in to this category [177,178]. However, these methods can work only down to the micrometer level. This is a strong limitation for these procedures. On the other hand, in bottom up strategies, the nanomaterial is built up from its constituents [179]. Synthesis by the bottom-up methods generally involves the following steps:

Nucleation phase: Metal ions contained in the precursors are reduced by a suitable reducing agent in the presence of a capping ligand to produce tiny seed particles. When the solution becomes supersaturated, these seed particles precipitate spontaneously. This is called a nucleation phase. Supersaturation can be accomplished by high temperature or by the reactants.

Growth phase: Nucleation phase is followed by the growth phase where the precipitated seeds capture dissolved atoms or molecules and grow in size. A process called Ostwald ripening whereby smaller particles dissolve releasing monomers or ions for consumption by bigger particles (since they have lower solubility than smaller particles) is significant in the growth. If nucleation and growth occur concurrently throughout particle formation, then the particles show a polydisperse nature. So, in order to obtain narrow size dispersion of nanoparticles, the nucleation phase should be temporally separated from the growth phase. This was shown in classic studies conducted by Lamer and Dinegar [180].
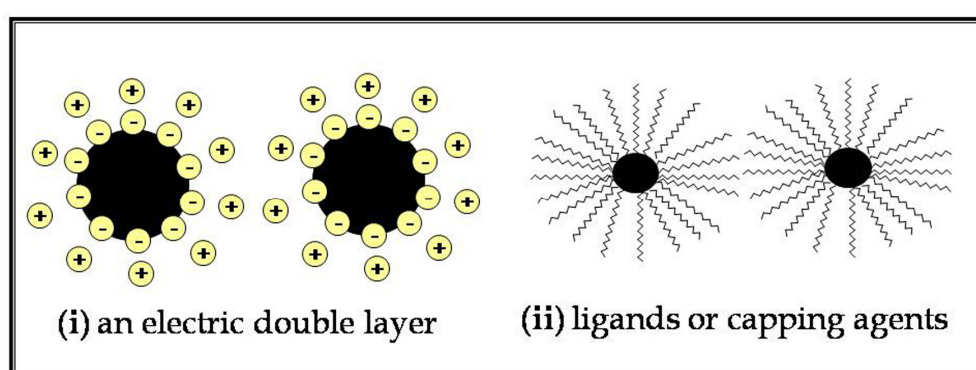
Fig. 1.8 *Picture depicting two ways of achieving stability of nanoparticles- electrostatic repulsion between ionic layer surrounding nanoparticles and steric interaction between ligands capping the nanoparticles.*

Since nanoparticles have high surface to volume ratio, they are reactive and thermodynamically unstable. If their surface is not protected, they would aggregate to bulk structures. Hence, a capping agent is added during the nanoparticle synthesis, to get stable solutions. The stability of nanoparticles can be achieved by two ways as shown in Fig. 1.8 –

(i) Electrostatic repulsion - If the nanoparticles are prepared in aqueous medium, they are surrounded by an electrical double layer formed by the adsorption of precursor ions. This layer is in turn surrounded by the counterions constituting the so-called double layer. Due to their same surface charge, there will be coulombic repulsion between two nanoparticles and hence their aggregation will be prevented.

(ii) Steric interaction- For nanoparticles in organic medium, the capping ligands consist of surfactants, polymers etc. Their head groups bind to the nanoparticles and hydrocarbon chains undergo steric interactions to avoid aggregation. Molecules like

long chain aliphatic thiols [181], amines [182], phosphines [183], amino acids [184,185] ; natural polymers like peptides [186] as well as synthetic polymers [187] etc. can be used as stabilizing agents.

Some of the prominent synthesis methods [188] based on deposition [189], reduction etc. have been described below.

1.4.1 Deposition methods

- In case of **Physical Vapour Deposition (PVD)** method, the bulk metal is heated in high vacuum and the vapours produced are condensed on a substrate to make thin films of metal of having few nm thickness [190].

- In **Chemical Vapour Deposition (CVD)**, the carrier gases containing the elements of the desired compound flow over the surface to be coated. This surface is heated to a suitable temperature so that the carrier gas thermally decomposes or reacts with other gases and its desired constituents are deposited on the surface [191].

- In **Solvated Metal Atom Deposition (SMAD)**, a bulk metal (metal wire) is heated under vacuum the vapours obtained contain highly reactive metal atoms. These vapours of the metal are co-condensed with vapours of excess of organic solvent like acetone to form nanoparticles in solution [192-195]. The resulting solution would consist only of colloids and solvent, with no by-products from precursors. Here, recombination to the bulk metal is suppressed since the vapours are immediately combined with a solvent.

- In **Inert gas condensation** procedure, a metal target foil or ingot placed in a ceramic crucible is heated in a chamber filled with an inert gas such as argon [196]. The vaporized metal cools fast, losing energy as it collides with argon atoms and hence leads to nanoparticle production.

- In **arc discharge method**, metal is evaporated by striking an arc between metal electrodes in the presence of an inert gas and the metal nanoparticles will be formed in the electrolyte solution [197].

- In **laser ablation method**, a metal target is irradiated with focussed and intense laser pulses [198-202]. The metal target can be immersed in a solvent containing surfactant. Due to laser pulses, the metal atoms vaporize and can be capped by

surfactant to obtain stable nanoparticles. The particle size is controlled by intensity of laser pulse and time of exposure. Generally, a pulsed excimer laser or a Nd:YAG laser is used.

1.4.2 Reduction based methods

Faraday adopted a reduction based method way back in 1857. He prepared gold nanoparticles by reduction of an aqueous solution of chloroaurate ($AuCl_4^-$) ions using phosphorus in CS_2 (a two-phase system) [32]. After that many reduction based protocols have been developed [203].

- **Citrate reduction:** It is one of the oldest synthesis methods, initiated by Turkevich in 1951 [204]. In this method, aqueous chloroauric acid is reduced by trisodium citrate to give gold nanoparticles. The tunability of nanoparticle size depending upon the ratio of stabilizer and reductant ratio was demonstrated later [205]. The advantage of this method is that the citrate is loosely bound and hence can be easily replaced by other ligands for functionalization.

- **Sodium borohydride reduction based methods:** This involves the hydrolysis of the borohydride accompanied by the evolution of hydrogen. Synthesis of nanoparticles in organic medium can be achieved by a two-phase Brust-Schiffrin method [206]. Here, aqueous chloroaurate ions are transferred into organic medium (toluene) by using tetraoctylammonium bromide. The phase transferred chloroaurate ions are then reduced by $NaBH_4$ in the presence of dodecanethiol which acted as stabilizers. This method results in gold organosols and with narrow size dispersion. These nanoparticles can be separated from solvent and redispersed in common organic solvents without irreversible aggregation or decomposition and hence can be easily functionalized. The strong binding of thiol ligands with gold has been exploited since the seminal work of Nuzzo and Allara [207] where the 'self-assembled monolayers' of alkane thiol on gold were obtained. Murray et al. named the alkanethiol capped gold nanoclusters as 'monolayer protected clusters' and studied the "place exchange" of a controlled proportion of thiol ligands by different functional thiols [208]. Gold nanoparticles can also be prepared in aqueous medium where sodium borohydride brings about reduction of chloroaurate ions. This resultant gold hydrosol is highly stable due to electrostatic repulsion and could be easily phase-transferred to an organic medium using phase

transferring agents like alkyl amines [209-211]. Silver and platinum nanoparticles can also be prepared by borohydride reduction and subsequently phase-transferred into organic medium by using octadecylamine [212,213]. Apart from these, polyol [214], lithium triethylborohydride (superhydride) [215] etc. are also being used for reduction. Polyol reduction is preferred for anisotropic particles while superhydride is preferred for synthesis in organic medium.

- **Photochemical (Photolytic and Radiolytic) methods:** A metal complex is decomposed by light in the presence of some donor ligands [216,217] while in radiolysis, a metal salt is reduced by photogenerated reducing agents such as solvated electrons. The radiolysis [218-222] of aqueous solutions of metal ions lead to formation of solvated electrons that can directly react with the metal ions or with other dissolved materials to produce secondary radicals, which then reduce the metal ions to produce nanoparticles For example, nanoparticles can be prepared when UV light is irradiated on the mixture of aqueous metal ions and alcohols.

- **Electrochemical methods:** This method [223,224] involves oxidative dissolution of anode, migration of metal ions to the cathode, reduction of ions to zero-valent state to form nanoparticles which are capped by ligands like quaternary ammonium salts containing long-chain alkanes such as tetraoctylammonium bromide. The particle size depends upon the current density, the distance between the electrodes, the reaction time, the temperature and the solvent polarity.

- **Sonochemical methods:** In this method, a mixture of reagents dissolved in a solvent is subjected to ultrasound radiation (20 kHz–10 MHz). This results into the creation, growth, and collapse of bubbles due to the suspended particulate matter and impurities in the solvent. Then, the bubbles expand, creating a vacuum due to which volatile reagents diffuse into the bubble. This is followed by the rapid collapse of the bubble accompanied by a temperature change of 5,000–25,000K in about a nanosecond, decomposing the matter within the bubble. There could be a generation of free radicals that cause further reactions e.g when water or alcohol is the solvent, hydroxyl radicals are generated. Such radicals can be involved in the reduction of metal ions in solution. Nanoparticles of gold, platinum, palladium etc. have been synthesized by this method [225-232].

- **Thermolysis:** In this method, organometallic complexes like metal carbonyls are decomposed in high-boiling organic solvents in the presence of ligands like tri-*n*-octylphosphine oxide (TOPO) [233-236]. The particle size and morphology are determined by ratios of the reagents, reaction temperature, reaction time, aging period etc [237]. Injection of organometallic precursors into a hot coordinating solvent containing a surfactant mixture under inert atmosphere, can result into a temporally discrete but homogeneous nucleation event followed by growth in solution. The surfactant acts as a capping agent, allows for monomer exchange, protects the nanocrystals from oxidation and controls the interparticle distance. If the surfactants preferentially bind to specific crystallographic surfaces of the growing crystal, the shape of the nanocrystals can also be controlled.

- **Reverse micelles and microemulsion:** Reverse micelles are aggregated structures of surfactants in organic medium [238]. Here, the hydrophobic chains of the surfactant point outwards while hydrophilic headgroups point towards the core of the micelle. So, the spherical droplets of water get trapped in the core of micelle. The dimension of the water droplet depends upon water–surfactant molar ratio. If the water droplets are bigger, the inverted micelle is called a microemulsion. The water droplets act as a reactor to synthesize nanoparticles [238-240]. The synthesis takes place by exchange of matter through coalescence of two reverse micelles containing the precursors and reagents where the size of droplet determines the size of nanoparticles produced.

- **Digestive Ripening method:** It has been pioneered by Klabunde's group [181,241,242], this method has been found to result in particles with exceptionally narrow size distribution, starting from a solution of polydisperse particles. Initially, gold nanoparticles are prepared by i) inverse micelle method or ii) SMAD method described earlier. Then, this colloidal suspension is heated at or near boiling point of the solvent and in the presence of a surface-active ligand like thiol. The solvents normally used are non-polar organic solvents having boiling points higher than 100 °C and then followed by digestive ripening method. Till now, different kinds of nanoparticles have been synthesized by this method.

- **Synthesis at air-water and liquid-liquid interface:** Organic derivative of the metal taken in the organic layer reacts at the air-water [243] or liquid-liquid

interface or with the appropriate reagent present in the aqueous layer to yield nanoparticles at interface.

- **Biological methods:** Taking a cue from nature, biological routes for nanoparticle synthesis have also been devised. Living microorganisms like bacteria, yeast, fungi have been employed to prepare metal nanoparticle like gold, silver etc. [244-247]. Such nanoparticles have also been prepared by using plant extracts as reducing agents [248-251].

1.5 Assembly of metal nanoparticles

Assemblies are the interconnecting bridges between nanoscale building blocks (synthesis stage) and nanodevices (application stage). For example, nanoparticles used in electronic devices based on tunneling effect should be in close proximity, separated only by tens of angstroms. Similarly, optical properties involving distance-dependent plasmon interactions require uniform arrays of nanoparticles. Assembly of nanoparticles can be obtained by (i) connecting them with other nanoparticles or nanomaterials, (ii) binding them to a functionalized surface, (iii) guiding them by a template. Size, stability, functionality and solubility of the nanomaterials play an important role in the formation of an assembly while electrostatic attractions, covalent bonding, (dipole-dipole interaction in case of magnetic nanoparticles) are the primary interactions that govern the assemblies [252,253]. The length and bulkiness of the stabilizing ligands of nanoparticles determine their interparticle distance in the assembly.

There are several ways to classify assemblies of nanoparticles [254-256]. They can be classified as one-dimensional (1-D), two-dimensional (2-D) and three-dimensional (3-D). Assemblies can also be categorized on the basis of the pathways of their formation e.g. template based, evaporation induced, involving specific biological interactions [257,258] (e.g. based on antibody – antigen coupling), lithographically achieved etc. [259]. Here, some key types of assemblies will be discussed.

- *Assembly by solvent evaporation*

    The most obvious way of preparing assemblies from nanoparticle solutions is by drop-coating them on a substrate. The evaporation of solvent leads to formation of spontaneous assemblies. The nature of assemblies is determined by i) properties of

the constituent nanoparticles including their size distribution, shape, concentration, capping ligand; ii) nature of solvent, rate of its evaporation, iii) characteristics of the substrate- its affinity to the solvent used; iv) the interaction between particle and substrate; v) presence of other reagents etc.

The packing and order of assemblies, nature of the solvent and its evaporation rate can differentiate between them in the following manner. If the interaction between particles is weak and repulsive, the driving force for forming ordered structures is less. Also, if the solvent evaporates fast, a glassy solid with short-range and random order, along with a frozen liquid-like structure is acquired. This glassy structure is reversible with respect to slow addition of structure. But, if the solvent is slowly evaporated and if the constituent nanoparticles have attractive interaction and narrow size dispersion; the resultant assembly is long-range and ordered. If the evaporation of the solvent is slow, the particles have enough time to move about to find their lowest energy sites in the superstructure, therefore an ordered organization is obtained. Hence, slow evaporation of a highly boiling solvent can result in long-range assembly of nanocrystals. The morphology of the organization could be a function of the substrate on which the assembly is obtained and also the shape of an individual nanostructure [260]. A large number of researchers have obtained evaporation induced assembly of metal nanoparticles [261-265]. Notable among them are Gelbert and co-workers [266,267] who have also explained the mechanism of formation of such assemblies.

- *Assembly of magnetic nanoparticles*

To achieve applications like ultra-high density recording media, arrays or superlattices of magnetic nanoparticles have to be prepared [268,269]. The driving forces for the assembly of ligand capped magnetic nanoparticles are van der waals interactions and magnetic interactions [270-272]. Dictated by the characteristics of the solvent and particles, the evaporation induced assembly of magnetic nanoparticles can lead to glassy solids or a hexagonal two-dimensional superlattice with less number of defects [273,274]. The arrangement may not be always in the form of an array. The nanoparticles can also arrange themselves in the form of loops or rings [275,276]. The properties of the assemblies can change due to an external stimulus like magnetic fields or temperature [277-279]. Ordered

magnetic nanostructures and arrays are being studied comprehensively due to the proposed applications [269,280] [281,282].

- *Assembly by lithography or patterning*

  Nanofabrication is an important tool for electronic applications. It can be done by many ways such as photolithography, electron beam lithography, focused ion beam lithography, dip-pen nanolithography, microcontact printing [283,284], nanoimprint lithography, scanning-probe-based techniques (e.g., atomic force microscope lithography) [285-287]. These pathways are advantageous due to the control over pattering, scaling up and uniformity of the resultant pattern.

- *Template Assisted assemblies of nanoparticles*

  Organization of nanocrystals can be achieved by using templates or scaffolds. Synthetic templates like porous alumina, polymers and natural templates like proteins, nucleic acids, fungus etc. [289-291] can be employed for nanoparticle assemblies.
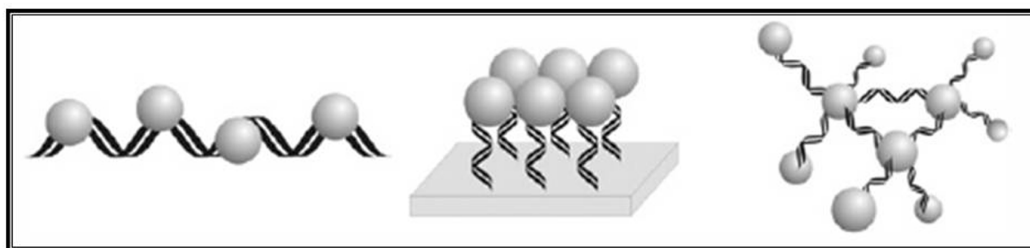
Fig. 1.9 *Schematic showing 1-D, 2-D and 3-D assembly of nanoparticles using DNA [288].*

One of the most popular examples of template based synthesis is the preparation of assemblies of gold nanoparticles using DNA [292-295]. This is based on the electrostatic interaction between the positively charged gold ions and negatively charged polyphosphate backbone of single and double stranded DNA [296,297]. DNA can be utilized to form 1-D [298], 2-D [299] as well as 3-D assemblies [300,301]. DNA linked gold nanoparticles were also utilized to study optical properties of gold nanoparticles [302].

- *Assembly by electrophoretic deposition*

  In this method, two metal electrodes (usually indium tin oxide electrode) are immersed in a small glass cell containing nanoparticle solution. The charged nanoparticles migrate under the influence of electric field and get deposited

accordingly. Applied voltage and nanoparticle concentration determine the nature of assembly. This method was pioneered by Giersig and Mulveney [303] where they obtained an assembly of aqueous citrate reduced gold nanoparticles and was followed by other reports of electrophoretic assembly.

- *Assembly at air-water and liquid-liquid interface*

Langmuir-Blodget (LB) is the main technique to assemble nanoparticles at air-water interface [304-306] and has been utilized extensively since its establishment by Langmuir and Blodgett [307,308]. Under this technique, assembly can be either in-situ where nanoparticles are synthesized and subsequently assembled at the air-water interface or ex-situ where the nanoparticles are synthesized by a different method, phase transferred if they are not hydrophobized and then spread on the LB trough [309,310]. Gold nanoparticles capped by ligands like laurylamine have been organized at the air-water interface [309]. Based on similar principles, nanoparticles have also been assembled at liquid-liquid interface [311,312].

- *Assembly using self-assembled monolayers*

The interesting chemistry between gold and sulfur has been utilized extensively by researchers. In 1983, Nuzzo and Allara reported the formation of self-assembled monolayers (SAMs) of disulfides on zerovalent gold substrate [313]. This was followed by the report of ordered monolayer films of long-chain alknathiol molecules formed on gold surface [314]. SAMs can be utilized to form nanodevices [315,316].

- *Assembly through non-covalent interactions*

In this method nanoparticles are assembled to non-covalent interaction e.g. strong hydrogen bonding. 2D and 3D superlattices of uniform-sized, capped nanoparticles can be prepared [317-320]. Hydrogen-bonding interaction is known to be attractive and direction-specific and hence is useful for organization.

1.6 Objective of the thesis

The importance of metal nanoparticles has been established in the previous sections which mainly owes to interesting properties displayed by them. It is shown to

arise from the large variety of applications offered by the metal nanoparticles. The dependence of properties of nanoparticles on the particle size has also been illustrated. Hence, it is desirable to synthesize monodisperse nanoparticles from the point of view of applications. A glimpse of literature on nanoscience and nanotechnology reveals different methods of synthesis and assembly of metal nanoparticles. But, there is a need of synthesis methods which lead to monodisperse nanoparticles. Hence, such a protocol has been developed as a part of this thesis. Using this protocol, nickel and cobalt nanoparticles (important for their catalytic and magnetic properties) have been synthesized.

Assembly is the bridge between nanoscience and nanotechnology or in other words it links synthesis of nanoparticles to their applications. As part of this thesis, a protocol was developed to synthesize monodisperse nanoparticles which formed a spontaneous assembly. Then, a known protocol was used to synthesize monodisperse nanoparticles which showed a variation in the type of assembly with respect to their capping ligands. The mechanism of assembly formation was probed here. Lastly, nanoparticles were functionalized to devise a photoresponsive assembly. Therefore, a significant part of this thesis has been devoted to devising different types of methods to assemble metal nanoparticles, specifically gold nanoparticles (important due to their interesting optical, electronic as well as catalytic properties and biocompatibility). The thesis consists of five chapters including this introductory chapter. The chapterwise description of the remaining thesis will now be outlined.

1.7 Brief outline of the thesis

The key concepts in nanoscience and a literature survey of properties, applications, synthesis protocols and assembly methods of metal nanoparticles have been discussed in the previous sections. These constitute the **First Chapter.**

The **Second Chapter** discloses the synthesis of monodisperse, magnetic metal nanoparticles. The chapter begins with the elucidation of the novel protocol developed by us to synthesize nickel and cobalt nanoparticles. The protocol is a simple wet chemical method involving reduction of metal salt by sodium borohydride in the presence of sodium dodecyl sulfate and oleic acid. Further, the spontaneous assembly formation of the nanoparticles has been illustrated in the chapter. The studies done towards obtaining optimum conditions for the stability, monodispersity and

crystallanity of the nanoparticles form an integral part of the chapter.

The **Third Chapter** deals with the synthesis and assembly formation of alkanethiol coated gold nanoparticles. The synthesis has been done by digestive ripening method. The first part of the chapter discusses the study of the melting properties and formation of superlattices of dodecanethiol coated gold nanoparticles. We have investigated the role of excess thiol in the superlattice formation by using experimental techniques like Differential Scanning caloriemetry and Thermogravimetric analysis.

The second part of this chapter discusses the formation of linear assemblies of hexadecanethiol coated gold nanoparticles. Initial demonstration of the assemblies through TEM images is followed by the description of experiments to probe the mechanism of their formation. We have proposed a hypothesis based on these experiments and then tried to validate it using different experimental techniques.

In the **Fourth Chapter**, the preparation of photoresponsive assembly of gold nanoparticles is described. The photoisomerization of azobenzene moiety has been exploited to obtain the photoresponsive networks. The molecule bearing an azobenzene moiety was extended on either side by linking it to molecules having affinity for gold nanoparticles. These molecules were incubated with gold nanoparticles coated by different kinds alkyl amine molecules. This results in gold nanoparticle-azobenzene (with linker molecule)-gold nanoparticle network. As azobenzene is known to demonstrate photoisomerization, this resultant network shows photoswitching behavior when subjected to irradiation with electromagnetic radiation (ultraviolet and visible). This photoswitching behaviour was monitored using UV-vis absorbance spectrophotometer and TEM. The UV-vis spectra show a shift in the position of surface plasmon resonance peak of gold nanoparticles which is attributed to the change in the interparticle spacings as a result of the formation of the photoresponsive assembly of gold nanoparticles. The TEM images obtained, after each step described above, have been in accordance with the observations of UV-vis spectra.

The **Fifth Chapter** summarizes the work described in this thesis by presenting the salient features of the work and also mentions the possible avenues for future investigations.

1.8 References

(1)   Ball, P. *Made To Measure: New Materials for the 21st Century*; Princeton University Press, New Jersey, 1997.

(2)   Heath, J. R. *Acc. Chem. Res.* **1999**, *32*, 388.

(3)   Klabunde, K. J. *Nanoscale materials in chemistry*; Wiley-Interscience: New York, 2001.

(4)   Schmid, G. *Nanoparticles: From Theory to Applications*; Wiley-VCH Weinheim, 2004.

(5)   Roduner, E. *Chem. Soc. Rev.* **2006**, *35*, 583.

(6)   Heath, J. R. *Science* **1995**, *270*, 1315.

(7)   Balzani, V. *Small* **2005**, *1*, 278.

(8)   Liz-Marzan, L. M. *Mater. Today* **2004**, *7*, 26.

(9)   Sato, O.; Kubo, S.; Gu, Z. Z. *Acc. Chem. Res.* **2009**, *42*, 1.

(10)   Goodsell, D. S. *Nano Today* **2006**, *1*, 44.

(11)   Xu, A. W.; Ma, Y. R.; Colfen, H. *J. Mater. Chem.* **2007**, *17*, 415.

(12)   Xia, F.; Jiang, L. *Adv. Mater.* **2008**, *20*, 2842.

(13)   Srinivasarao, M. *Chem. Rev.* **1999**, *99*, 1935.

(14)   Crookes-Goodson, W. J.; Slocik, J. M.; Naik, R. R. *Chem. Soc. Rev.* **2008**, *37*, 2403.

(15)   Faivre, D.; Schuler, D. *Chem. Rev.* **2008**, *108*, 4875.

(16)   Whitesides, G. M. *Nat. Biotechnol.* **2003**, *21*, 1161.

(17)   *Nanobiotechnology: Concepts, applications and Perspectives*; Wiley-VCH, Weinheim, 2004.

(18)   Goodsell, D. S. *Bionanotechnology: Lessons from nature*; Wiley-Liss, Hoboken, New Jersy, 2004.

(19)   Nel, A. E.; Madler, L.; Velegol, D.; Xia, T.; Hoek, E. M. V.; Somasundaran, P.; Klaessig, F.; Castranova, V.; Thompson, M. *Nat. Mater.* **2009**, *8*, 543.

(20)   Mann, S. *Angew. Chem. Int. Ed.* **2008**, *47*, 5306.

(21)   Dickerson, M. B.; Sandhage, K. H.; Naik, R. R. *Chem. Rev.* **2008**, *108*, 4935.

(22)   Mandal, S.; Phadtare, S.; Sastry, M. *Curr. Appl. Phys.* **2005**, *5*, 118.

(23)   Gerber, C.; Lang, H. P. *Nat. Nanotechnol.* **2006**, *1*, 3.

(24)   Fagaly, R. L. *Rev. Sci. Instrum.* **2006**, *77*, 101101.

(25)   Rasmussen, A.; Deckert, V. *Anal. Bioanal.Chem.* **2005**, *381*, 165.

(26)   Thomas, J. M.; Midgley, P. A. *Chem. Commun.* **2004**, 1253.

(27)   Lang, H. P.; Gerber, C. *Mater. Today* **2009**, *12*, 18.

(28)   Eigler, D. M.; Schweizer, E. K. *Nature* **1990**, *344*, 524.

(29)   Daniel, M. C.; Astruc, D. *Chem. Rev.* **2004**, *104*, 293.

(30)   Wagner, F. E.; Haslbeck, S.; Stievano, L.; Calogero, S.; Pankhurst, Q. A.; Martinek, P. *Nature* **2000**, *407*, 691.

(31)   Brown, D. H.; Smith, W. E. *Chem. Soc. Rev.* **1980**, *9*, 217.

(32)   Faraday, M. *Philos. Trans.* **1857**, *147*, 145.

(33)   Edwards, P. P.; Thomas, J. M. *Angew. Chem. Int. Ed.* **2007**, *46*, 5480.

(34)   Graham, T. *Philos. Trans. R. Soc.* **1861**, *151*, 183.

(35)   Zsigmondy, R.; Alexander, J. *Colloids and the Ultramicroscope: A Manual of Colloid Chemistry and Ultramicroscopy*; John Wiley & Sons, New York, 1914.

(36)   Ruska, E. *Angew. Chem. Int. Ed.* **1987**, *26*, 595.

(37)   Feynman, R. P. *Eng. Sci.* **1960**, *23*, 22.

(38)   Taniguchi, N. *Proceedings of the international conference on production engineering. Tokyo, Part II, Japan Society of Precision Engineering: Tokyo: JSPE* **1974**, 18.

(39)   Binnig, G.; Rohrer, H. *Rev. Mod. Phys.* **1987**, *59*, 615.

(40)   Binnig, G.; Quate, C. F.; Gerber, C. *Phys. Rev. Lett.* **1986**, *56*, 930.

(41)   Alivisatos, A. P. *ACS Nano* **2008**, *2*, 1514.

(42)   Kroto, H. W.; Heath, J. R.; O'Brien, S. C.; Curl, R. F.; Smalley, R. E. *Nature* **1985**, *318*, 162.

(43)   Iijima, S. *Nature* **1991**, *354*, 56.

(44)   Geim, A. K.; Novoselov, K. S. *Nat. Mater.* **2007**, *6*, 183.

(45)   Geim, A. K. *Science* **2009**, *324*, 1530.

(46)   Terrones, M. *Annu. Rev. Mater. Res.* **2003**, *33*, 419.

(47)   Biju, V.; Itoh, T.; Anas, A.; Sujith, A.; Ishikawa, M. *Anal. Bioanal.Chem.* **2008**, *391*, 2469.

(48)   Chen, X.; Mao, S. S. *Chem. Rev.* **2007**, *107*, 2891.

(49)   Wang, Z. L. *J. Phys. Condens. Matter* **2004**, *16*, R829.

(50)   Rao, C. N. R.; Kulkarni, G. U.; Thomas, P. J. *Nanocrystals Synthesis, Properties and Applications*; Springer-Verlag Berlin Heidelberg 2007.

(51)   Zhang, J. Z. *Acc. Chem. Res.* **1997**, *30*, 423.

(52)   Halperin, W. P. *Rev. Mod. Phys.* **1986**, *58*, 533.

(53)   Simon, U. *Adv. Mater.* **1998**, *10*, 1487.

(54)   Johnson, P. B.; Christy, R. W. *Phys. Rev. B* **1972**, *6*, 4370.

(55)   Creighton, J. A.; Eadon, D. G. *J. Chem. Soc., Faraday Trans.* **1991**, *87*, 3881.

(56)   Henglein, A. *Chem. Rev.* **1989**, *89*, 1861.

(57)   Xia, Y.; Halas, N. J. *MRS Bulletin* **2005**, *30*, 338.

(58)   El-Sayed, M. A. *Acc. Chem. Res.* **2001**, *34*, 257.

(59)   Ghosh, S. K.; Pal, T. *Chem. Rev.* **2007**, *107*, 4797.

(60)   Storhoff, J. J.; Lazarides, A. A.; Mucic, R. C.; Mirkin, C. A.; Letsinger, R. L.; Schatz, G. C. *J. Am. Chem. Soc.* **2000**, *122*, 4640.

(61)   Moores, A.; Goettmann, F. *New J. Chem.* **2006**, *30*, 1121.

(62)   Su, K. H.; Wei, Q. H.; Zhang, X.; Mock, J. J.; Smith, D. R.; Schultz, S. *Nano Lett.* **2003**, *3*, 1087.

(63)   Miller, M. M.; Lazarides, A. A. *J. Phys. Chem. B* **2005**, *109*, 21556.

(64)   Liz-Marzán, L. M. *Langmuir* **2006**, *22*, 32.

(65)   Underwood, S.; Mulvaney, P. *Langmuir* **1994**, *10*, 3427.

(66)   Zhong, Z. Y.; Patskovskyy, S.; Bouvrette, P.; Luong, J. H. T.; Gedanken, A. *J. Phys. Chem. B* **2004**, *108*, 4046.

(67)   Lu, X. M.; Rycenga, M.; Skrabalak, S. E.; Wiley, B.; Xia, Y. N. *Ann. Rev. Phys. Chem.* **2009**, *60*, 167.

(68)   Sendroiu, I. E.; Mertens, S. F. L.; Schiffrin, D. J. *PCCP* **2006**, *8*, 1430.

(69)   Schmid, G.; Corain, B. *Eur. J. Inorg. Chem.* **2003**, 3081.

(70)   Buffat, P.; Borel, J. P. *Phys. Rev. A* **1976**, *13*, 2287.

(71)   Jeong, U.; Teng, X.; Wang, Y.; Yang, H.; Xia, Y. *Adv. Mater.* **2007**, *19*, 33.

(72)   Tartaj, P. *Eur. J. Inorg. Chem.* **2009**, 333.

(73)   Darling, S. B.; Bader, S. D. *J. Mater. Chem.* **2005**, *15*, 4189.

(74)   Jun, Y. W.; Seo, J. W.; Cheon, A. *Acc. Chem. Res.* **2008**, *41*, 179.

(75)   Krishnan, K. M.; Pakhomov, A. B.; Bao, Y.; Blomqvist, P.; Chun, Y.; Gonzales, M.; Griffin, K.; Ji, X.; Roberts, B. K. *J. Mater. Sci.* **2006**, *41*, 793.

(76)   Bean, C. P.; Livingston, J. D. *J. Appl. Phys.* **1959**, *30*, S120.

(77)   LesliePelecky, D. L.; Rieke, R. D. *Chem. Mater.* **1996**, *8*, 1770.

(78)   Ozin, G. A.; Cademartiri, L. *Small* **2009**, *5*, 1240.

(79)   Narayanan, R.; El-Sayed, M. A. *Nano Lett.* **2004**, *4*, 1343.

(80)   Astruc, D.; Lu, F.; Aranzaes, J. R. *Angew. Chem. Int. Ed.* **2005**, *44*, 7852.

(81)   Haruta, M.; Kobayashi, T.; Sano, H.; Yamada, N. *Chem. Lett.* **1987**, 405.

(82)   Lewis, L. N. *Chem. Rev.* **1993**, *93*, 2693.

(83)   Bukhtiyarov, V. I.; Slin'ko, M. G. *Russ. Chem. Rev.* **2001**, *70*, 147.

(84)   Roucoux, A.; Schulz, J.; Patin, H. *Chem. Rev.* **2002**, *102*, 3757.

(85)   Somorjai, G. A.; Contreras, A. M.; Montano, M.; Rioux, R. M. *Proc. Natl. Acad. Sci. USA* **2006**, *103*, 10577.

(86)   Hashmi, A. S. K.; Rudolph, M. *Chem. Soc. Rev.* **2008**, *37*, 1766.

(87)   Fierro-Gonzalez, J. C.; Gates, B. C. *Chem. Soc. Rev.* **2008**, *37*, 2127.

(88)   Yeung, L. K.; Crooks, R. M. *Nano Lett.* **2000**, *1*, 14.

(89)   Li, Y.; Petroski, J.; El-Sayed, M. A. *The J. Phys. Chem. B* **2000**, *104*, 10956.

(90)   Ohde, H.; Wai, C. M.; Kim, H.; Kim, J.; Ohde, M. *J. Am. Chem. Soc.* **2002**, *124*, 4540.

(91)   Spiro, M.; de Jesus, D. M. *Langmuir* **2000**, *16*, 2464.

(92)   Haruta, A. *Chem. Rec.* **2003**, *3*, 75.

(93)   Haruta, M. *Cata.Today* **1997**, *36*, 153.

(94)   Haruta, M. *Gold Bulletin* **2001**, *34*, 40.

(95)   Haruta, M. *Gold Bulletin* **2004**, *37*, 27.

(96)   Haruta, M. *Nature* **2005**, *437*, 1098.

(97)   Haruta, M. *ChemPhysChem* **2007**, *8*, 1911.

(98)   Haruta, M.; Date, M. *Appl. Cata., A: General* **2001**, *222*, 427.

(99)   Haruta, M.; Souma, Y. *Cata.Today* **1997**, *36*, 1.

(100)   Narayanan, R.; El-Sayed, M. A. *J. Phys. Chem. B***2005**, *109*, 12663.

(101)   Moreno-Manas, M.; Pleixats, R. *Acc. Chem. Res.* **2003**, *36*, 638.

(102)   Kumar, A.; Kumar, S.; Saxena, A.; De, A.; Mozumdar, S. *Cata. Commun.* **2008**, *9*, 778.

(103)   Park, J.; Kang, E.; Son, S. U.; Park, H. M.; Lee, M. K.; Kim, J.; Kim, K. W.; Noh, H. J.; Park, J. H.; Bae, C. J.; Park, J. G.; Hyeon, T. *Adv. Mater.* **2005**, *17*, 429.

(104)   Son, S. U.; Lee, S. I.; Chung, Y. K.; Kim, S. W.; Hyeon, T. *Org. Lett.* **2002**, *4*, 277.

(105)   Saxena, A.; Kumar, A.; Mozumdar, S. *Appl. Cata., A-General* **2007**, *317*, 210.

(106)   Saxena, A.; Kumar, A.; Mozumdar, S. *J. Mol. Cata. A-Chemical* **2007**, *269*, 35.

(107)   Kidwai, M.; Bansal, V.; Saxena, A.; Shankar, R.; Mozumdar, S. *Tetrahedron*

Lett. **2006**, *47*, 4161.

(108) Son, S. U.; Jang, Y.; Park, J.; Na, H. B.; Park, H. M.; Yun, H. J.; Lee, J.; Hyeon, T. *J. Am. Chem. Soc.* **2004**, *126*, 5026.

(109) Pachon, L. D.; Rothenberg, G. *Appl. Organometal. Chem.* **2008**, *22*, 288.

(110) Moshfegh, A. Z. *J. Phys. D: Appl. Phys.* **2009**, *42*, 233001.

(111) Tansil, N. C.; Gao, Z. Q. *Nano Today* **2006**, *1*, 28.

(112) De, M.; Ghosh, P. S.; Rotello, V. M. *Adv. Mater.* **2008**, *20*, 4225.

(113) Niemeyer, C. M. *Angew. Chem. Int. Ed.* **2001**, *40*, 4128.

(114) Salata, O. V. *J. Nanobiotechnol.* **2004**, *2*.

(115) Hu, M.; Chen, J.; Li, Z. Y.; Au, L.; Hartland, G. V.; Li, X.; Marquez, M.; Xia, Y. *Chem. Soc. Rev.* **2006**, *35*, 1084.

(116) Gooding, J. J. *Small* **2006**, *2*, 313.

(117) Jun, Y. W.; Choi, J. S.; Cheon, J. *Chem. Commun.* **2007**, 1203.

(118) Gu, H. W.; Xu, K. M.; Xu, C. J.; Xu, B. *Chem. Commun.* **2006**, 941.

(119) Jin, R. C. *Angew. Chem. Int. Ed.* **2008**, *47*, 6750.

(120) Perez, J. M.; Simeone, F. J.; Saeki, Y.; Josephson, L.; Weissleder, R. *J. Am. Chem. Soc.* **2003**, *125*, 10192.

(121) Wilson, R. *Chem. Soc. Rev.* **2008**, *37*, 2028.

(122) Elghanian, R.; Storhoff, J. J.; Mucic, R. C.; Letsinger, R. L.; Mirkin, C. A. *Science* **1997**, *277*, 1078.

(123) Loweth, C. J.; Brett Caldwell, W.; Peng, X.; Alivisatos, A. P.; Schultz, P. G. *Angew. Chem. Int. Ed.* **1999**, *38*, 1808.

(124) Rosi, N. L.; Mirkin, C. A. *Chem. Rev.* **2005**, *105*, 1547.

(125) Baron, R.; Willner, B.; Willner, I. *Chem. Commun.* **2007**, 323.

(126) Shukla, R.; Bansal, V.; Chaudhary, M.; Basu, A.; Bhonde, R. R.; Sastry, M. *Langmuir* **2005**, *21*, 10644.

(127) Ghosh, P. S.; Kim, C. K.; Han, G.; Forbes, N. S.; Rotello, V. M. *ACS Nano* **2008**, *2*, 2213.

(128) Han, G.; Ghosh, P.; Rotello, V. M. *Nanomedicine* **2007**, *2*, 113.

(129) Joshi, H. M.; Bhumkar, D. R.; Joshi, K.; Pokharkar, V.; Sastry, M. *Langmuir* **2006**, *22*, 300.

(130) Latham, A. H.; Williams, M. E. *Acc. Chem. Res.* **2008**, *41*, 411.

(131) Aryal, S.; Grailer, J. J.; Pilla, S.; Steeber, D. A.; Gong, S. Q. *J. Mater. Chem.* **2009**, *19*, 7879.

(132) Hacliipanayis, C. G.; Bonder, M. J.; Balakrishanan, S.; Wang, X.; Mao, H.; Hadjipanayis, G. C. *Small* **2008**, *4*, 1925.

(133) Murphy, C. J.; Gole, A. M.; Stone, J. W.; Sisco, P. N.; Alkilany, A. M.; Goldsmith, E. C.; Baxter, S. C. *Acc. Chem. Res.* **2008**, *41*, 1721.

(134) Sperling, R. A.; Rivera Gil, P.; Zhang, F.; Zanella, M.; Parak, W. J. *Chem. Soc. Rev.* **2008**, *37*, 1896.

(135) Jain, P. K.; Huang, X.; El-Sayed, I. H.; El-Sayed, M. A. *Acc. Chem. Res.* **2008**, *41*, 1578.

(136) Tartaj, P.; Del Puerto Morales, M.; Veintemillas-Verdaguer, S.; Gonzaález-Carreño, T.; Serna, C. J. *J. Phys. D: Appl. Phys.* **2003**, *36*, R182.

(137) Pankhurst, Q. A.; Connolly, J.; Jones, S. K.; Dobson, J. *J. Phys. D: Appl. Phys.* **2003**, *36*, R167.

(138) Bouchard, L. S.; Anwar, M. S.; Liu, G. L.; Hann, B.; Xie, Z. H.; Gray, J. W.; Wang, X. D.; Pines, A.; Chen, F. F. *Proc. Natl. Acad. Sci. USA* **2009**, *106*, 4085.

(139) Sondi, I.; Salopek-Sondi, B. *J. Colloid Interface Sci.* **2004**, *275*, 177.

(140) Panacek, A.; Kvitek, L.; Prucek, R.; Kolar, M.; Vecerova, R.; Pizurova, N.; Sharma, V. K.; Nevecna, T.; Zboril, R. *J. Phys. Chem. B* **2006**, *110*, 16248.

(141) Wu, Q. Z.; Cao, H. Q.; Luan, Q. Y.; Zhang, J. Y.; Wang, Z.; Warner, J. H.; Watt, A. A. R. *Inorg. Chem.* **2008**, *47*, 5882.

(142) Kim, Y.; Johnson, R. C.; Hupp, J. T. *Nano Lett.* **2001**, *1*, 165.

(143) Huang, C. C.; Yang, Z.; Lee, K. H.; Chang, H. T. *Angew. Chem. Int. Ed.* **2007**, *46*, 6824.

(144) Raguse, B.; Chow, E.; Barton, C. S.; Wieczorek, L. *Anal. Chem.* **2007**, *79*, 7333.

(145) Ahn, H.; Chandekar, A.; Kang, B.; Sung, C.; Whitten, J. E. *Chem. Mater.* **2004**, *16*, 3274.

(146) Obare, S. O.; Hollowell, R. E.; Murphy, C. J. *Langmuir* **2002**, *18*, 10407.

(147) Slocik, J. M.; Zabinski Jr, J. S.; Phillips, D. M.; Naik, R. R. *Small* **2008**, *4*, 548.

(148) Briglin, S. M.; Gao, T.; Lewis, N. S. *Langmuir* **2004**, *20*, 299.

(149) Franke, M. E.; Koplin, T. J.; Simon, U. *Small* **2006**, *2*, 36.

(150) Guo, S.; Wang, E.   **2007**, *598*, 181.

(151) Peng, G.; Tisch, U.; Adams, O.; Hakim, M.; Shehada, N.; Broza, Y. Y.;

Billan, S.; Abdah-Bortnyak, R.; Kuten, A.; Haick, H. *Nat. Nanotechnol.* **2009**, *4*, 669.

(152)   Talapin, D. V.; Lee, J.-S.; Kovalenko, M. V.; Shevchenko, E. V. *Chem. Rev.* **2009**, DOI: 10.1021/cr900137k.

(153)   Schwartzberg, A. M.; Zhang, J. Z. *J. Phys. Chem. C* **2008**, *112*, 10323.

(154)   Murphy, C. J.; Sau, T. K.; Gole, A. M.; Orendorff, C. J.; Gao, J.; Gou, L.; Hunyadi, S. E.; Li, T. *J. Phys. Chem. B* **2005**, *109*, 13857.

(155)   Banholzer, M. J.; Millstone, J. E.; Qin, L. D.; Mirkin, C. A. *Chem. Soc. Rev.* **2008**, *37*, 885.

(156)   Tian, Z. Q.; Yang, Z. L.; Ren, B.; Li, J. F.; Zhang, Y.; Lin, X. F.; Hu, J. W.; Wu, D. Y. *Faraday Discuss.* **2006**, *132*, 159.

(157)   Porter, M. D.; Lipert, R. J.; Siperko, L. M.; Wang, G.; Narayanan, R. *Chem. Soc. Rev.* **2008**, *37*, 1001.

(158)   Qian, X.; Peng, X. H.; Ansari, D. O.; Yin-Goen, Q.; Chen, G. Z.; Shin, D. M.; Yang, L.; Young, A. N.; Wang, M. D.; Nie, S. *Nat. Biotechnol.* **2008**, *26*, 83.

(159)   Doering, W. E.; Piotti, M. E.; Natan, M. J.; Freeman, R. G. *Adv. Mater.* **2007**, *19*, 3100.

(160)   Qian, X. M.; Nie, S. M. *Chem. Soc. Rev.* **2008**, *37*, 912.

(161)   Dieringer, J. A.; McFarland, A. D.; Shah, N. C.; Stuart, D. A.; Whitney, A. V.; Yonzon, C. R.; Young, M. A.; Zhang, X. Y.; Van Duyne, R. P. *Faraday Discuss.* **2006**, *132*, 9.

(162)   Tian, Z. Q.; Ren, B.; Wu, D. Y. *J. Phys. Chem. B* **2002**, *106*, 9463.

(163)   Kamat, P. V. *The J. Phys. Chem. B* **2002**, *106*, 7729.

(164)   Maier, S. A.; Brongersma, M. L.; Kik, P. G.; Meltzer, S.; Requicha, A. A. G.; Atwater, H. A. *Adv. Mater.* **2001**, *13*, 1501.

(165)   Maier, S. A.; Atwater, H. A. *J. Appl. Phys.* **2005**, *98*, 1.

(166)   Murray, W. A.; Barnes, W. L. *Adv. Mater.* **2007**, *19*, 3771.

(167)   Speliotis, D. E. *J. Magn. Magn. Mater.* **1999**, *193*, 29.

(168)   Weller, D.; Doerner, M. F. *Annu. Rev. Mater. Sci.* **2000**, *30*, 611.

(169)   *Nanoparticle Assemblies and Superstuctures* CRC Press, Taylor & Francis: Boca Raton, 2006.

(170)   Sun, S. *Adv. Mater.* **2006**, *18*, 393.

(171)   Reiss, G.; Hutten, A. *Nat. Mater.* **2005**, *4*, 725.

(172)   Chen, J.; Cheng, F. Y. *Acc. Chem. Res.* **2009**, *42*, 713.

(173)   Winter, M.; Brodd, R. J. *Chem. Rev.* **2004**, *104*, 4245.

(174)   Harris, A. T.; See, C. H.; Liu, J.; Dunens, O.; MacKenzie, K. *J. Nanosci. Nanotechnol.* **2008**, *8*, 2450.

(175)   Gschneidner Jr, A.; Pecharsky, V. K.; Tsokol, A. O. *Rep. Prog. Phys.* **2005**, *68*, 1479.

(176)   Barth, J. V.; Costantini, G.; Kern, K. *Nature* **2005**, *437*, 671.

(177)   Koch, C. C. *Rev. Adv. Mater. Sci.* **2003**, *5*, 91.

(178)   Munoz, J. E.; Cervantes, J.; Esparza, R.; Rosas, G. *J. Nanopart. Res.* **2007**, *9*, 945.

(179)   Wilcoxon, J. P.; Abrams, B. L. *Chem. Soc. Rev.* **2006**, *35*, 1162.

(180)   Lamer, V. K.; Dinegar, R. H. *J. Am. Chem. Soc.* **1950**, *72*, 4847.

(181)   Prasad, B. L. V.; Stoeva, S. I.; Sorensen, C. M.; Klabunde, K. J. *Langmuir* **2002**, *18*, 7515.

(182)   Leff, D. V.; Brandt, L.; Heath, J. R. *Langmuir* **1996**, *12*, 4723.

(183)   Weare, W. W.; Reed, S. M.; Warner, M. G.; Hutchison, J. E. *J. Am. Chem. Soc.* **2000**, *122*, 12890.

(184)   Selvakannan, P. R.; Mandal, S.; Phadtare, S.; Gole, A.; Pasricha, R.; Adyanthaya, S. D.; Sastry, M. *J. Colloid Interface Sci.* **2004**, *269*, 97.

(185)   Joshi, H.; Shirude, P. S.; Bansal, V.; Ganesh, K. N.; Sastry, M. *J. Phys. Chem. B* **2004**, *108*, 11535.

(186)   Levy, R. *ChemBioChem* **2006**, *7*, 1141.

(187)   Shan, J.; Tenhu, H. *Chem. Commun.* **2007**, 4580.

(188)   Masala, O.; Seshadri, R. *Annu. Rev. Mater. Res.* **2004**, *34*, 41.

(189)   Swihart, M. T. *Curr. Opinion Colloid Interface Sci.* **2003**, *8*, 127.

(190)   Wang, J.; Huang, H.; Kesapragada, S. V.; Gall, D. *Nano Lett.* **2005**, *5*, 2505.

(191)   Park, S.; Lim, S.; Choi, H. *Chem. Mater.* **2006**, *18*, 5150.

(192)   Kanai, H.; Tan, B. J.; Klabunde, K. J. *Langmuir* **1986**, *2*, 760.

(193)   Stoeva, S.; Klabunde, K. J.; Sorensen, C. M.; Dragieva, I. *J. Am. Chem. Soc.* **2002**, *124*, 2305.

(194)   Stoeva, S. I.; Prasad, B. L. V.; Uma, S.; Stoimenov, P. K.; Zaikovski, V.; Sorensen, C. M.; Klabunde, K. J. *J. Phys. Chem. B* **2003**, *107*, 7441.

(195)   Kalidindi, S. B.; Jagirdar, B. R. *Inorg. Chem.* **2009**, *48*, 4524.

(196)   Baker, C.; Pradhan, A.; Pakstis, L.; Pochan, D. J.; Shah, S. I. *J. Nanosci. Nanotechnol.* **2005**, *5*, 244.

(197)   Qiu, J.; Li, Y.; Wang, Y.; Zhao, Z.; Zhou, Y. *Fuel* **2004**, *83*, 615.

(198)   Mafune, F.; Kohno, J.; Takeda, Y.; Kondow, T.; Sawabe, H. *J. Phys. Chem. B* **2000**, *104*, 9111.

(199)   Mafune, F.; Kohno, J.; Takeda, Y.; Kondow, T.; Sawabe, H. *J. Phys. Chem. B* **2001**, *105*, 5114.

(200)   Mafune, F.; Kohno, J. Y.; Takeda, Y.; Kondow, T. *J. Phys. Chem. B* **2002**, *106*, 7575.

(201)   Mafune, F.; Kohno, J. Y.; Takeda, Y.; Kondow, T. *J. Phys. Chem. B* **2003**, *107*, 4218.

(202)   Amendola, V.; Meneghetti, M. *PCCP* **2009**, *11*, 3805.

(203)   Cushing, B. L.; Kolesnichenko, V. L.; O'Connor, C. J. *Chem. Rev.* **2004**, *104*, 3893.

(204)   Turkevich, J.; Stevenson, P. C.; Hillier, J. *Discuss. Faraday Soc.* **1951**, *11*, 55.

(205)   Kimling, J.; Maier, M.; Okenve, B.; Kotaidis, V.; Ballot, H.; Plech, A. *J. Phys. Chem. B* **2006**, *110*, 15700.

(206)   Brust, M.; Walker, M.; Bethell, D.; Schiffrin, D. J.; Whyman, R. *J. Chem. Soc., Chem. Commun.* **1994**, 801.

(207)   Allara, D. L.; Nuzzo, R. G. *Langmuir* **1985**, *1*, 45.

(208)   Hostetler, M. J.; Templeton, A. C.; Murray, R. W. *Langmuir* **1999**, *15*, 3782.

(209)   Kumar, A.; Mandal, S.; Selvakannan, P. R.; Pasricha, R.; Mandale, A. B.; Sastry, M. *Langmuir* **2003**, *19*, 6277.

(210)   Sastry, M.; Kumar, A.; Mukherjee, P. *Colloids Surf., A* **2001**, *181*, 255.

(211)   Sastry, M. *Curr. Sci.* **2003**, *85*, 1735.

(212)   Kumar, A.; Joshi, H. M.; Mandale, A. B.; Srivastava, R.; Adyanthaya, S. D.; Pasricha, R.; Sastry, M. *J. Chem. Sci.* **2004**, *116*, 293.

(213)   Kumar, A.; Joshi, H.; Pasricha, R.; Mandale, A. B.; Sastry, M. *J. Colloid Interface Sci.* **2003**, *264*, 396.

(214)   Couto, G. G.; Klein, J. J.; Schreiner, W. H.; Mosca, D. H.; de Oliveira, A. J. A.; Zarbin, A. J. G. *J. Colloid Interface Sci.* **2007**, *311*, 461.

(215)   Yee, C.; Scotti, M.; Ulman, A.; White, H.; Rafailovich, M.; Sokolov, J. *Langmuir* **1999**, *15*, 4314.

(216)   Pietrobon, B.; Kitaev, V. *Chem. Mater.* **2008**, *20*, 5186.

(217)   Li, H. X.; Lin, M. Z.; Hou, J. G. *J. Cryst. Growth* **2000**, *212*, 222.

(218)   Henglein, A.; Meisel, D. *Langmuir* **1998**, *14*, 7392.

(219)   Gachard, E.; Remita, H.; Khatouri, J.; Keita, B.; Nadjo, L.; Belloni, J. *New J. Chem.* **1998**, *22*, 1257.

(220)   Henglein, A. *Langmuir* **2001**, *17*, 2329.

(221)   Dimitrijevic, N. M.; Bartels, D. M.; Jonah, C. D.; Takahashi, K.; Rajh, T. *J. Phys. Chem. B* **2001**, *105*, 954.

(222)   Henglein, A.; Giersig, M. *J. Phys. Chem. B* **1999**, *103*, 9533.

(223)   Hu, X. G.; Dong, S. J. *J. Mater. Chem.* **2008**, *18*, 1279.

(224)   Huang, S.; Ma, H.; Zhang, X.; Yong, F.; Feng, X.; Pan, W.; Wang, X.; Wang, Y.; Chen, S. *J. Phys. Chem. B* **2005**, *109*, 19823.

(225)   Suslick, K. S.; Fang, M.; Hyeon, T. *J. Am. Chem. Soc.* **1996**, *118*, 11960.

(226)   Chen, W.; Cai, W. P.; Lei, Y.; Zhang, L. D. *Mater. Lett.* **2001**, *50*, 53.

(227)   Fujimoto, T.; Terauchi, S.; Umehara, H.; Kojima, I.; Henderson, W. *Chem. Mater.* **2001**, *13*, 1057.

(228)   Nemamcha, A.; Rehspringer, J. L.; Khatmi, D. *J. Phys. Chem. B* **2006**, *110*, 383.

(229)   Suslick, K. S.; Price, G. J. *Annu. Rev. Mater. Sci.* **1999**, *29*, 295.

(230)   Okitsu, K.; Yue, A.; Tanabe, S.; Matsumoto, H.; Yobiko, Y. *Langmuir* **2007**, *23*, 13244.

(231)   Gedanken, A. *Curr. Sci.* **2003**, *85*, 1720.

(232)   Gedanken, A. *Ultrason. Sonochem.* **2004**, *11*, 47.

(233)   Dinega, D. P.; Bawendi, M. G. *Angew. Chem. Int. Ed.* **1999**, *38*, 1788.

(234)   Sun, S.; Murray, C. B.; Weller, D.; Folks, L.; Moser, A. *Science* **2000**, *287*, 1989.

(235)   Hyeon, T. *Chem. Commun.* **2003**, *9*, 927.

(236)   Xu, C.; Sun, S. *Polym. Int.* **2007**, *56*, 821.

(237)   Lagunas, A.; Jimeno, C.; Font, D.; Sola, L.; Pericas, M. A. *Langmuir* **2006**, *22*, 3823.

(238)   Pileni, M. P. *J. Phys. Chem.* **1993**, *97*, 6961.

(239)   Petit, C.; Taleb, A.; Pileni, M. P. *Adv. Mater.* **1998**, *10*, 259.

(240)   Lisiecki, I. *J. Phys. Chem. B* **2005**, *109*, 12231.

(241)   Lin, X. M.; Sorensen, C. M.; Klabunde, K. J. *J. Nanopart. Res.* **2000**, *2*, 157.

(242)   Prasad, B. L. V.; Stoeva, S. I.; Sorensen, C. M.; Klabunde, K. J. *Chem. Mater.* **2003**, *15*, 935.

(243)   Swami, A.; Kumar, A.; Pasricha, R.; Mandale, A. B.; Sastry, M. *J. Colloid*

Interface Sci. **2004**, *271*, 381.

(244)   Ahmad, A.; Senapati, S.; Khan, M. I.; Kumar, R.; Sastry, M. *Langmuir* **2003**, *19*, 3550.

(245)   Mukherjee, P.; Ahmad, A.; Mandal, D.; Senapati, S.; Sainkar, S. R.; Khan, M. I.; Parishcha, R.; Ajaykumar, P. V.; Alam, M.; Kumar, R.; Sastry, M. *Nano Lett.* **2001**, *1*, 515.

(246)   Mukherjee, P.; Ahmad, A.; Mandal, D.; Senapati, S.; Sainkar, S. R.; Khan, M. I.;Ramani, R.; Parischa, R.; Ajayakumar, P. V.; Alam, M.; Sastry, M.; Kumar, R. *Angew. Chem. Int. Ed.* **2001**, *40*, 3585.

(247)   Mukherjee, P.; Senapati, S.; Mandal, D.; Ahmad, A.; Khan, M. I.; Kumar, R.; Sastry, M. *ChemBioChem* **2002**, *3*, 461.

(248)   Chandran, S. P.; Chaudhary, M.; Pasricha, R.; Ahmad, A.; Sastry, M. *Biotechnol. Progr.* **2006**, *22*, 577.

(249)   Shankar, S. S.; Ahmad, A.; Pasricha, R.; Sastry, M. *J. Mater. Chem.* **2003**, *13*, 1822.

(250)   Shankar, S. S.; Rai, A.; Ahmad, A.; Sastry, M. *J. Colloid Interface Sci.* **2004**, *275*, 496.

(251)   Shankar, S. S.; Rai, A.; Ankamwar, B.; Singh, A.; Ahmad, A.; Sastry, M. *Nat. Mater.* **2004**, *3*, 482.

(252)   Min, Y.; Akbulut, M.; Kristiansen, K.; Golan, Y.; Israelachvili, J. *Nat. Mater.* **2008**, *7*, 527.

(253)   Bishop, K. J. M.; Wilmer, C. E.; Soh, S.; Grzybowski, B. A. *Small* **2009**, *5*, 1600.

(254)   Zhang, H.; Edwards, E. W.; Wang, D. Y.; Möhwald, H. *PCCP* **2006**, *8*, 3288.

(255)   Hamley, I. W. *Angew. Chem. Int. Ed.* **2003**, *42*, 1692.

(256)   Gomar-Nadal, E.; Puigmartí-Luis, J.; Amabilino, D. B. *Chem. Soc. Rev.* **2008**, *37*, 490.

(257)   Mann, S.; Shenton, W.; Li, M.; Connolly, S.; Fitzmaurice, D. *Adv. Mater.* **2000**, *12*, 147.

(258)   Berry, V.; Saraf, R. F. *Angew. Chem. Int. Ed.* **2005**, *44*, 6668.

(259)   Velev, O. D.; Gupta, S. *Adv. Mater.* **2009**, *21*, 1897.

(260)   Puntes, V. F.; Zanchet, D.; Erdonmez, C. K.; Alivisatos, A. P. *J. Am. Chem. Soc.* **2002**, *124*, 12874.

(261)   Brinker, C. J.; Lu, Y.; Sellinger, A.; Fan, H. *Adv. Mater.* **1999**, *11*, 579.

(262)   Kiely, C. J.; Fink, J.; Brust, M.; Bethell, D.; Schiffrin, D. J. *Nature* **1998**, *396*, 444.

(263)   Fan, H.; Leve, E.; Gabaldon, J.; Wright, A.; Haddad, R. E.; Brinker, C. J. *Adv. Mater.* **2005**, *17*, 2587.

(264)   Stowell, C.; Korgel, B. A. *Nano Lett.* **2001**, *1*, 595.

(265)   Sigman, M. B.; Saunders, A. E.; Korgel, B. A. *Langmuir* **2004**, *20*, 978.

(266)   Ohara, P. C.; Gelbart, W. M. *Langmuir* **1998**, *14*, 3418.

(267)   Ohara, P. C.; Heath, J. R.; Gelbart, W. M. *Angew. Chem. Int. Ed.* **1997**, *36*, 1078.

(268)   Murray, C. B.; Sun, S.; Doyle, H.; Betley, T. *MRS Bulletin* **2001**, *26*, 985.

(269)   Martín, J. I.; Nogués, J.; Liu, K.; Vicent, J. L.; Schuller, I. K. *J. Magn. Magn. Mater.* **2003**, *256*, 449.

(270)   Murray, C. B.; Sun, S.; Gaschler, W.; Doyle, H.; Betley, T. A.; Kagan, C. R. *IBM J. Res. Develop.* **2001**, *45*, 47.

(271)   Murray, C. B.; Kagan, C. R.; Bawendi, M. G. *Annu. Rev. Mater. Sci.* **2000**, *30*, 545.

(272)   Sachan, M.; Walrath, N. D.; Majetich, S. A.; Krycka, K.; Kao, C.-C.; J. Appl. Phys. **2006**, *99*, 08C302.

(273)   Puntes, V. F.; Krishnan, K. M.; Alivisatos, P. *Appl. Phys. Lett.* **2001**, *78*, 2187.

(274)   Sun, S.; Murray, C. B. *J. Appl. Phys.* **1999**, *85*, 4325.

(275)   Puntes, V. F.; Krishnan, K. M.; Alivisatos, A. P. *Science* **2001**, *291*, 2115.

(276)   Tripp, S. L.; Dunin-Borkowski, R. E.; Wei, A. *Angew. Chem. Int. Ed.* **2003**, *42*, 5591.

(277)   Cheng, G. J.; Romero, D.; Fraser, G. T.; Walker, A. R. H. *Langmuir* **2005**, *21*, 12055.

(278)   Chitu, L.; Chushkin, Y.; Luby, S.; Majkova, E.; Leo, G.; Satka, A.; Giersig, M.; Hilgendorff, M. *Appl. Sur. Sci.* **2006**, *252*, 5559.

(279)   Park, J. I.; Jun, Y. W.; Choi, J. S.; Cheon, J. *Chem. Commun.* **2007**, 5001.

(280)   Bader, S. D. *Rev. Mod. Phys.* **2006**, *78*, 1.

(281)   Chitu, L.; Chushkin, Y.; Luby, S.; Majkova, E.; Satka, A.; Ivan, J.; Smrcok, L.;Buchal, A.; Giersig, M.; Hilgendorff, M. *Mater. Sci. Eng., C-Biomimetic and Supramolecular Systems* **2007**, *27*, 23.

(282)   Frey, N. A.; Peng, S.; Cheng, K.; Sun, S. H. *Chem. Soc. Rev.* **2009**, *38*, 2532.

(283)   Santhanam, V.; Andres, R. P. *Nano Lett.* **2004**, *4*, 41.

(284)   Santhanam, V.; Liu, J.; Agarwal, R.; Andres, R. P. *Langmuir* **2003**, *19*, 7881.

(285)   Xia, Y.; Whitesides, G. M. *Annu. Rev. Mater. Sci.* **1998**, *28*, 153.

(286)   Xia, Y.; Rogers, J. A.; Paul, K. E.; Whitesides, G. M. *Chem. Rev.* **1999**, *99*, 1823.

(287)   Mirkin, C. A. *Acs Nano* **2007**, *1*, 79.

(288)   Fischler, M.; Simon, U. *J. Mater. Chem.* **2009**, *19*, 1518.

(289)   Li, Z.; Chung, S. W.; Nam, J. M.; Ginger, D. S.; Mirkin, C. A. *Angew. Chem. Int. Ed.* **2003**, *42*, 2306.

(290)   Sotiropoulou, S.; Sierra-Sastre, Y.; Mark, S. S.; Batt, C. A. *Chem. Mater.* **2008**, *20*, 821.

(291)   Lazzari, M.; Rodrí-guez-Abreu, C.; Rivas, J.; Arturo López-Quintela, M. *J. Nanosci. Nanotechnol.* **2006**, *6*, 892.

(292)   Niemeyer, C. M.; Simon, U. *Eur. J. Inorg. Chem.* **2005**, 3641.

(293)   Mirkin, C. A.; Letsinger, R. L.; Mucic, R. C.; Storhoff, J. J. *Nature* **1996**, *382*, 607.

(294)   Alivisatos, A. P.; Johnsson, K. P.; Peng, X.; Wilson, T. E.; Loweth, C. J.; Bruchez Jr, M. P.; Schultz, P. G. *Nature* **1996**, *382*, 609.

(295)   Gourishankar, A.; Shukla, S.; Pasricha, R.; Sastry, M.; Ganesh, K. N. *Curr. Appl. Phys.* **2005**, *5*, 102.

(296)   Warner, M. G.; Hutchison, J. E. *Nat. Mater.* **2003**, *2*, 272.

(297)   Mirkin, C. A. *Inorg. Chem.* **2000**, *39*, 2258.

(298)   Schmid, G.; Simon, U. *Chem. Commun.* **2005**, 697.

(299)   Taton, T. A.; Mirkin, C. A.; Letsinger, R. L. *Science* **2000**, *289*, 1757.

(300)   Nykypanchuk, D.; Maye, M. M.; Van Der Lelie, D.; Gang, O. *Nature* **2008**, *451*, 549.

(301)   Park, S. Y.; Lytton-Jean, A. K. R.; Lee, B.; Weigand, S.; Schatz, G. C.; Mirkin, C. A. *Nature* **2008**, *451*, 553.

(302)   Lazarides, A. A.; Schatz, G. C. *J. Phys. Chem. B* **2000**, *104*, 460.

(303)   Giersig, M.; Mulvaney, P. *Langmuir* **1993**, *9*, 3408.

(304)   Tao, A. R.; Huang, J. X.; Yang, P. D. *Acc. Chem. Res.* **2008**, *41*, 1662.

(305)   Khomutov, G. B.; Koksharov, Y. A. *Adv. Colloid Interface Sci.* **2006**, *122*, 119.

(306)   Sastry, M.; Rao, M.; Ganesh, K. N. *Acc. Chem. Res.* **2002**, *35*, 847.

(307)   Blodgett, K. B. *J. Am. Chem. Soc.* **1935**, *57*, 1007.

(308) Blodgett, K. B. *J. Am. Chem. Soc.* **1934**, *56*, 495.

(309) Swami, A.; Kumar, A.; Selvakannan, P. R.; Mandal, S.; Sastry, M. *J. Colloid Interface Sci.* **2003**, *260*, 367.

(310) Selvakannan, P. R.; Swami, A.; Srisathiyanarayanan, D.; Shirude, P. S.; Pasricha, R.; Mandale, A. B.; Sastry, M. *Langmuir* **2004**, *20*, 7825.

(311) Kumar, A.; Mandal, S.; Mathew, S. P.; Selvakannan, P. R.; Mandale, A. B.; Chaudhari, R. V.; Sastry, M. *Langmuir* **2002**, *18*, 6478.

(312) Rao, C. N. R.; Kalyanikutty, K. P. *Acc. Chem. Res.* **2008**, *41*, 489.

(313) Nuzzo, R. G.; Allara, D. L. *J. Am. Chem. Soc.* **1983**, *105*, 4481.

(314) Bain, C. D.; Troughton, E. B.; Tao, Y. T.; Evall, J.; Whitesides, G. M.; Nuzzo, R. G. *J. Am. Chem. Soc.* **1989**, *111*, 321.

(315) Ulman, A. *Chem. Rev.* **1996**, *96*, 1533.

(316) Love, J. C.; Estroff, L. A.; Kriebel, J. K.; Nuzzo, R. G.; Whitesides, G. M. *Chem. Rev.* **2005**, *105*, 1103.

(317) Yao, H.; Minami, T.; Hori, A.; Koma, M.; Kimura, K. *J. Phys. Chem. B* **2006**, *110*, 14040.

(318) Yao, H.; Kojima, H.; Sato, S.; Kimura, K. *Langmuir* **2004**, *20*, 10317.

(319) Prins, L. J.; Reinhoudt, D. N.; Timmerman, P. *Angew. Chem. Int. Ed.* **2001**, *40*, 2382.

(320) Han, L.; Luo, J.; Kariuki, N. N.; Maye, M. M.; Jones, V. W.; Zhong, C. J. *Chem. Mater.* **2003**, *15*, 29.

Chapter II

Synthesis and Spontaneous Assembly of Transition Metal Nanoparticles
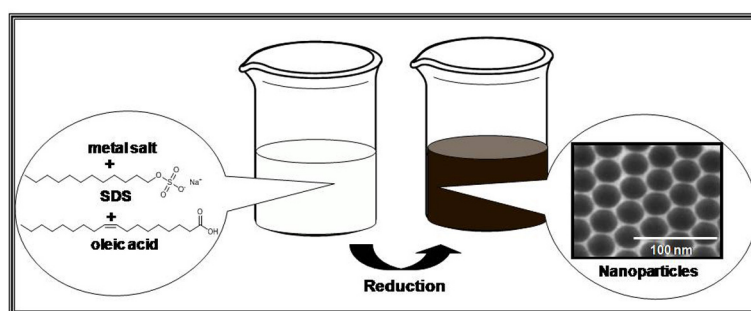
This chapter describes the formation of nearly monodisperse nanoparticles of nickel and cobalt. The chapter begins with the elucidation of the novel protocol developed to synthesize these nanoparticles. Further, the spontaneous assembly of the nanoparticles has been illustrated in the chapter. The studies done towards obtaining optimum conditions for the stability, monodispersity and crystallanity of the nanoparticles have been delineated.

2.1 Introduction

Magnetic nanoparticles of different kinds are being prepared owing to the bountiful applications they offer including ultra-high density data storage [1], magnetic seals [2], magnetic separation [3] etc. In addition to these, there are large number bio-medical applications such as diagnosis, therapeutics, drug delivery and imaging [4]. The prominent examples of magnetic nanoparticles are single metal nanoparticles like Co, Ni and Fe [5], metal oxides like γ-Fe_2O_3 [6], alloys like $CoPt_3$ and FePt containing one magnetic component [7], core-shell systems- with one or both magnetic components [8] and ferrites [9]. Among the magnetic nanoparticles, nickel and cobalt nanoparticles are significant because apart from their magnetic property based applications [10]; they have applications in other areas such as catalysis [11], synthesis of one dimensional nanostructures like nanotubes and nanowires [12] etc.

The main strategies for synthesis of magnetic nanoparticles involve the use of organometallic precursors. For metal nanoparticles, the reaction is based on decomposition of metal carbonyl or reduction of metal salt in the presence of bulky and weakly bound ligand like trioctylphosphine oxide (TOPO) which stabilizes the particles and plays a crucial role in determining their size [13]. Different groups have already reported the formation of Co and Ni nanoparticles at high temperature by such organometallic precursor based methods [14]. Some prominent reports for synthesis of nickel nanoparticles include the report by Hou *et al*. where nickel acetylacetonate [Ni(acac)$_2$] was reduced of by sodium borohydride or superhydride in the presence of hexadecylamine (HDA) and (TOPO) to give nickel nanoparticles of size 3 to 11 nm [15a]. Hyeon and co-workers prepared monodisperse nickel nanoparticles by thermal decomposition of a Ni–oleylamine complex in a hot phosphine solvent. These nanoparticles were seen to self-assemble to form long-range supperlattices [11b]. In a research account by Chaudret *et al.,* nickel nanoparticles of different shapes were synthesized in tetrahydrofuran (THF) by using nickel complex as a precursor and in the presence of hexadecylamine (HDA) or trioctylphosphineoxide (TOPO) where HDA was seen to act as a shape controlling agent [15b].

Cobalt nanoparticles with three different crystal structures can be prepared by organo-metallic methods. The phases are (i) hexagonal close packed (hcp) phase, (ii)

face-centered cubic (fcc) phase and (iii) metastable cubic ε phase. Murray *et al.* prepared hcp cobalt nanocrystals by the high-temperature reduction of cobalt acetate through a polyol process using 1,2-dodecanediol as both the reductant and the solvent in the presence of oleic acid and trioctylphosphine (TOP) [16a]. They also synthesized monodisperse fcc cobalt nanocrystals by thermal decomposition of dicobalt octacarbonyl in the presence of a surfactant mixture composed of oleic acid and tributylphosphine (TBP) at 200 °C followed by size-selective precipitation [16b]. The ε phase of cobalt was obtained by thermal decomposition of octacarbonyldicobalt in the presence of trioctylphosphane oxide (TOPO) as a coordinating ligand [16c]. It was also synthesized by the reduction of a cobalt salt with superhydride (LiBEt$_3$H), in the organic phase and in the presence of surfactants such as oleic acid and trioctylphosphine (TOP) [16d]. Even Alivisatos *et al.* obtained monodisperse ε-Co nanoparticles by rapid pyrolysis of dicobalt octacarbonyl [Co$_2$ (CO)$_8$] in the presence of a surfactant mixture composed of oleic acid, lauric acid and TOP [16e].

Other synthesis routes for cobalt and nickel nanoparticles involve the utilization of microemulsions/reverse micelles and soft templates. Klabunde's group synthesized cobalt nanoparticles by microemulsion / inverse micelle based method where cobalt salt was reduced by sodium borohydride [17]. Pileni and co-workers have developed a synthesis protocol by using reverse micelles as a micro reactor [18]. To synthesize cobalt nanoparticles using this protocol, micellar solutions containing sodium bis(2-ethylhexyl)sulfosuccinate [Na(AOT)] and (Co(AOT)$_2$) are made to react with sodium borohydride dissolved in a solution of Na[AOT]. Chen *et al.* have prepared nickel nanoparticles by reducing nickel chloride with hydrazine in an aqueous solution of cationic surfactants like cetyltrimethylammonium bromide (CTAB) [19]. To prepare Co nanoparticles with polyvinylpyrrolidone (PVP) as a soft template, Zhang *et al.* reduced cobalt chloride by anhydrous monohydrate (NH$_2$· NH$_2$) where ethylene glycol (EG) and PVP acted as solvent and stabilizer, respectively [20].

Synthesis of metal nanoparticles involving organometallic precursors can be cumbersome, as it may require very high temperatures. It is generally performed using volatile precursors, under inert atmosphere and may need a prolonged heating. However, in spite of such problems, these methods are popular because they usually lead to monodisperse nanoparticles which form uniform arrays [21]. Monodisperse

magnetic nanoparticles offer an advantage from the application point of view [22]. On the other hand, the reverse micelle or soft-template based methods are easier to handle but they often lead to polydisperse nanoparticles [23]. Hence, a synthesis protocol which is easier to handle and also leads to spontaneous organization of monodisperse nanoparticles is desirable.

In this context, development of a simple wet chemical process for synthesizing nearly monodisperse Ni and Co nanoparticles that self-assemble to form ordered structures has excellent potential for applications. The role of a capping agent is very crucial in synthesis of magnetic nanoparticles because the attractive magnetic interactions between nanoparticles can lead to aggregation and hence unstable solution. Oleic acid (octadec-9-ene-1-carboxylic acid) has been known as a strongly binding capping agent which prevents growth of the particles [13a]. Hence, after an initial report by Hyeon and co-workers [24], it has been used extensively during the synthesis of a range of magnetic nanoparticles [25], even in combination with other weakly binding ligands such as TOPO. Due to such advantages, oleic acid has been utilized in the present work as well. An anionic surfactant - sodium dodecyl sulfate (SDS) has also been used along with it.

This chapter describes synthesis of monodisperse nickel and cobalt nanoparticles that spontaneously form self-assembled close-packed structures. First, the protocol developed for the synthesis of cobalt and nickel nanoparticles has been elucidated. Then, experimental conditions required for the stability of nanoparticle solutions have been described. The spontaneous organization of nanoparticles has been illustrated using the TEM images. The particles are observed to become crystalline by heating. The structural changes in the sample before and after heating, characterized by TEM and powder XRD have been discussed. Similarly, magnetic properties of the samples have also been displayed. A mechanism for the formation of nanoparticles and their subsequent assembly has been proposed. Finally, the advantages offered by this synthesis protocol have been presented.

2.2 Synthesis and study of nickel nanoparticles and their spontaneous assembly

The experimental results are first described by taking nickel as a typical example. The results obtained for cobalt nanoparticles were similar to nickel and have been presented later in this chapter.

2.2.1 Synthesis protocol and stability optimization of nickel nanoparticles

Fig. 2.1 shows the scheme for the synthetic methodology developed as part of the present work for the synthesis of nanoparticles. As shown in the scheme, aqueous nickel ions were reduced in the presence of two surfactants- SDS and oleic acid to produce the nickel nanoparticles.
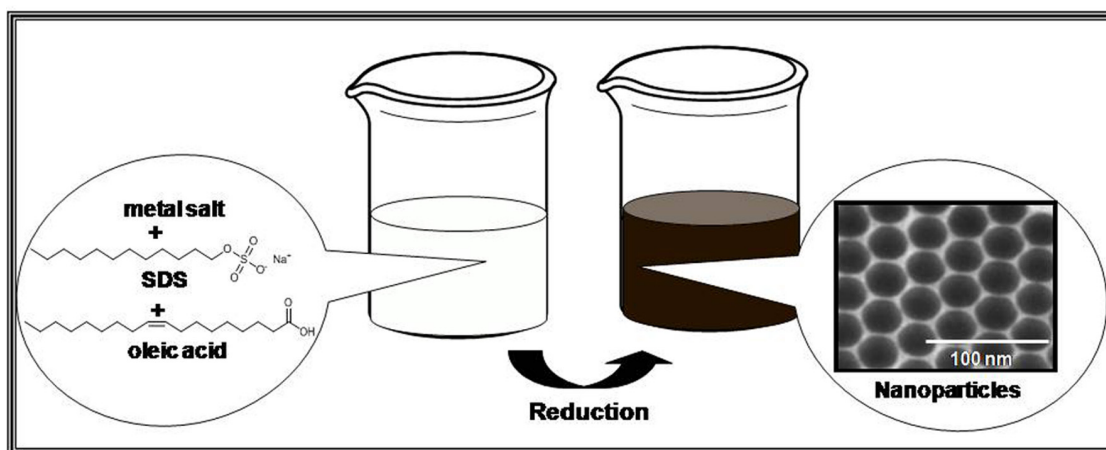

Figure 2.1 *The scheme illustrating the synthesis protocol where metal salt is reduced in the presence of SDS and oleic acid to produce nanoparticles.*

In a typical experiment, an aqueous solution of nickel salt [1×10^{-3} M solution of $Ni(NO_3)_2.6H_2O$] was reduced by a strong reducing agent sodium borohydride ($\sim 0.025\%$) in the presence of SDS and oleic acid to obtain nickel nanoparticles. The synthesis was done at ambient temperature and pressure. This synthesis protocol was further optimized to attain stability, size monodispersity and crystallanity.

The concentrations of SDS and oleic acid were varied to obtain a combination necessary to get a stable solution of monodisperse nickel nanoparticles. As oleic acid is insoluble in water, its methanolic solution was used with its concentration restricted to 10^{-4} M because further increase in concentration was seen to lead to a turbid solution. The different concentration combinations used for optimization are given in Table 2.1.

Table 2.1 *Various concentration combinations of SDS and oleic acid to determine the optimum condition.*

Case	SDS (M)	Oleic acid (M)
A	1×10^{-2}	1×10^{-4}
B	5×10^{-4}	5×10^{-6}
C	5×10^{-2}	-
D	-	1×10^{-4}

As seen from Table 2.1, four combinations were made which would be referred to as the cases A, B, C and D. In case A and B, both SDS and oleic acid were present but the concentration of SDS was above its Critical Micelle Concentration (CMC of SDS is 8.1 mM [26]) in case A while below its CMC value in case B. In case C, only SDS was used while in case D, only oleic acid was used. These conditions were same for preparation of both cobalt and nickel nanoparticles. The respective solutions of nickel will be referred to as A_{Ni}, B_{Ni}, C_{Ni} and D_{Ni} while respective solutions of cobalt will be denoted by A_{Co}, B_{Co}, C_{Co} and D_{Co}.
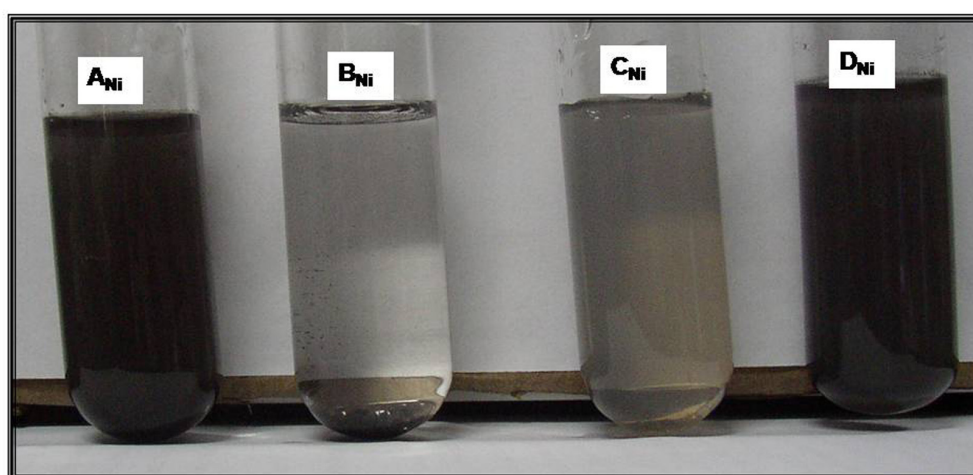

Figure 2.2 *Photograph depicting the difference in the stability of solutions of nickel nanoparticles. The solutions A_{Ni}, B_{Ni}, C_{Ni} and D_{Ni} represent their corresponding cases as given in Table 2.1.*

Upon addition of the reducing agent to the mixture of above mentioned oleic acid/SDS solutions and Ni^{2+} ions, the solutions immediately turned brownish-black.

They were then left undisturbed to check for their stability with respect to time. The photograph of the four solutions is depicted in Fig. 2.2. As clearly seen in the photograph, solution A_{Ni} and D_{Ni} remain completely stable and retain their original colour. Among the remaining two solutions, precipitation can be seen for solution B_{Ni} while solution C_{Ni} has lost its colour. Please note that both Solutions A_{Ni} and D_{Ni} contained same concentration of oleic acid whereas solution C_{Ni} did not contain any oleic acid.

The solutions were then subjected to centrifugation at 9000 rpm for 20 min to remove excess surfactant and reaction byproducts. In each case, the supernatent obtained after centrifugation was colourless and was discarded. The pellets were redissolved in deionized water, centrifuged again under the same condition and then analyzed by characterization techniques like Transmission Electron Microscopy.

2.2.2 Spontaneous assembly of highly monodisperse nickel nanoparticles

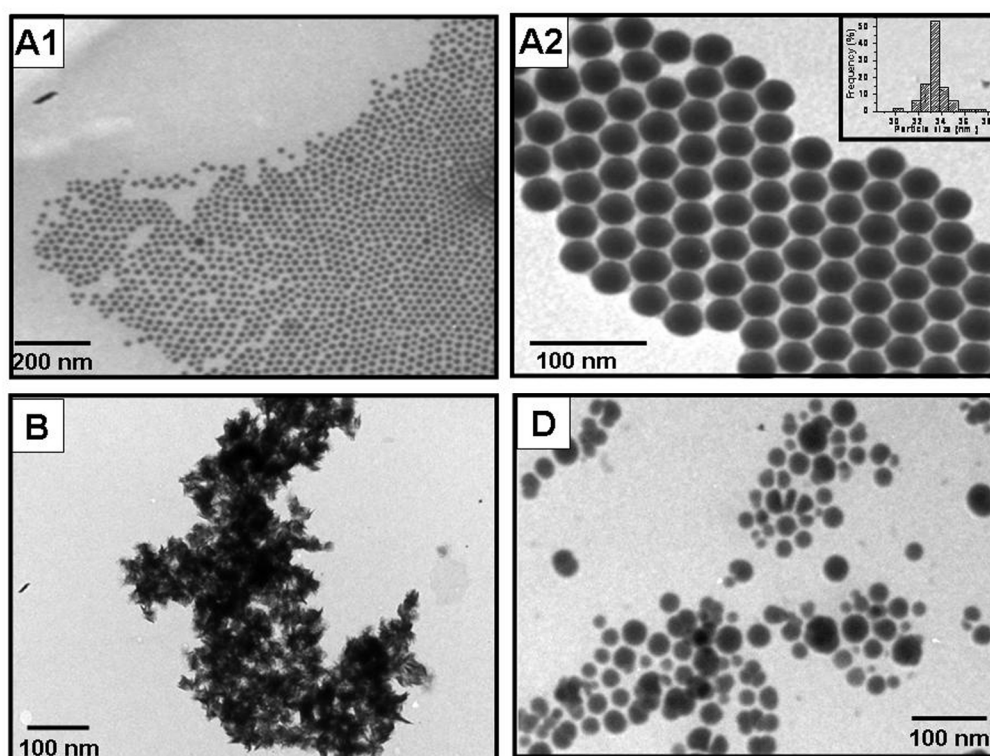**Figure 2.3 A1,A2***) Representative TEM images obtained corresponding to solution A_{Ni} demonstrating spontaneous ordered arrangement of highly monodisperse nickel nanoparticles* **B)** *TEM images obtained from solution B_{Ni} where SDS concentration is below the CMC.* **D)** *TEM images corresponding to solution D_{Ni} (with only oleic acid) showing polydisperse nickel nanoparticles.*

In order to obtain TEM images from a sample, it was drop-casted on a carbon-coated copper grid. The TEM images obtained from solutions A_{Ni}, B_{Ni} and D_{Ni} are shown in Fig. 2.3.

Fig. 2.3 A1 and A2 correspond to solution A_{Ni} where SDS (with concentration above its CMC) plus oleic acid were used. Highly monodispesre nanoparticles were obtained in this case as clearly seen in the TEM images. The nanoparticles are also seen to spontaneously assemble into hexagonal close packed (hcp) arrangement. The low magnification TEM image clearly shows one such representative long range assembly (see Fig. 2.3A1). The hcp assembly of these nanoparticles is evident from the high magnification TEM image shown in Fig. 2.3 A2. The inset of Fig. 2.3 A2 shows the histogram of particle size distribution of the nanoparticles. It indicates size monodispersity with an average particle size of 33.30 ± 1.05 nm.

Fig. 2.3 B corresponds to solution B_{Ni} that had undergone precipitation. The image shows agglomerated particles. The nanoparticles seen in Fig. 2.3 D are of highly polydisperse nature and correspond to solution D_{Ni} which contained only oleic acid and no SDS. No image could be obtained from solution C_{Ni} (SDS was present and oleic acid absent) suggesting degradation of the particles along with decolourization. Thus, TEM analysis indicates that the presence of SDS (concentration > CMC) along with oleic acid ensures monodisperse nanoparticle formation. Thus, solution A_{Ni} seemed to have the optimum combination of surfactants and was used for further characterization.

2.2.3 Spectroscopic studies of nickel nanoparticles

Stable solution of nanoparticles (solution A_{Ni}) was subjected to UV-vis absorption and FTIR spectral analysis to study optical properties and functional group signatures respectively.

Fig. 2.4 A shows the UV-vis absorption spectrum of nickel nanoparticles. Typically, Ni nanoparticles do not have any characteristic features in the optical absorption [25d], and the spectrum obtained here is in accordance with it. The intensity is seen to decrease monotonically with respect to the increase in wavelength.
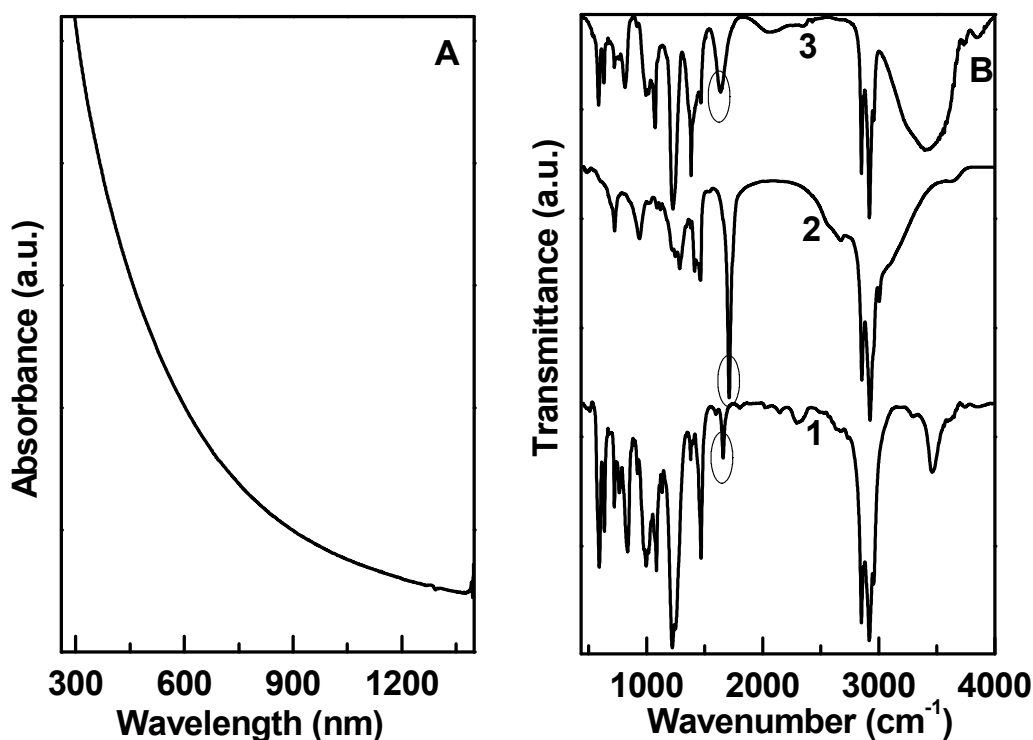
Fig. 2.4 A) *UV-visible absorption spectrum of solution* A_{Ni} **B)** *FTIR spectra corresponding to pure SDS (Curve 1), to pure oleic acid (curve 2) and to Ni nanoparticles coated by both SDS and oleic acid (curve 3).*

Since, the optimum condition for the monodispersity and stability indicated that both SDS and oleic acid were necessary for obtaining monodisperse nanoparticles, an attempt was made to probe their way of binding to the nanoparticle surface. Fig.2.4 B shows the FTIR spectra where curve 1 and 2 correspond to pure SDS and pure oleic acid respectively while curve 3 is for nickel nanoparticles coated with both SDS and oleic acid (solution A). The carboxylic stretch of pure oleic acid molecule is seen at 1709 cm^{-1} (see curve 2) whereas a sharp peak is observed at 1660 cm^{-1} in the spectrum of pure SDS (see curve 1). But, these two peaks are absent in the spectrum of nickel nanoparticles. Instead, a single peak is seen at 1629 cm^{-1} (curve 3).

2.2.4 Study of crystallnity of nickel nanoparticles

Powder X-Ray analysis of nanoparticles before and after heating has been carried out to understand the changes in crystallinity of these nanoparticles due to heating. Curve 1 from Fig. 2.5 corresponds to the as-prepared sample of nickel nanoparticles. At this point, no distinguishing peak was observed. The sample was then subjected to heating at 300 ºC. The XRD spectrum taken after heating is shown

as curve 2 and reveals improved crystalline nature of the sample. The three peaks marked by * are observed at 2θ values of 44.6º, 52º and 76.6º (wavelength- Cu k_α =1.542 Å).
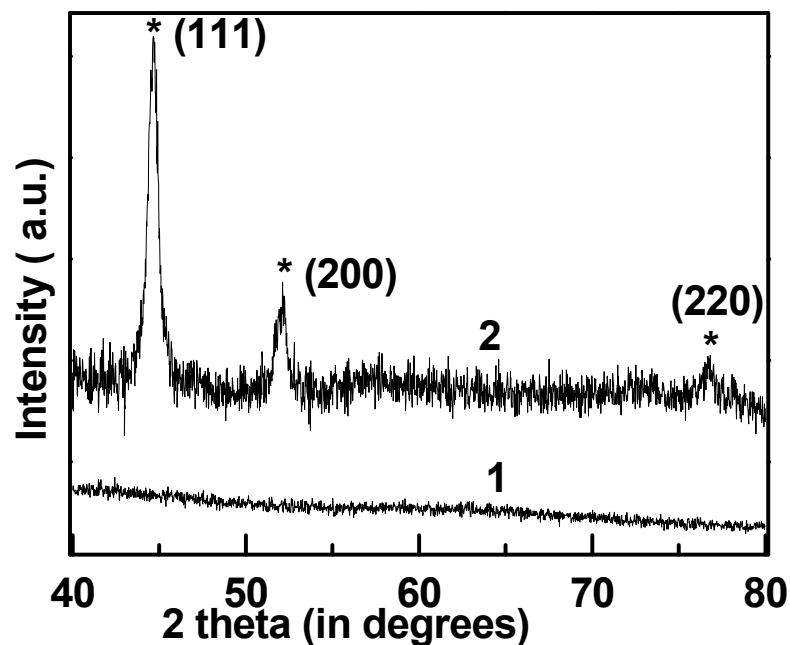
Figure 2.5 *X-Ray diffractograms of nickel nanoparticles before (curve 1) and after heating at 300 ºC (curve 2). Curve 1 does not consist of any peak but curve 2 shows three prominent peaks marked by symbol * .*

The improvement in crystalline nature was further confirmed by the TEM images of the heated sample as depicted in Fig. 2.6.
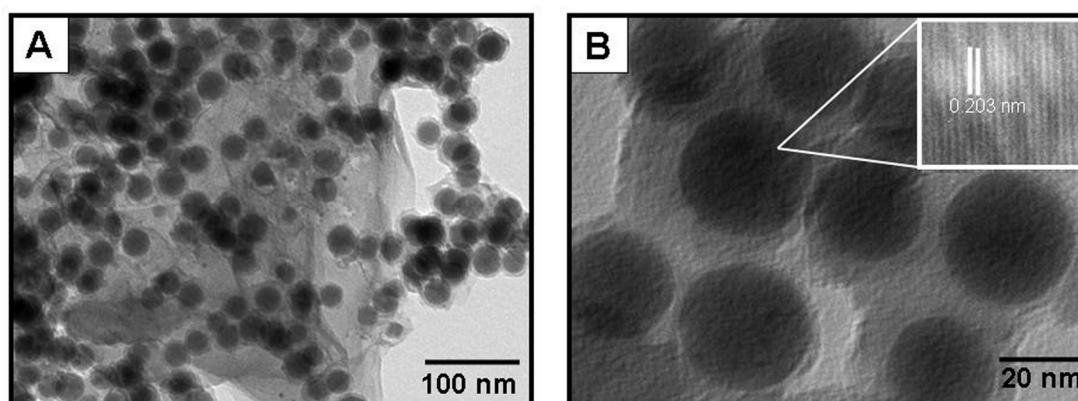
Figure 2.6 *TEM images corresponding to the heated sample. Inset of B shows d value obtained from lattice spacing.*

As can be seen from the figure, the TEM images for the heated sample demonstrate that the constituent nanoparticles have not aggregated after heating. Instead, they remain distinct and of similar size to the original ones. Inset of Fig. 2.6 B is an HRTEM image of one of the nanoparticles and discloses crystalline nature of the nanoparticles with the lattice planes of interplaner spacing of 0.203 nm clearly visible.

Since the improvement in crystalline nature was observed after heating the sample at 300 °C; it was to be probed whether there was a corresponding weight-loss as well. The original and the heated samples were then subjected to thermogravimetric analysis.

2.2.5 Thermogravimetric analysis (TGA)

Fig. 2.7 *Thermogravimetric analysis of original sample (curve 1) and the heated sample (curve 2).*

Fig. 2.7 demonstrates the TG profile (curve 1) for the as-prepared sample and it shows total weight-loss of about 23 wt%. While the TG profile of heated sample (curve 2) shows the total weight-loss of only 9 wt%.

2.2.6 Magnetic measurements

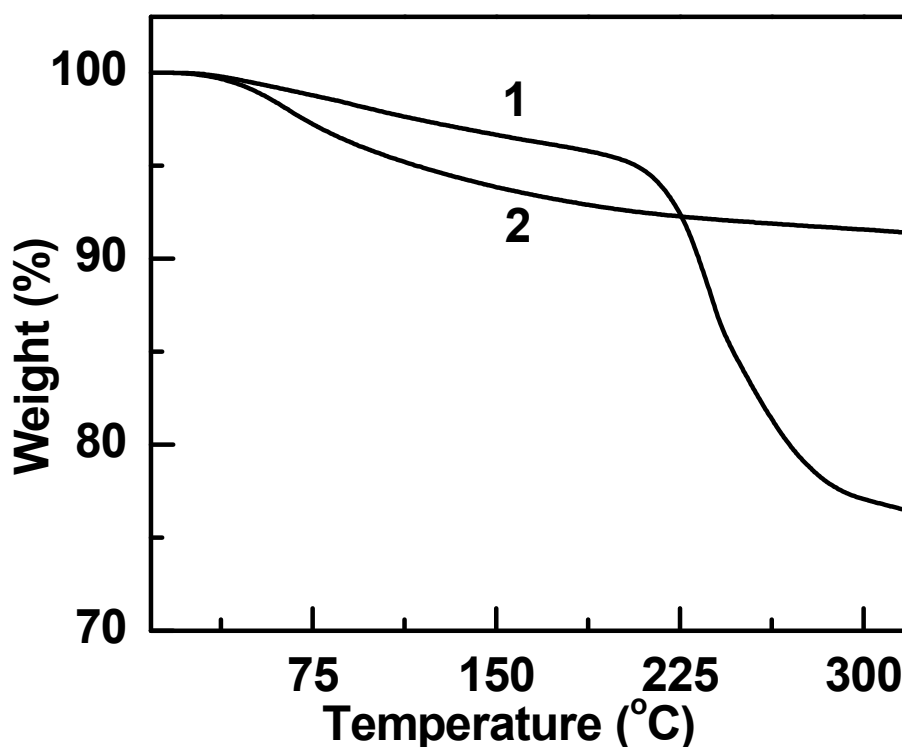As the crystallinity is different for as prepared samples and heated samples, it will have surely be reflected in their magnetic properties. Hence, the nickel nanoparticles were also characterized for their magnetic measurements. The field dependent magnetization (M-H) measurements for nickel nanoparticles before and after heating are shown in Figure 2.8A and B respectively with the temperature dependent magnetization curves as the insets.
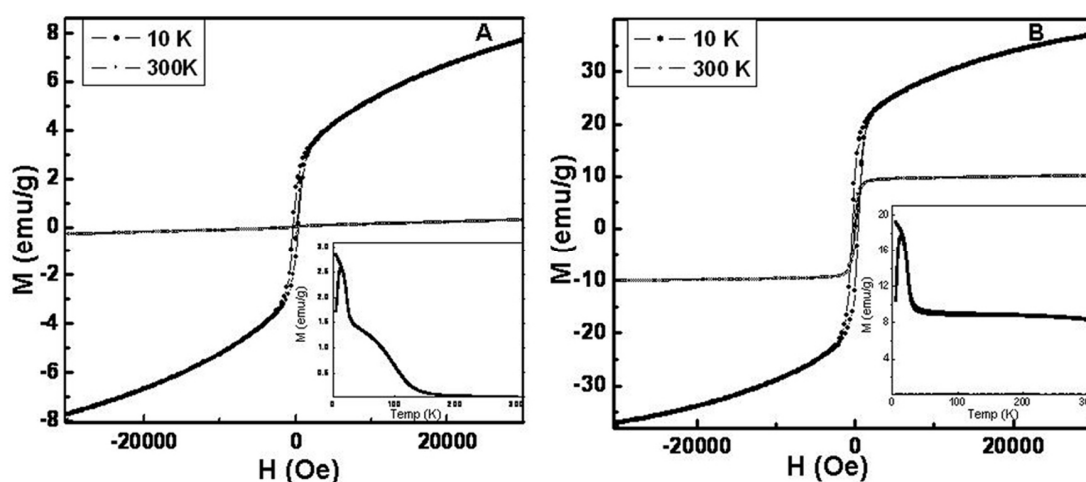
Figure 2.8 *A) Field dependent magnetization curves for Ni nanoparticles (original sample) above (300K) and below (10K) the blocking temperature (T_B). Temperature dependent magnetization of the Ni nanoparticles in zero field cooled and field cooled mode are given in the inset. B) Field dependent magnetic measurements of the heated sample with the inset showing its temperature dependent magnetic measurements.*

When the magnetic measurements for original and annealed nanoparticles are compared, it is found that in both cases, the zero-field cooled (ZFC) and field cooled (FC) curves for Ni nanaoparticles represent the typical curves for superparamagnetic particles. The peak observed at ~ 14 K in the ZFC curve can be attributed to be the blocking temperature (T_B). Superparamagnetic nanoparticles are known to exhibit hysteresis loop below the blocking temperature and not above it, which is clearly supported by the field dependent magnetization studies. Here, the field dependent magnetization curves display no hysteresis at 300 K and a distinct loop is seen at 10 K. Also, the magnetization values are seen to increase in case of the annealed samples. At 10 K, the saturation magnetization value for the unheated and heated

samples are ~10 emu/g and ~ 44 emu/g respectively. Hence, heating of the nanoparticles is seen to lead to better magnetic characteristics along with better crystallanity. The implications of all the results obtained so far will be elaborated upon in the Discussion section.

2.3 Synthesis and spontaneous assembly of cobalt nanoparticles

To check the validity of the protocol for the synthesis of other transition metal nanoparticles, we tried synthesis of cobalt nanoparticles with exactly same procedure. The formation of nanopaticles and their hcp assembly were observed for cobalt nanoparticles as well.

2.3.1 Synthesis and stability of cobalt nanoparticles

In a typical experiment to synthesize cobalt nanoparticles, 100 mL aqueous solution of cobalt ions [1×10^{-3}M solution of $CoCl_2.6H_2O$] was reduced by sodium borohydride (~0.025%) in the presence of SDS and oleic acid and at ambient temperature and pressure.
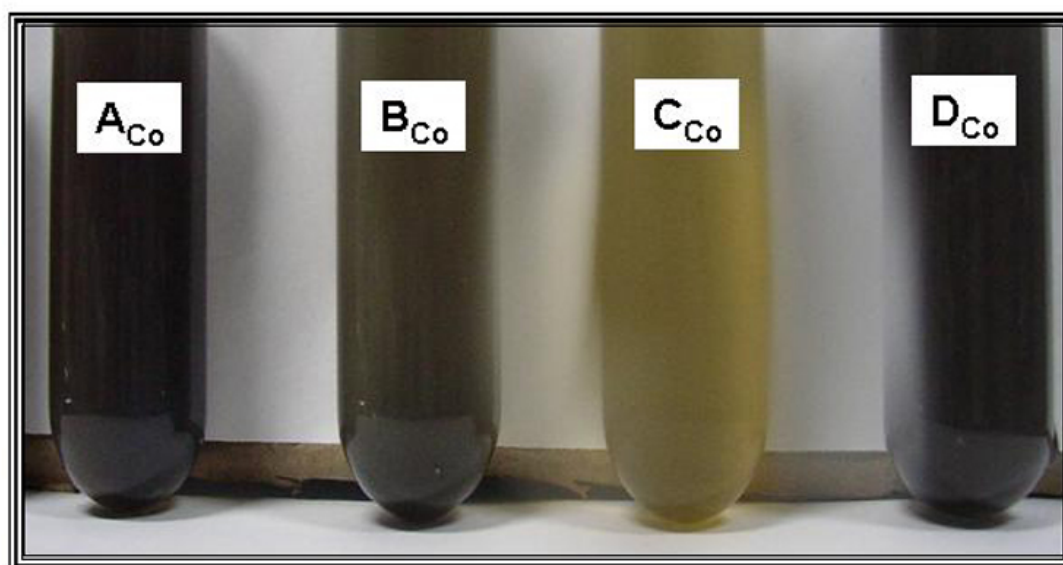
Figure 2.9 *Photograph depicting the difference in the stability of solutions of cobalt nanoparticles. The solutions A_{Co}, B_{Co}, C_{Co} and D_{Co} represent their corresponding cases A, B, C, D respectively as given in Table 2.1.*

Cobalt solutions corresponding to cases A, B, C and D will be denoted as solutions A_{Co}, B_{Co}, C_{Co} and D_{Co} respectively. As evident from the photograph and as observed in nickel case, only solution A_{Co} (SDS concentration above CMC, oleic

acid) and solution D_{Co} (only oleic acid) have remained stable. The solutions were then centrifuged (9000 rpm, 20 min.) and the pellets were used for further analysis.

2.3.2 TEM analysis of cobalt nanoparticles
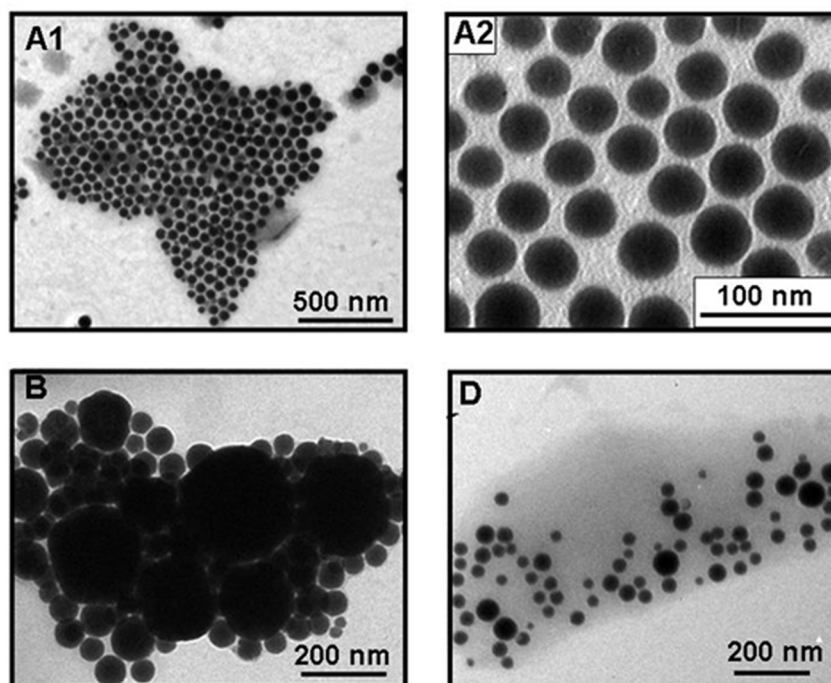
Figure 2.10*) Representative TEM images from **A1, A2)** solution* A_{Co} *showing nearly monodisperse cobalt nanoparticles which arranged themselves in hcp manner. **B)** Solution* B_{Co} *where SDS concentration is below the CMC resulting in an agglomeration. **D)** Solution* $D_{Co,}$ *(with only oleic acid) in which nanoparticles are of polydisperse nature.*

TEM images of cobalt nanoparticles show similar trends like their nickel counterparts. Fig. 2.10 shows representative TEM images from solution A_{Co} (images A1 and A2), solution B_{Co} (image B) and solution D_{Co} (image D). In this case as well, the solution containing both SDS (above CMC) and oleic acid gives rise to isolated nanoparticles. But the nature of these nanoparticles is not as highly monodisperse as nickel nanoparticles. These nanoparticles are also seen to organize spontaneously to form assemblies.

The nanoparticles from solution B_{Co} demonstrate aggregation. No TEM image could be obtained from solution C_{Co} as it was unstable. The nanoparticles obtained from solution D_{Co} display highly polydisperse nature. So, here again, the solution containing both SDS (above CMC) and oleic acid is found to be highly stable and is seen to

contain nanoparticles of narrow size dispersion. The nanoparticles from the solution were used for further characterization.

2.3.3 Spectroscopic studies of cobalt nanoparticles

Nanoparticles prepared by the above-mentioned method were characterized by UV-Visible absorption and FTIR spectral analysis to study their optical properties and functional groups signature respectively. Fig. 2.11 A shows the UV-vis absorption spectrum of cobalt nanoparticles. It has no peaks but the intensity is seen to increase monotonically towards lower wavelength.
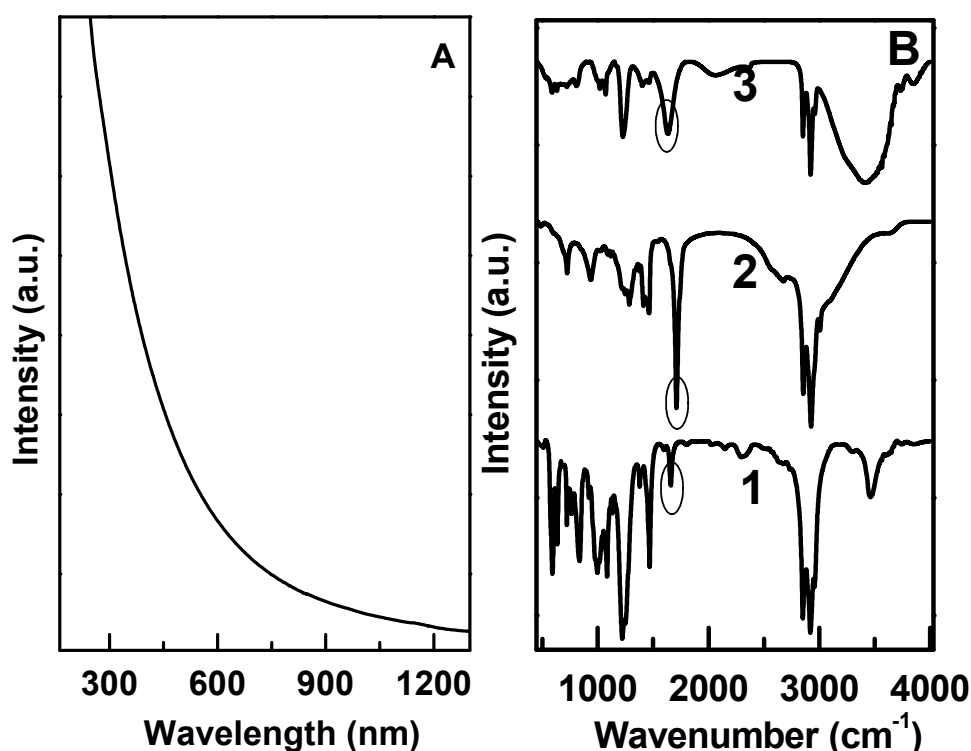
Fig. 2.11 A) *UV-visible absorption curve for solution A_{Co} displaying no distinguishing peak.* **B)** *FTIR spectra of pure SDS (Curve 1), pure oleic acid (curve 2) and cobalt nanoparticles coated by both SDS and oleic acid (curve 3).*

The cobalt nanoparticles were also subjected to FTIR measurements, the results of which are shown in Fig.2.11 B. Curves 1, 2 and 3 correspond to the FTIR spectra of pure SDS, pure oleic acid and cobalt nanoparticles functionalized by both SDS and oleic acid respectively. Cobalt nanoparticles show a peak at 1635 cm^{-1} as against the peaks seen for pure oleic acid (1709 cm^{-1}) and pure SDS (1660 cm^{-1}).

2.3.4 Magnetic measurements of cobalt nanoparticles
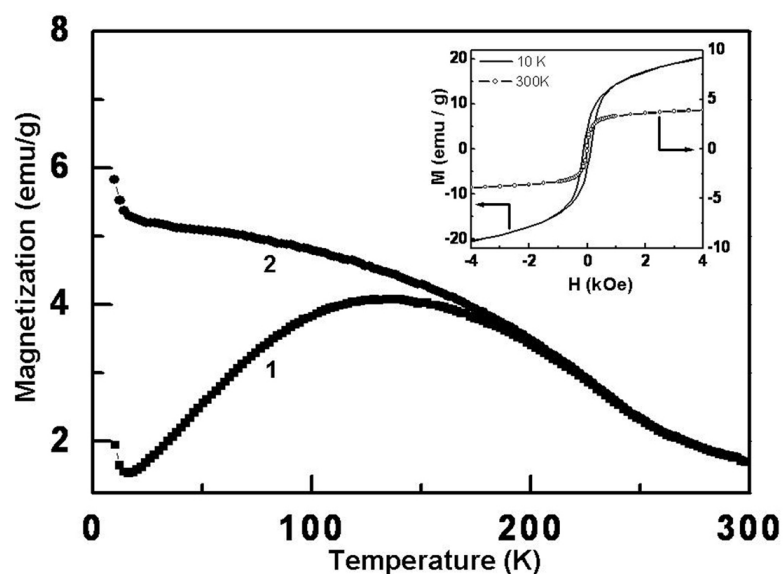
Figure 2.12 *The temperature dependent magnetization curves in zero field cooled (curve 1) and field cooled (curve 2) mode. The field dependent magnetization curves for cobalt nanoparticles above (300K) and below (10K) the blocking temperature (T_B) are given in the inset.*

Cobalt nanoparticles were then subjected to magnetic measurements. Here also, two kinds of measurements were done- temperature dependent and field dependent. In case of temperature dependent measurements, zero field curve and field cooled curve were obtained at 50 Oe. The blocking temperature was determined from it. For the field dependent measurements, the M-H curve was obtained at two temperatures, one below the blocking temperature and the other above it.

The temperature dependent magnetization measurements for Co (sample IIB) nanoparticles are shown in Figure 2.12 with the field dependent magnetization (M-H) curves as the insets. The zero-field cooled (ZFC) and field cooled (FC) curves are typical of superparamagnetic particles. The ZFC curve peaks at around ~ 150 K, indicating it to be the blocking temperature (T_B). Cobalt nanoparticles should exhibit hysteresis below this temperature but not at room temperature, which is clearly supported by the field dependent magnetization studies (inset of Fig. 2.12).

2.3.5 XRD analysis of cobalt nanoparticles
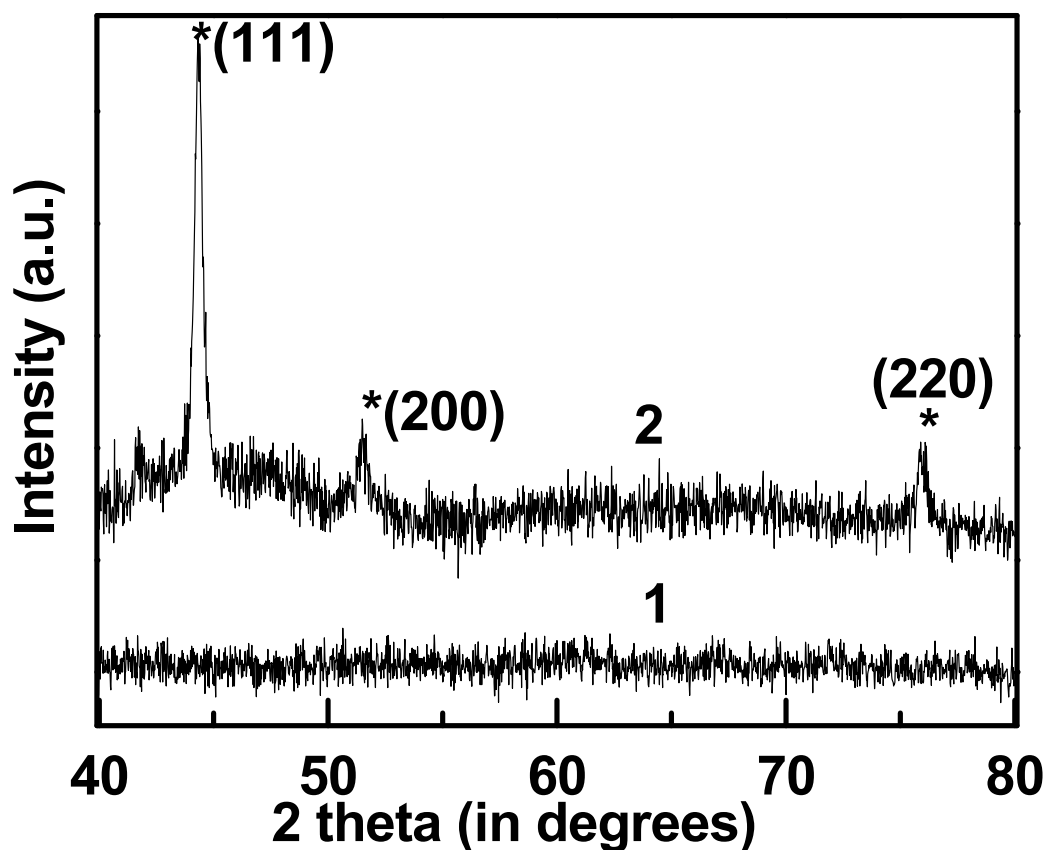
Figure 2.13 *X-Ray diffractograms of cobalt nanoparticles recorded before heating (curve 1) and after heating at 500 ºC (curve 2). The XRD spectrum showed no discernible peak before heating but 3 distinguishing peaks (marked by *) were seen after heating.*

The as-prepared sample did not display any peak in its XRD spectrum (as seen in curve 1 of Fig. 2.13). Hence, it was heated at 500 ºC and then the XRD spectrum was recorded. This spectrum is shown as curve 2 in Fig. 2.13. It revealed 3 prominent peaks which were used to find corresponding d values.

The implications of all the results obtained for both the systems viz. nickel and cobalt will be discussed in the next section.

2.4 Discussion

In this section, intially, the analysis of the results would be given roughly in the same order as they were described in the experimental section and finally they would be summed up. Initially, a protocol was formulated to obtain stable solution of monodisperse metal nanoparticles from the corresponding metal salt. The protocol employed is reduction of metal ions in the presence of oleic acid and SDS. The

concentrations of SDS and oleic acid were seen to play a crucial role in obtaining the nanoparticles with desirable features like stability and monodispersity.

To determine the optimum concentration condition for nanoparticles, four combinations of SDS and oleic acid were used (Table 2.1). Metal reduction took place in every case irrespective of the surfactant concentration as evident from the fact that all the solutions showed the same kind of colour transformation and finally attained the dark brownish-black colour. But then, with time, each of the solution was seen to behave differently (Photographs from Fig. 2.2 and Fig. 2.9). The time dependent changes, as seen from the photographs, the TEM images (Fig. 2.3 and Fig. 2.10) and table 2.1, point to the following-

i) To obtain stable nanoparticles solutions, presence of oleic acid is a necessary condition (solutions corresponding to case A and D).

ii) If, alongwith oleic acid, SDS is present with its concentration above its CMC, only then, the resultant nanoparticles form a stable solution containing monodisperse nanoparticles (solutions corresponding to case A) and not otherwise (case B).

iii) If only SDS is present (case C), the resultant nanoparticles are highly susceptible to degradation.

iv) If only oleic acid is present, then a stable solution of nanoparticles is obtained but the nanoparticles are polydisperse in nature (solutions corresponding to case D). This points towards the role of SDS to achieve monodispersity.

These observations indicate that oleic acid is necessary to stabilize the nanoparticles or in other words, it could be acting as a capping agent, whereas SDS would be needed to achieve monodispersity. So, the presence of both SDS (above CMC) and oleic acid constitute the optimum condition to obtain stable solution of monodisperse nanopaticles using our synthesis protocol.

Apart from these desirable features, the nanoparticles were also seen to spontaneously form long-range assemblies in a hexagonally closed packed manner. Such assemblies were present all-over the TEM grid. The assemblies of monodisperse nanoparticles are useful from the application point of view.

In case of the spectroscopic studies, the UV-visible absorption spectra in both the cases (Fig. 2.4 A and Fig. 2.11 A) were as expected [25 c, 25 d, 27]. Both nickel and cobalt nanoparticles are known to display a spectrum without any peak and only with a monotonic increase in intensity while moving towards the lower wavelength. The role of oleic acid as a capping agent is as expected because it has been used for capping magnetic nanoparticles by many research groups [25]. The double bond of oleic acid is found to play a crucial role in stabilizing action [13, 24]. In the present work, oleic acid is supplemented by SDS. FTIR is a valuable technique to understand the interaction of SDS and oleic acid with the nanoparticles (Fig. 2.4B and Fig. 2.11B). In both nickel and cobalt cases, the FTIR bands are observed at a position different from that in spectra for oleic acid and SDS. The shift in carboxylic stretch of oleic acid indicates an interaction of these groups with the nanoparticles, thus contributing to their stability.

Both the as-prepared samples (Ni and Co) showed no feature in X-ray diffractogram, which was seen to improve on heating. This is in agreement with literature reports [13]. In the work by Pileni *et al*. [18c] and Bawendi *et al*. [16c], initially amorphous samples have been heat-treated to improve their crystallanity and showed prominent peaks in the x-ray diffractograms of the heated samples. Following a similar strategy, wein the present work, nickel and cobalt as-prepared samples were heated at 300 °C and 500 °C respectively. The peaks obtained in the heated sample of Ni nanoparticles match with the fcc phase (JCPDS card no. 1-1258). The prominent peak at d = 2.03Å corresponds to interplaner spacing of (111) plane. Other intense peaks correspond to (200) and (220) peaks respectively matching well with the fcc phase. Similarly, peak values in heated samples of cobalt also matched with d values for (111), (200) and (220) confirming their fcc nature (JCPDS card no. 1-1255).

Preparation of nanoparticles by borohydride reduction can be susceptible to contamination with their respective borides [28]. But it has been shown that when the reduction is carried out in ambient air conditions, there is a greater chance of pure metal nanoparticle formation [29]. Synthesis in the present work has also been carried out under ambient air conditions. The heating could result into elimination of metal boride if present [28]. It can also remove defects (stacking faults, twinned planes) to improve crystallanity [30].

The composition and nature of nickel and cobalt nanoparticles was realized by the spectroscopic and microscopic measurements. But, to understand the change in crystallanity in a better way, the heated sample of nickel nanoparticles was subjected to HRTEM, TGA and magnetic measurements and its results were compared with those for the as-prepared sample.

The improvement in the crystallanity due to heating was also illustrated by the HRTEM image of the heated sample (inset of Fig. 2.6B) where d spacing corresponding to (111) planes for fcc phase of nickel (JCPDS card no. 1-1258) was observed. Heating induced a slight decrease in the interparticle distance between the nanoparticles but they retained their isolated nature (Fig. 2.6). TGA curve (Fig. 2.7, curve 1) corresponding to the as-prepared sample showed greater weight-loss than the heated sample.

The magnetic properties of nanoparticles are known to be a function of their crystallanity [30]. This was reflected from the comparison of magnetic properties of as-prepared and heated nickel nanoparticles (Fig. 2.8). The zero-field cooled (ZFC) and field cooled (FC) curves for the samples resembled the curves observed for superparamagnetic nanoparticles [31]. In both the cases, corresponding ZFC curves depicted peak position at $\sim$ 14 K. Hence, the blocking temperature (T_B) was ascertained to be 14 K. Superparamagnetic nanoparticles are known to exhibit hysteresis only below the blocking temperature. Hence, the field dependent measurements were performed at 10 K (below blocking temperature) and 300 K (above the blocking temperature). As expected, for both the samples, hysteresis loop was observed only at 10K and not at 300K. Although the nature was similar for both samples; corresponding magnetization values showed a difference. At 10 K, the saturation magnetization value for the heated samples was $\sim$ 44 emu/g which was four times that observed for as-prepared sample ($\sim$ 10 emu/g). Hence, heating of the nanoparticles is seen to lead to improved magnetic characteristics along with crystallanity.

The as-prepared sample of cobalt nanoparticles was also subjected to magnetic measurements (Fig. 2.12). The temperature dependent magnetization measurements revealed a blocking temperature of 150 K. In keeping with this observation, the nanoparticles did not show a distinct loop at room temperature (300 K) while the

hysteresis was clearly seen below the blocking temperature (10 K). The magnetization value was observed to be ~ 20 emu/g. The comparatively lower magnetization value for both nickel and cobalt could be occurring due to the presence of surfactant SDS and oleic acid in the samples.

Efforts were made to investigate the mechanism behind formation of nanoparticles and their subsequent organization. Based on all the above results, it was hypothesized that the formation of nanoparticles can take place by two ways –

1) The optimum synthetic condition for both Ni and Co nanoparticle systems includes both SDS (above CMC) and oleic acid. As the nanoparticles are formed in an aqueous medium and constitute a stable dispersion, one could think of formation of vesicles, inside which these nanoparticles can be formed. Oleic acid is known to form vesicles with anionic surfactant [32]. But, typically, the vesicles have sizes greater than 100 nm; hence the particles formed inside them would also be of this size but the nanoparticles observed are far too smaller than this size. (Fig. 2.3 and Fig. 2.10) So, this hypothesis may not be correct.

2) As other possibility, micellar formation of SDS and oleic acid is proposed. After addition of metal ions, there may be an organization of monodisperse clusters of micelles and the metal ions can get trapped in the interstitial spaces of these micelle aggregates. Upon addition of sodium borohydride, the ions will get reduced to form nanoparticles. In this process, they may be stabilized mainly by oleic acid. Such hypothesis can be only proved by carrying out detailed in-situ dynamic light scattering experiments and could be taken up for further studies. Such understanding of the mechanism can pave way for better utilization of the synthetic procedure developed here.

2.5 Conclusion

A simple protocol to synthesize monodisperse magnetic metal nanoparticles has been developed. The metal nanoparticles were prepared by reducing the corresponding metal salt in the presence of SDS and oleic acid. The protocol has been optimized to obtain stable solutions consisting of monodisperse nanoparticles. The crystallanity and magnetic properties of the nanoparticles have also been studied. The nanoparticles demonstrate spontaneous formation of beautiful assemblies. In comparison with other available protocols, the experimental advantages of the present

method would be as follows -its simplicity, feasibility at ambient temperature and pressure conditions and usage of precursors which can be handled very easily, instantaneous occurance of reaction, no requirement for separate size-selective separation procedure. In terms of the output, the current approach produces stable solutions of monodisperse nanoparticles and they are present in aqueous medium which is one of the essential requirements for biological applications. Further advantage comes from the fact that the nanoparticles form spontaneous assemblies.

2.6 References

1) (a) Ross; C. A. *Annu. Rev. Mater. Res.* **2001**, *31*, 203.

  (b) Skomski, R. *J. Phys.: Condens. Matter* **2003**, *15*, R841.

  (c) Weller, D.; Doerner, M. F. *Annu. Rev. Mater. Sci.* **2000**, *30*, 611.

2) (a) De Volder, M.; Reynaerts, D. *Sens. Actuators, A* **2009**, *152*, 234.

  (b) Odenbach, S. *Colloids Surf., A* **2003**, *217*, 171.

3) (a) Zhao, X.; Shi, Y.; Cai, Y.; Mou, S. *Environ. Sci. Tech.* **2008**, *42*, 1201.

  (b) Horák, D.; Babič, M.; Macková, H.; Beneš, M. J. *J. Sep. Sci.* **2007**, *30*, 1751.

  (c) Jun, Y.-W.; Seo, J.-W.; Cheon, A. *Acc. Chem. Res.* **2008**, *41*, 179.

4) (a) Pankhurst, Q. A.; Connolly, J.; Jones, S. K.; Dobson, J. *J. Phys. D: Appl. Phys.* **2003**, *36,* R167.

  (b) Lok, C. *Nature* **2001**, *412*, 372.

  (c) Dutz, S.; Clement, J. H.; Eberbeck, D.; Gelbrich, T.; Hergt, R.; Müller, R.; Wotschadlo, J.; Zeisberger, M. *J. Magn. Magn. Mater.* **2009**, *321*, 1501.

  (d) Kalambur, V. S.; Han, B.; Hammer, B. E.; Shield, T. W.; Bischof, J. C. *Nanotechnology* **2005**, *16*, 1221.

  (e) Bouchard, L.-S.; Anwar, M. S.; Liu, G. L.; Hann, B.; Xie, Z. H.; Gray, J. W.; Wang, X.; Pines, A.; Chen, F. F. *Proc. Natl. Acad. Sci. USA* **2009**, *106*, 4085.

  (f) O'Grady, K. *J. Phys. D: Appl. Phys.* **2009**, *42*, 220301.

  (g) Pankhurst, Q. A.; Thanh, N. K. T.; Jones, S. K .; Dobson, J. *J. Phys.D: Appl. Phys.* **2009**, *42*, 224001.

  (h) Roca, A. G.; Costo, R.; Rebolledo, A. F.; Veintemillas-Verdaguer, S.; Tartaj, P.; Gonzalez-Carreno, T.; Morales, M. P.; Serna, C. J. *J. Phys.D: Appl. Phys.* **2009**, *42*, 224002.

  (i) Berry, C. C. J. Phys. D: Appl. Phys. **2009,** *42***,** 224003.

  (j) Pellegrino, T.; Kudera, S.; Liedl, T.; Javier, A. M.; Manna, L.; Parak, J. *Small* **2005**, *1*, 48.

  (k) Xu, C.; Sun, S. *Dalton Trans.* **2009**, 5583.

5) (a) Jeong, U.; Teng, X.; Wang ,Y.; Yang, H.; Xia, Y. *Adv. Mater.* **2007**, *19*, 33.

  (b) Huber, D. L. S*mall* **2005**, *1*, 482.

  (c) Park, S. J.; Kim, S.; Lee, S.; Khim, Z. G.; Char, K.; Hyeon, T. *J. Am. Chem.*

Soc. **2000**, *122*, 8581.

(d) Peng, S.; Wang, C.; Xie, J.; Sun, S. *J. Am. Chem. Soc.* **2006**, *128*, 10676.

6) (a) Woo, K.; Hong, J.; Choi, S.; Lee, H.-W.; Ahn, J.-P.; Kim, C. S.; Lee, S. W. *Chem. Mater.* **2004**, *16*, 2814.

(b) Laurent, S.; Forge, D.; Port, M.; Roch, A.; Robic, C.; Elst, L. V.; Müller, R. N. *Chem. Rev.* **2008**, *108,* 2064.

(c) Hyeon, T.; Lee, S. S.; Park, J.; Chung, Y.; Na, H. B. *J. Am. Chem. Soc.* **2001**, *123*, 12798.

7) (a) Park, J.; Cheon, J. *J. Am. Chem. Soc.* **2001,** *123,* 5743.

(b) Jun, Y.-w.; Choi, J.-S.; Cheon, J. *Chem. Commun.* **2007**, 1203.

(c) Shevchenko, E. V.; Talapin, D. V.; Rogach, A. L.; Kornowski, A.; Haase, M.; Weller H. *J. Am. Chem. Soc.* **2002**, *124*, 11480.

(d) Shevchenko, E. V.; Talapin, D. V.; Schnablegger, H.; Kornowski, A.; Festin, Ö.; Svedlindh, P.; Haase, M.; Weller, H. *J. Am. Chem. Soc.* **2003**, *125*, 9090.

(e) Borchert, H.; Shevchenko, E. V.; Robert, A.; Mekis, I.; Kornowski, A.; Grübel, G.; Weller, H. *Langmuir* **2005**, *21*, 1931.

(f) Chen, M.; Liu, J. P.; Sun, S. *J. Am. Chem. Soc.* **2004**, *126*, 8394.

(g) Sun, S. *Adv. Mater.* **2006**, *18*, 393.

8) (a)Kim, H; Achermann, M;. Balet, L. P.; Hollingsworth, J. A.; Klimov, V. I. *J. Am. Chem. Soc.* **2005**, *127*, 544.

(b) Zeng, H.; Li, J.; Wang, Z. L.; Liu, J. P.; Sun, S. *Nano Lett.* **2004,** *4*, 187.

(c) Zeng, H.; Sun, S. *Adv. Funct. Mater.* **2008**, *18*, 391.

(d) Son, S. U.; Jang, Y.; Park, J.; Na, H. B.; Park, H. M.; Yun, H. J.; Lee, J.; Hyeon, T. *J. Am. Chem. Soc.* **2004**, *126*, 5026.

(e) Leslie-Pelecky, D. L.; Rieke, R. D. *Chem. Mater.* **1996**, *8*, 1770.

9) (a) Hyeon, T.; Chung, Y.; Park, J.; Lee, S. S.; Kim, Y.-W.; Park, B. H. *J. Phys. Chem. B* **2002**, *106*, 6831.

(b) Sun, S.; Zeng, H.; Robinson, D. B.; Raoux, S.; Rice, P. M.; Wang, S. X.; Li, G. *J. Am. Chem. Soc*. **2004**, *126*, 273.

10) Zeisberger, M.; Dutz, S.; Müller, R.; Hergt, R.; Matoussevitch, N.; Bönnemann, H. *J. Magne. Magne. Mater.* **2007**, *311*, 224.

11) (a) Moreno-Mañas, M.; Pleixats, R. *Acc. Chem. Res.* **2003**, *36*, 638.

(b) Park, J.; Kang, E.; Son, S. U;. Park, H. M.; Lee, M. K.; Kim, J.; Kim, K. W.; Noh, H.- J.; Park, J.-H.; Bae, C. J.; Park, J.-G.; Hyeon; T. *Adv.Mater.* **2005**, *17*, 429.

(c) Son, S. U.; Lee, S. I.; Chung, Y. K.; Kim, S.-W.; Hyeon, T. *Org. Lett.* **2002***, 4*, 277.

(d) Kumar, A.; Kumar, S.; Saxena, A.; De, A.; Mozumdar, S. *Cata. Commun.* **2008**, *9*, 778.

(e) Saxena, A.; Kumar, A.; Mozumdar, S. *J. Mol. Catal. A: Chem.* **2007**, *269*, 35.

(f) Saxena, A.; Kumar, A.; Mozumdar, S. *Appl. Catal. A: Gen.* **2007**, *317*, 210.

(g) Kidwai, M.; Bansal, V.; Saxena, A.; Shankar, R.; Mozumdar, S. *Tetra. Lett.* **2006**, *47*, 4161.

12) (a) Harris, A. T.; See, C. H.; Liu, J.; Dunens, O.; MacKenzie, K. *J. Nanosci. Nanotech.* **2008**, *8*, 2450.

(b) Moshfegh, A. Z. *J. Phys. D: Appl. Phys.* **2009**, *42*, 233001.

(c) Tuan, H. Y.; Lee, D. C.; Hanrath, T.; Korgel, B. A. *Chem. Mater.* **2005**, *17*, 5705.

(d) Tuan, H. Y.; Lee, D. C.; Hanrath, T.; Korgel, B. A. *Nano Lett.* **2005**, *5*, 681.

13) (a) Green, M. *Chem. Commun.* **2005**, 3002.

(b) Bao, Y.; An, W.; Turner, C. H.; Krishnan, K. M. *Langmuir* **2009,** DOI: 10.1021/la902120e.

(c) Chaudret, B. *C. R. Physique* **2005,** *6*, 117.

14) (a) Hyeon, T. *Chem. Commn.* **2003**, 927.

(b) Chen, Y. Z.; Luo, X. H.; She, H. D.; Yue, G. H.; Peng, D. L. *J. Nanosci. Nanotechnol.* **2009**, *9*, 5157.

(c) Winnischofer, H.; Rocha, T. C. R.; Nunes, W. C.; Socolovsky, L. M.; Knobel, M.; Zanchet, D. *ACS Nano* **2008**, *2*, 1313.

(d) Dennis, C. L.; Cheng, G.; Baler, K. A.; Maranville, B. B.; Walker, A. R. H.; Shull, R. D. *IEEE Trans. Magn.* **2007**, *43*, 2448.

(e) Han, M.; Liu, Q.; He, J. H.; Song, Y.; Xu, Z.; Zhu, J. M. *Adv. Mater.* **2007**, *19*, 1096.

15) (a) Hou, Y.; Kondoh, H.; Ohta, T.; Gao S. *Appl. Sur. Sci.* **2005**, *241,* 218.

(b) Cordente, N.; Respaud, M.; Senocq, F.; Casanove, M. J.; Amiens, C.; Chaudret, B. *Nano Lett.* **2001**, *1*, 565.

16) (a) Murray, C. B.; Sun, S.; Doyle, H.; Betley, T. A. *MRS Bull.* **2001**, *26*, 985.

(b) Murray, C. B.; Sun, S.; Gaschler, W.; Doyle, H.; Betley, T. A.; Kagan, C. R. *IBM J. Res. & Dev.* **2001**, *45*, 47.

(c) Dinega, D. P.; Bawendi, M. G. *Angew. Chem. Int. Ed.* **1999**, *38*, 1788.

(d) Sun, S.; Murray, C. B. *J. Appl. Phys.* **1999**, *85*, 4325.

(e) Puntes, V. F.; Krishnan, K. M.; Alivisatos, A. P. *Appl. Phys. Lett.* **2001**, *78*, 2187.

17) (a) Chen, J. P.; Lee, K. M.; Sorensen, C. M.; Klabunde, K. J.; Hadjipanayis, G. C. *J. Appl. Phys.* **1994**, *75*, 5876.

(b) Chen, J. P.; Sorensen, C. M.; Klabunde, K. J.; Hadjipanayis, G. C. *J. Appl. Phys.* **1994**, *76*, 6316.

18) (a) Pileni, M. P. *J. Phys. Chem.* **1993,** *97,* 6961.

(b) Petit, C.; Taleb, A.; Pileni, M. P. *Adv. Mater* **1998**, *10*, 259.

(c) Petit, C.; Taleb, A.; Pileni, M. P. *J. Phys. Chem. B* **1999**, *103*, 1805.

(d) Petit, C.; Wang, Z. L.; Pileni, M. P. *J. Phys. Chem. B* **2005**, *109*, 15309.

19) Chen, D.-H.; Hsieh, C.-H. *J. Mater. Chem.* **2002**, *12*, 2412.

20) Zhang, Y. ; Liang, F.; Wang, N.; Guo, L.; He, L.; Chen, C.; Zhang, Q.; Zhong, Q. *J. Nanosci. Nanotech.* **2008**, *8*, 2057.

21) (a) Murray, C. B.; Kagan, C. R.; Bawendi, M. G. *Annu. Rev. Mater. Sci.* **2000**, *30*, 545.

(b) Bao, Y.; Beerman, M.; Krishnan, K. M. *J. Magn. Magn. Mater.* **2003**, 266, L245.

(c) Wang, Z. L.; Dai, Z.; Sun, S. *Adv. Mater.* **2000**, *12*, 1944.

(d) Diehl, M. R.; Yu, J. Y.; Heath, J. R.; Held, G. A.; Doyle, H.; Sun, S.; Murray, C. B. *J. Phys. Chem. B* **2001**, *105*, 7913.

22) (a) Park, J.; Joo, J.; Kwon, S. G.; Jang, Y.; Hyeon T. *Angew. Chem. Int. Ed.* **2007**, *46*, 4630.

(b) Darling, S. B.; Bader, S. D. *J. Mater. Chem.,* **2005**, *15*, 4189.

23) Lin, X. M.; Samia, A. C. S. *J. Magn. Magn. Mater.* **2006**, *305*, 100.

24) Suslick, K. S. ; Fang, M.; Hyeon, T. *J. Am. Chem. Soc.* **1996**, *118,* 11960.

25) (a) Wu, N.; Fu, L.; Su, M.; Aslam, M.; Wong, K. C.; Dravid, V. P. *Nano Lett.*
       2004, *4*, 383.
    (b) Samia, A. C. S.; Hyzer, K.; Schleuter, J. A.; Qin, C-J.; Jiang, J. S.; Bader, S.
       D.; Lin, X.- M. *J. Am. Chem. Soc.* **2005**, *127*, 4126.
    (c) Bala, T.; Arumugam, S.; Pasricha, R.; Prasad, B. L. V.; Sastry, M. *J. Mater.
       Chem.* **2004**, *14*, 1057.
    (d) Bala, T.; Bhame, S. D.; Joy, P. A.; Prasad, B. L. V.; Sastry, M. *J. Mater.
       Chem.* **2004**, *14*, 2941.
    (e) Fried, T.; Shemer, G.; Markovich, G. *Adv. Mater.* **2001**, *13*, 1158.
    (f) Samia, A. C. S.; Schlueter, J. A.; Jiang, J. S.; Bader, S. D.; Qin, C. J.; Lin, X.-
       M. *Chem. Mater.* **2006**, *18*, 5203.
    (g) Luna, C.; Morales, M. P.; Serna, C. J.; Vazquez, M. *Mater. Sci. Eng., C-
       Biomimetic and Supramolecular Systems* **2003**, *23*, 1129.

26) Israelachvili, J. N. *Intermolecular and Surface Forces*; Academic Press Ltd.: San
    Diego, **2003**.

27) Ershov, B. G.; Sukhov, N. L.; Janata, E. *J. Phys. Chem. B* **2000**, *104,* 6138.

28) Glavee,G. N.; Klabunde, K. J.; Sorensen, C. M.; Hadjipanayis, G. C. *Langmuir*
    1993, *9,* 162.

29) Legrand, J.; Taleb, A.; Gota, S.; Guittet, M.- J.; Petit, C. *Langmuir* **2002**, *18*,
    4131.

30) *Nanoparticle Assemblies and Superstuctures,* N. A. Kotov, (ed); CRC Press:Boca
    Raton, **2006**.

31) (a) Sorensen, C. M. *Nanoscale Materials in Chemistry*, K. J. Klabunde, (ed.);
       Wiley: New York, **2001**.
    (b) Cullity, B. D. *Introduction To Magnetic Materials*; Addison-Wesley: London,
       1972.

32) Watanabe, K.; Nakama, Y.; Yanaki, T.; Hoffmann, H. *Langmuir* **2001**, *17, 7219.*

Chapter III

Role of alkanethiol in the formation of organized assemblies of gold nanoparticles
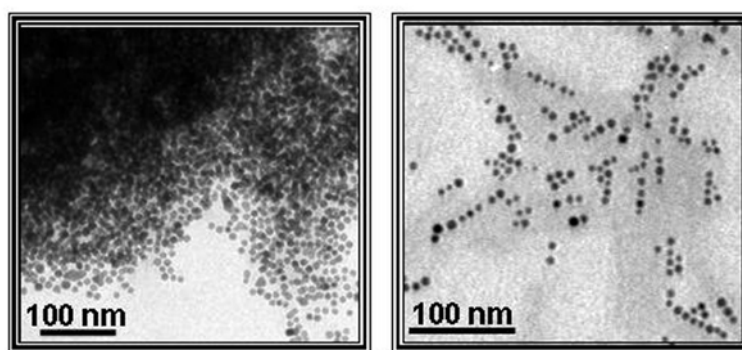
This chapter describes the synthesis of alkanethiol functionalized gold nanoparticles by digestive ripening method and the role of excess thiol in their subsequent organization. The first part of the chapter describes the preparation and closely packed 3 dimensional assembly of dodecanethiol capped gold nanoparticles. The melting properties of these capped nanoparticles have been studied using techniques like TGA and DSC. The second part of the chapter explains the production and linear organization of hexadecanethiol capped gold nanoparticles. The mechanism for linear assembly formation has also been probed.

3.1 Introduction

Gold nanoparticles are potential candidates for diverse applications in fields such as bio-medicine and optoelectronics [1]. A variety of ligands have been used to functionalize gold nanoparticles. Thiol molecules are widely used for capping gold nanoparticles due to the comparatively greater affinity between gold and sulfur. In addition, these nanoparticles can be separated from the solvent as a dry powder and also redispersed in different solvents. Thus, synthesis methods for thiol capped nanoparticles are witnessing a great surge in recent years [2]. But, in order to use nanoparticles for an application, it is necessary to have control over their properties. Since, properties of the nanoparticles are significantly size dependent [3], a narrow size dispersion of nanoparticles is desirable from the point of view of applications. Synthesis methodology based on digestive ripening is well-known to yield such monodisperse nanoparticles [4]. Hence, the same method has been used in this work to synthesize thiol functionalized gold nanoparticles of monodisperse nature.

Apart from synthesis, assembly of nanoparticles is a crucial step in order to reach the stage of applications. Traditionally, to obtain long-range and uniform assemblies of particles, top-down approach is preferred. But due to factors like cost and resolution, researchers are striving to prepare assemblies by bottom-up approach or by self-assembly. The nature of assembly can be determined by several parameters. Some of the salient factors are as follows 1) particle size – usually uniform particles i.e. with narrow size dispersion are desirable. 2) morphology of constituent nanoparticles 3) length and bulkiness of stabilizing ligand decide the interparticle spacing in the assembly 4) characteristics of solvents 5) rate of evaporation of solvent 6) interactions between nanoparticle – steric, van der Waal, dipole interactions etc. 7) nature of substrate 8) temperature and pressure conditions 9) presence of external stimulus.

Superlattices are densely packed three-dimensional assemblies of nanoparticles. They involve self-assembly of nanocrystals encapsulated within a protective ligand into a crystalline material. Klabunde's group has reported the formation of superlattices of alkanethiol coated nanoparticles [5]. Au nanocluster superlattices were obtained by Giersig and Mulvaney where the gold nanoparticles were prepared by citrate reduction and the assembly was obtained by applying voltage [2a]. Since then, there has been a rising interest in formation of superlattices of a

single [6] or a variety of compositions e.g. binary superlattices [7]. The superlattices are further useful when made up of monodisperse nanoparticles. The next step in this field will be the preparation of 'designer' superlattices where their ordering can be modulated. In order to do that, the mechanistic aspects of formation of superlattices or the closely packed ordered assemblies need to be understood. It could be possible that the capping agent might be playing a crucial role in the formation of such assemblies. In this chapter, an attempt has been made to understand, in a more detailed way, the role of capping agent in the assembly process.

Keeping this in mind, compact assemblies of highly monodisperse dodecanethiol capped gold nanoparticles have been prepared first. Then, the mechanism of their formation and the effect of temperature on them have been investigated. During the literature survey regarding temperature effects on the ligand protected metal nanoparticles and their superlattices, two types of reports were found. The first one dealt with order-disorder transitions of the self assembled monolayers of the ligands. For example, Lennox and co-workers [8], in their reports, have pointed out the similarity between self-assembled monolayers on the bulk surfaces and capping ligands of the nanoparticles. The second type dealt with transitions and melting of the entire superlattice. Pradeep *et al.* [9] studied the melting of superlattices revealing the melting point transitions. Vijayamohanan and co-workers studied the effect of temperature on long-range and ordered superlattice structures of dodecanethiol coated gold nanocrystals [10]. They observed an irreversible phase transition to a disordered state upon heating. Landman and Luedtke also studied the structural transformations induced by thermal effects [11]. In such studies, many times, the amount of thiol present in the samples was found to be greater than that expected if a monolayer of thiol was capping the gold nanoparticles. But, this factor was not probed further. Hence, in the present work, it was probed whether this excess thiol could dictate the formation of assemblies and then in any way influence their properties .

Apart from 2D and 3D superlattices of nanoparticles, one-dimensional (1D) chains of regularly spaced nanoparticles are also interesting especially for applications in the field of optoelectronics. A variety of techniques have been employed to prepare 1-D assemblies of metal nanoparticles which mainly include nanopatterning techniques, methods using linear templates such as DNA, polymer, liquid crystal

ligands, nanofibers, nanotubes [12-14] or by co-ordination chemistry [15], controlled washing [16], evaporation induced assembly [17], electrostatic attraction [18], selective functionalization [19], controlled ligand exchange [20], interparticle interaction [21] electrical stimulation [22] etc.

One-dimensional assembly of hexadecanethiol capped gold nanoparticles was acquired. Consequently, the mechanistic aspects of this linear organization were investigated. Previously, there have been attempts to understand the mechanism of one dimensional organization of alkanethiol coated gold nanoparticles. Rao and co-workers have worked out a detailed phase diagram of two-dimensional arrays of palladium nanoparticles where the thiol-capped nanocrystals were treated as soft spheres [23]. The phase diagram revealed the dependence of the array structure crucially depends on the particle diameter (d) and alkanethiol chain length (l). Also, when the value of diameter - chain length ratio reaches 1.5, these 1-D strings of palladium nanoparticles are said to be observed. There have been some reports of formation of evaporation induced 1-D assembly [24]. However, the reasons for such linear assemblies are poorly understood. The experiments reported in this work also lead to linear organization of nanoparticles. The mechanism behind this linear organization was investigated and a combination of a lamellar template and solvent evaporation was found to be the driving force for such organization. There has been a lot of interest in studying structures involving Au-thiol interaction [25] and this work can be significant in this regard as well.

3.2 Preparation and superlattice formation of dodecanethiol capped gold nanoparticles

In this section, initially, the protocol for synthesis of dodecanethiol capped gold nanoparticles is delineated. It is followed by characterization results for individual nanoparticles and their assemblies.

3.2.1 Preparation of dodecanethiol coated gold nanoparticles

The protocol used for the synthesis has been pioneered by Klabunde's group and involves digestive ripening method to achieve size monodispersity [4]. The scheme and the mechanism of this protocol are portrayed in fig. 3.1.
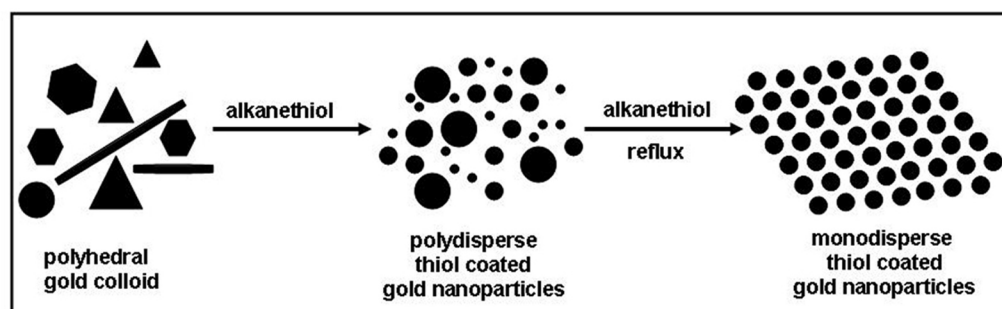
Fig. 3.1 *The schematic displaying synthesis protocol for alkanethiol coated gold nanoparticles. The protocol is based on digestive ripening method. (Schematic not to scale, adapted from [4j]).*

As seen in the scheme, initially, gold colloid comprising of different shapes of particles including rods, polyhedra and spheres is obtained by reduction of gold salt in the presence of a surfactant. This colloid breaks down into polydisperse alkanethiol coated spherical nanoparticles after addition of alkanethiol. Further, on refluxing with more portion of thiol, these nanoparticles convert to highly monodispersed ones.

In a typical experiment, initially, 0.1841 g of didodecyldimethylammonium bromide (DDAB) was dissolved in 20 mL of toluene to prepare inverse miceller solution of 0.02M. Next, 68 mg of $AuCl_3$ was added to this colourless solution followed by sonication during which, colour of the solution was seen to turn dark orange. This solution turned red after the dropwise addition of the reducing agent (72 μL of 9.4 M aqueous solution of sodium borohydride) accompanied by stirring. The stirring was continued for 15 min. to ensure the completion of reaction.

The next step was the addition of dodecanethiol to the gold nanoparticle solution maintaining the Au/thiol molar ratio to be 1:30. To remove the excess DDAB and the reaction side products from this solution, ethanol was added to it and the solution was left undisturbed overnight after which the gold colloid was seen to settle down. The supernatant was discarded and the isolated precipitate was dried. This dried precipitate was then redispersed in 20 mL toluene to form a homogeneous solution, to which, dodecanedecanethiol was added, again keeping the Au/thiol molar ratio to be 1:30. This final solution was then refluxed for 1.5 h. under argon atmosphere. The refluxed solution was cooled and the precipitate was extracted and was used for further analysis. This as-prepared sample would be denoted as sample "Au-th12" hereafter in the text. The second sample would be denoted as "Au-

th12_wash" as it was prepared by washing a part of sample Au-th12 extensively by using ethanol and acetone.

The main characterization technique used was transmission electron microscopy. For this, gold nanoparticle solution was drop-casted on a carbon coated TEM grid and was allowed to air-dry without any external assistance. The TEM studies revealed the formation of spontaneous assemblies. To probe the formation of assembly, the samples were subjected to TGA and DSC measurements. UV-vis absorbance and XRD analysis were used to find out composition of the samples. The results obtained after characterization would be described in the subsequent section.

3.2.2 Characterization results

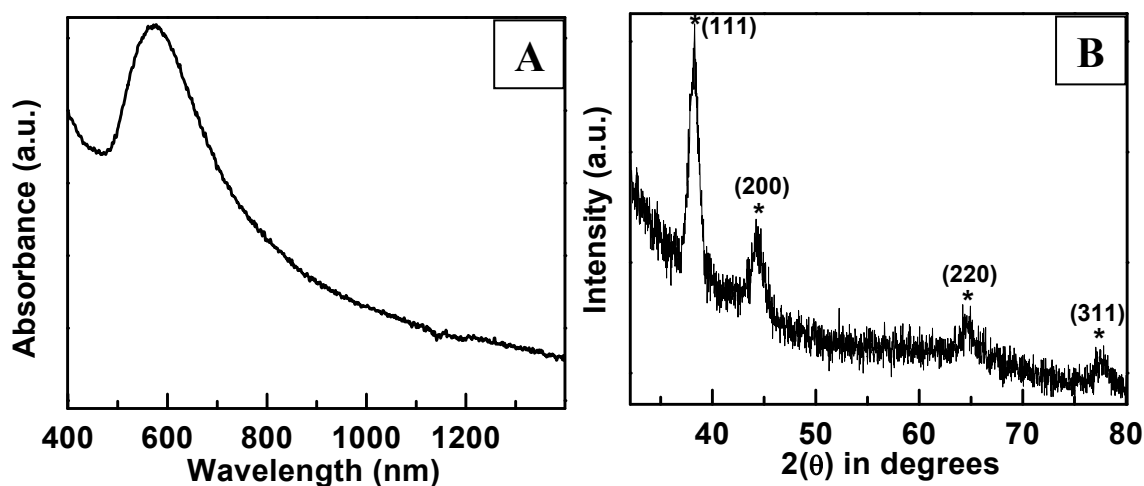### 3.2.2.1 Properties of dodecanethiol coated nanoparticles

Fig. 3.2.1 A) *UV-visible absorption spectrum of the dodecanethiol coated gold nanoparticles obtained by digestive ripening method* **B)** *X-ray diffraction curve of dodecanethiol capped gold nanoparticles showing four prominent peaks (marked by *) with 2θ values of 38.28°, 44.40°, 64.67° and 77.28° respectively.*

UV- visible absorption spectrum of sample Au-th12 is shown in Fig. 3.2.1 A. The peak position is seen at 570 nm. The peak for isolated gold nanoparticles is expected to be at around 520 nm [3]. The shift of the peak position towards higher wavelength suggests the decrease in interparticle distance of gold nanoparticles [3].

The XRD spectrum corresponding to sample Au-th12 is displayed in fig. 3.2.1 B The spectrum shows four prominent peaks at 2θ values of 38.28°, 44.40°, 64.67° and 77.28° .The d spacings corresponding to them are 0.235 nm, 0.205 nm, 0.144 nm

and 0.123 nm respectively. These values match exactly with standard d values of fcc gold (PCPDF card no. 04-0784).

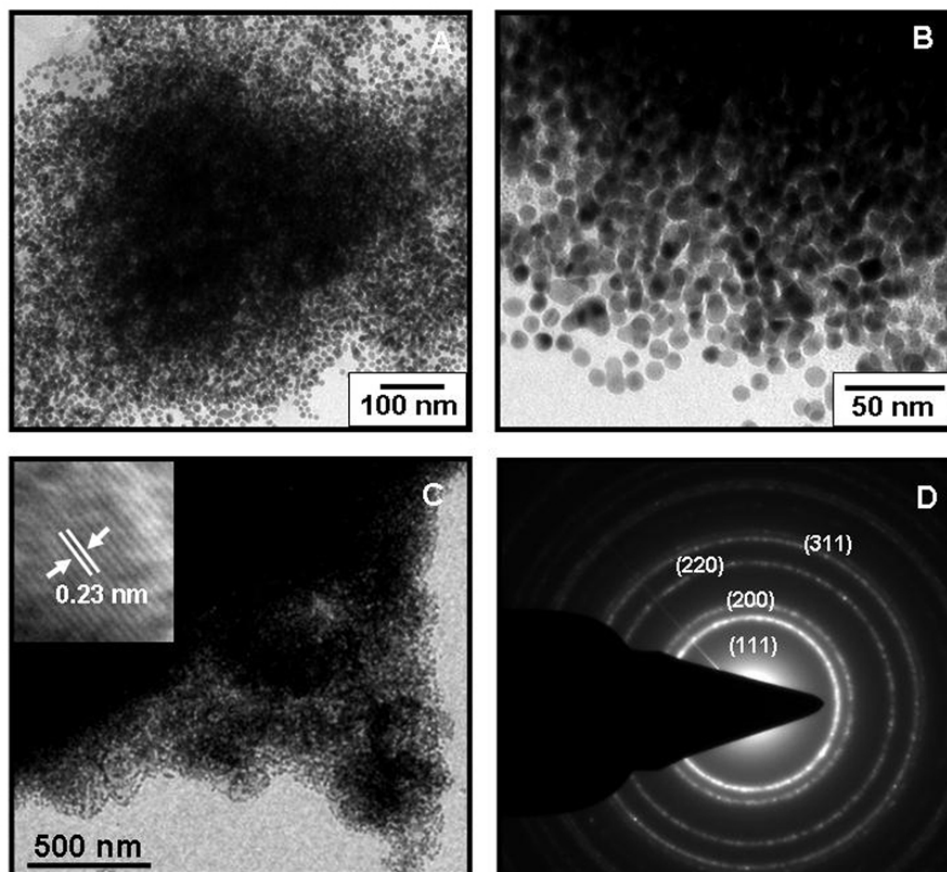### 3.2.2.2 Assembly formation of dodecanethiol coated nanoparticles

Fig. 3.2.2 A, B and C) *Representative TEM images of sample dodecanethiol coated gold nanoparticles showing densely populated and spontaneous organization of the gold nanoparticles. Inset of C shows the HRTEM image of a single nanoparticle showing lattice spacing of 0.23 nm.* **D)** *SAED pattern showing four prominent rings .*

Fig. 3.2.2 shows the results of TEM analysis for the dodecanethiol coated gold nanoparticles. Fig. 3.2.2 A, B and C are the representative TEM images of sample Au12-th while Fig. 3.2.2 D is the selective area electron diffraction (SAED) obtained from it. The inset of Fig. 3.2.2 C shows the high resolution TEM image of the sample with a lattice spacing of 0.23 nm which is in agreement with the lattice spacing for fcc phase of gold nanoparticles (PCPDF card no. 04-0784).

The TEM images reveal spontaneous self-assembly of the gold nanoparticles. The central portion of these assemblies is so densely populated that the electron beam could not pass through and hence is seen as dark area in the TEM images. Such

structures are present all over the TEM grid and resemble the superlattices. The HRTEM image (inset of Fig. 3.2.2 C) displays the lattice planes and hence confirms the crystalline nature of the nanoparticles. The obtained interplaner spacing of 0.23 nm matches with that of fcc phase of gold. SAED also shows rings having d-values matching with (111), (200), (220) and (311) planes further confirming the crystallanity and fcc phase of gold.
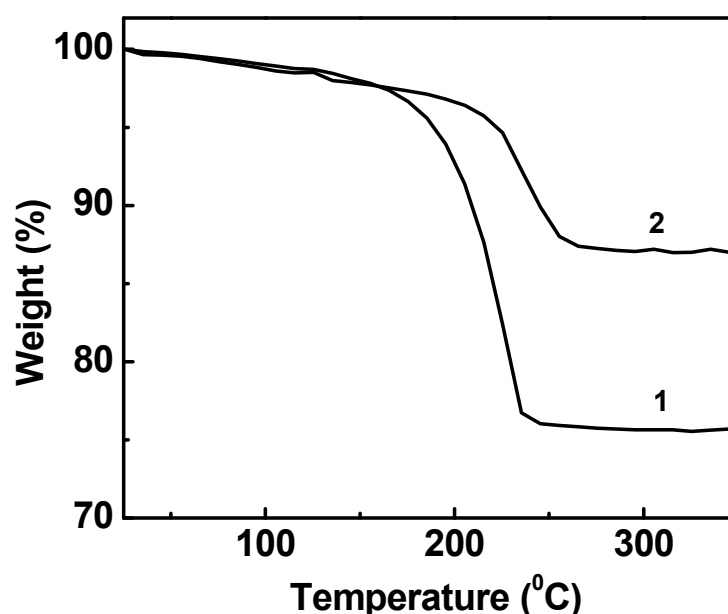
3.2.2.3 Thermogravimetric analysis (TGA)

Fig. 3.2.3 *TGA curves corresponding to sample Au-th12 (curve1) and Au-th12_wash   (curve 2) showing total weight loss of 18% and 11% respectively.*

In order to probe the driving forces for the formation of superlattices, thermogravimetric analysis of samples Au-th12 and Au-th12_wash was done. The TGA curves are shown in Fig. 3.2.3 where curve 1 corresponds to sample Au-th12 while curve 2 corresponds to sample Au-th12_wash. Curve 1 from Fig. 3.2.4 corresponds to sample Au-th12 and shows a total weight loss of 18% while curve 2 is recorded from sample Au-th12_wash and demonstrates a weight loss of 11%. The decrease in weight-loss could be attributed to extensive washing of the sample. TEM images from Sample Au-th12_wash were recorded and are shown in Fig. 3.2.5. The samples were further subjected to Differential scanning caloriemetry (DSC) studies.

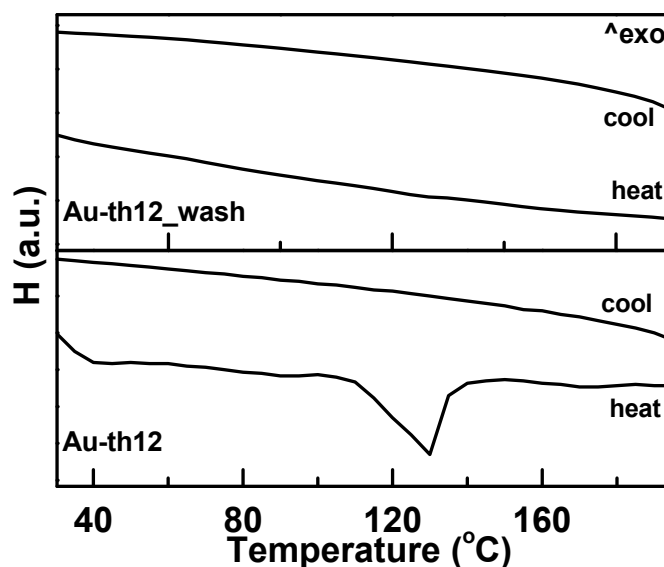**3.2.2.4 DSC studies (room temperature-200 °C– room temperature cycle)**

Fig. 3.2.4 *DSC analysis curves (enthalpy (H) plotted against temperature) of the samples Au-th12 and Au-th12_wash corresponding to the heating and cooling part of the room temperature-200 °C– room temperature cycle.*

Fig. 3.2.4 shows the melting characteristics of the samples Au-th12 and Au-th12_wash obtained from DSC. The temperature variation was done in the following way. The analysis was started at room temperature. First, the samples were heated to 200 °C and then cooled back to room temperature. An endothermic peak was seen at 129 ° C during the heating part whereas no peak is seen in the cooling curve. This peak was absent in the DSC curves for Au-th12_wash which showed no prominent peak. To find whether the absence of peak was an indication of changes in the superalttices, TEM images of sample Au-th12_wash were taken.

3.2.2.5 TEM analysis of sample Au-th12-wash

The TEM images show disappearance of the dense nature of assemblies after extensive washing of the sample. The nanoparticles appear to be more isolated and retain their crystallanity as seen from the HRTEM image of a single electron (inset of Fig. 3.2.5 C) and the SAED (Fig. 3.2.5 D). The value of lattice spacing obtained from HRTEM image corresponds to (111) plane of fcc Au in consonance with the sharp ring patterns of SAED that could be indexed to give d values matching excellently with the standard d values of (111), (200), (220) and (311) planes of fcc Au.
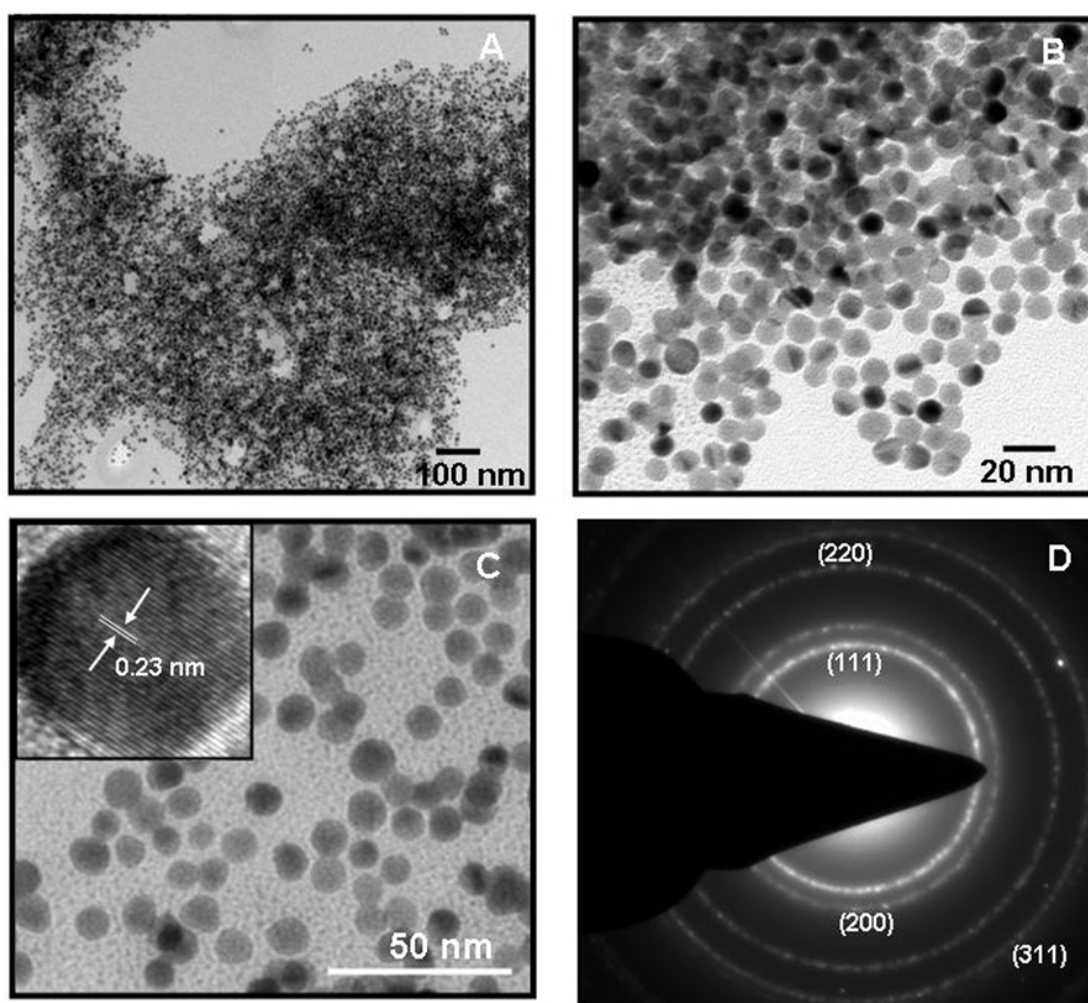
Fig. 3.2.5 A, B and C) *Representative TEM images obtained from sample Au-th12-wash reveal that the spontaneously organized assemblies are not densely populated. Inset of C shows the HRTEM image of a single nanoparticle displaying crystalline nature with lattice spacing of 0.23 nm.* **D)** *SAED pattern showing rings having corresponding d values equivalent to those of (111), (200), (220) and (311) planes of fcc phase of gold.*

The weaker interaction of the nanoparticles and the voids seen in the assembly could be due to the absence of forces leading to the assembly caused by washing of the sample. The TGA results seem to be in accordance with the TEM images of the two samples (Fig. 3.2.2 and Fig. 3.2.5) where, the compactness of the assemblies was seen to reduce for the washed samples.

3.2.2.6 Comparative DSC studies (room temperature-300 °C– room temperature cycle)

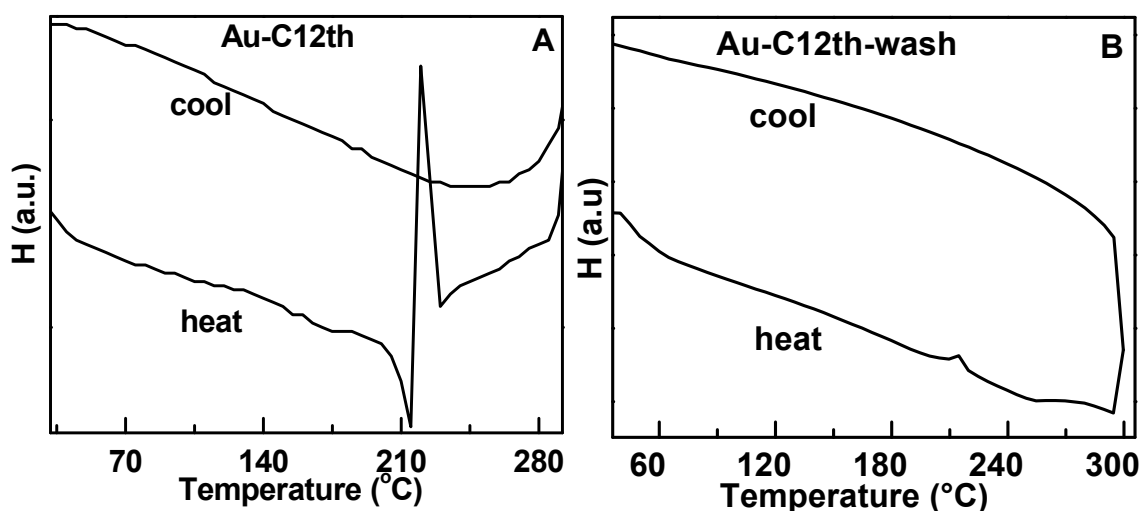**Fig. 3.2.6** *DSC analysis curves of the dodecanethiol coated gold nanoparticles (sample Au-th12) and sample Au-th12_wash corresponding to the heating and cooling part of the room temperature-300°C– room temperature cycle.*

Fig. 3.2.6 shows comparative DSC studies (room temperature-300 °C– room temperature cycle). Here, the DSC analysis was started at room temperature. First, the samples were heated to 300 °C and then cooled back to room temperature. The DSC curves for the two samples are shown in Fig. 3.2.6. Heating curves for samples Au-th12 and sample Au-th12_wash show an exothermic peak and hump respectively at ~215 °C. The cooling curves corresponding to both the samples do not display any peak. The difference between the DSC curves for sample Au-th12 and Au-th12_wash is in accordance with the results obtained from the TEM and TGA measurements of both samples.

3.2.3 Discussion

The formation of crystalline gold nanoparticles with fcc phase is confirmed from the UV-visible absorption spectrum, XRD patterns, HRTEM image and the SAED image of sample Au-th12. The HRTEM image and SAED of sample Au-th12_wash confirms that the crystalline fcc nature of gold nanoparticles has been retained even after extensive washing.

As a part of the synthesis protocol, excess dodecanethiol has been added for refluxing the nanoparticles. The dodecanethiol molecules acting as a capping agent for the gold nanoparticles would remain confined to the nanoparticle surface while the remaining molecules would be present in the solution.

The results obtained from this study thus can be summarized as follows:

- Digestive ripening of a polydisperse colloid with dodecanthiol leads to highly monodisperse particles.

- Such monodisperse particles come together and form 3D self-assembled superlattice structures.

- These superlattices show melting like characteristics as can be seen from an endothermic peak at 129 ^{o} C in the DSC curve in the room temperature- 200 ^{o}C- room temperature cycle of sample Au-th12.

- Interestingly, these superlattices are associated with the presence of excess thiol i.e. more than expected if the thiol was forming only a monolayer on each gold nanoparticle surface. This excess thiol could be removed by excessive washing. The weight loss obtained from the TGA of sample Au-th12 is 18 wt % (see curve 1, Fig. 3.2.3). In case of sample Au-th12_wash, the weight loss is seen to reduce to 11 wt % . (see curve 2, Fig. 3.2.3).

- The washed sample neither forms dense superlattice structures nor shows melting-like characteristics in DSC scan.

- In the room temperature-300 ^{o}C-room temperature cycle, the heating curves from both samples depict an exothermic peak at ~215 ^{o}C. Such a peak could be attributed to the desorption of alkanethiol. Plausible explanation for the exothermicity is the concomitant formation of disulfide bond when the disorbed thiol molecules combine to form a disulfide and hydrogen.

From these, it can be hypothesized that the superlattice formation critically depends on the presence of excess thiol that probably is getting trapped in the interstitial sites of superlattices. Upon heating these superlattices, this excess thiol present in the interstitial sites leads to disintegration of the superlattices showing melting like feature in the form of an endothermic peak in DSC. This peak is not

reversible suggesting this to be similar to a glass-like transition. In case of the washed sample, as the excess thiol has already been washed off, the nanoparticles interact weakly and are comparatively isolated; therefore, do not form a superlattice. The absence of the superlattice precludes any melting behavior, which explains the absence of the peak in the washed sample. However, heating beyond 200 $^{\circ}$C leads to an exothermic peak in DSC, which could be caused due to desorption and concurrent formation of disulfide from the thiol molecules adsorbed on the gold nanoparticles- as observed for sample Au-th12.

This means that if the proportion of the excess alkanethiol can be tuned, the formation of superlattices would be controlled. Such studies can be extended to other alkanethiols like octanethiol which are also known to form superlattices. The superlattices can be used for various applications like for example in the field of metamaterials [26].

3.3 Synthesis and linear assembly formation of hexadecanethiol coated gold nanoparticles

3.3.1 Preparation and assembly of hexadecanethiol coated Au nanoparticles

The hexadecanethiol coated gold nanoparticles were synthesized as described above in section 3.2.1 but the difference was that they were not refluxed in argon atmosphere. The as-prepared sample obtained after synthesis would be denoted as sample "Au-th16". It was used as it is or as a redispersion for further characterization. A drop of the solution of hexadecanethiol coated gold nanoparticles was added on a TEM grid and was allowed to air-dry without any external assistance. The powder was subjected to TGA and SAXS studies. Sample Au-th16 was washed multiple times using ethanol and acetone. The resultant washed and dried precipitate will be denoted as sample "Au-th12_wash". The sample Au-th16_wash was also analyzed by the TEM, TGA and SAXS techniques.

3.3.2 Characterization results and discussion

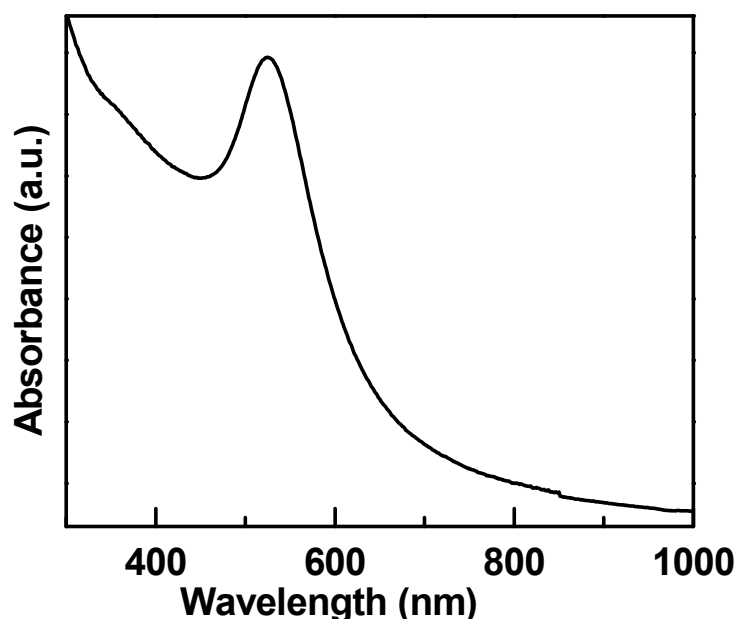### 3.3.2.1 UV-visible absorption spectroscopy and XRD analysis

Fig. 3.3.1) *UV-visible absorbance spectrum recorded from sample Au-th16 demonstrating the surface plasmon resonance peak from gold nanoparticles.*

The characterization of sample "Au-th16" was initiated with the measurement of optical properties. Fig. 3.3.1 shows the UV-visible absorbance spectrum depicting

a prominent peak at 525 nm corresponding to the surface plasmon resonance peak of gold nanoparticles.
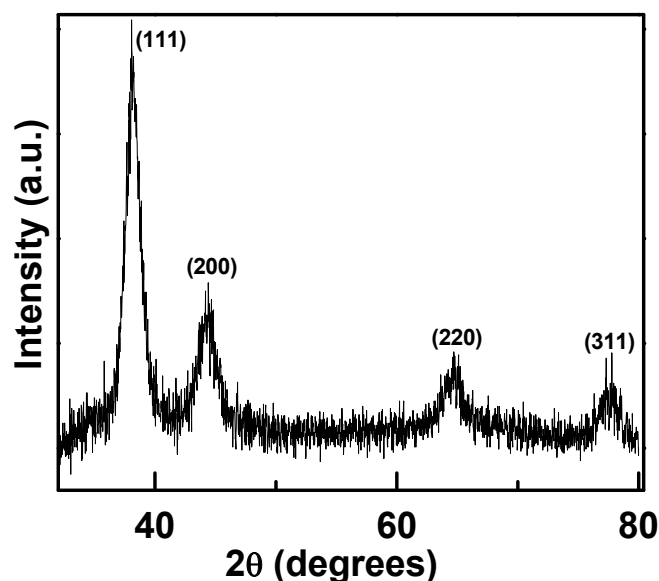

Fig. 3.3.2 *XRD pattern of sample Au-th16 showing Bragg reflections at 2θ values of 38. 20°, 44.40°, 64.63° and 77.66° respectively.*

The existence of gold nanoparticles was further confirmed from the X-ray diffraction analysis of the sample Au-th16. Bragg reflections recorded from drop-cast films of the sample are seen in Fig. 3.3.2. Four major peaks are found to be at 2θ values of 38. 20°, 44.40°, 64.63° and 77.66° corresponding to d values of 0.235 nm, 0.203 nm, 0.144 nm and 0.123 nm respectively.

3.3.2.2 TEM Analysis

The most important evidence of formation of linear assembly comes from its TEM images. Fig.3.3.3 shows TEM images taken at different magnifications. Initially, at the lowest magnification, there is just an indication of the presence of a region of low contrast as seen in Fig. 3.3.3 A. As this region was magnified by TEM, a criss-cross network of darker bands was seen to lie on top of it (Fig. 3.3.3 B).

Further magnified images reveal that these bands were made up of short-range linear assemblies containing around 5 to 6 nanoparticles. The average diameter of nanoparticles is found to be ~ 7 nm. The orientation of the lines differed, though locally 2-3 lines were seen to be parallel with each other. But the most noticeable fact is the coexistence of the linear assemblies with the low-contrast material seen in the
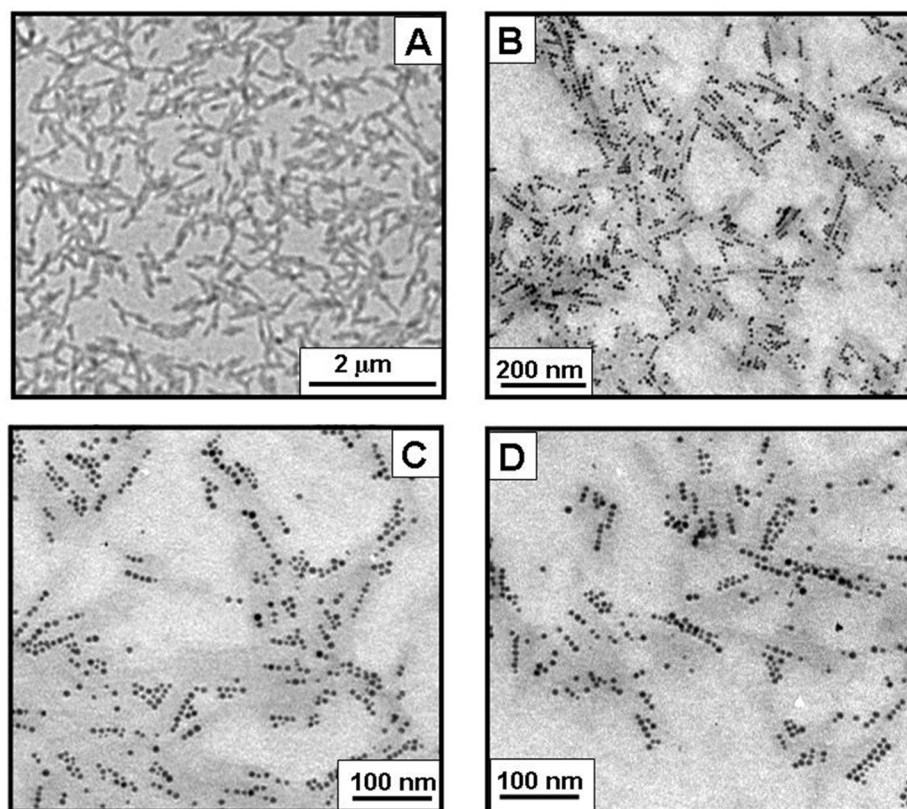
Fig. 3.3.3 *Representative TEM images corresponding to sample Au-th16 illustrating the linear assembly of gold nanoparticles. The magnification increases as one moves on from image A to image B and then finally to images C and D. The short range assemblies are seen to ride over a region of lower contrast.*

lower magnification images of the TEM. This hints at the assembly being template directed. But then the composition of the template needs to be found out and its origin has to be investigated. In order to do this, sample Au-th16_wash was prepared after careful washing.

It was expected that the moiety giving low contrast would be washed off and hence the TEM images of this sample would be different from that of sample Au-th16. The representative TEM image of a thoroughly washed sample, depicted in Fig. 3.3.4, indeed does not reveal any linear assemblies. Here, the loss of linear nature of the assemblies is clearly associated with simultaneous disappearance of a region of low contrast surrounding the linear assembly observed in case of as-prepared sample Au-th16. This indicates that the hexadecanethiol capped gold nanoparticles have been directed to organize in a linear fashion by the moiety giving low contrast. The

removal of low contrast giving moiety after washing of the sample can be quantitatively verified by TGA measurements.
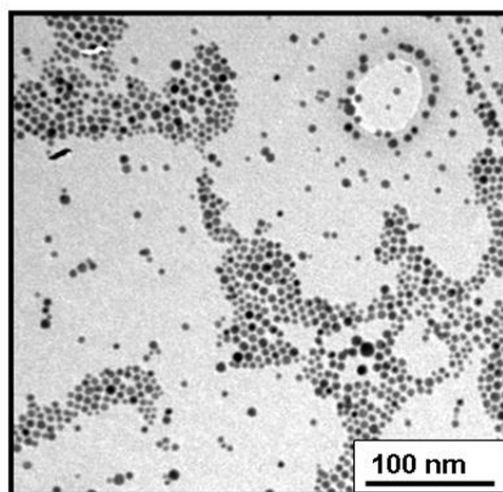
Fig. 3.3.4 *TEM images of sample Au-th16_wash depicting non-linear assembly of gold nanoparticles with a concomitant absence of region of low contrast.*

3.3.2.3 Thermogravimetric Analysis

Both, as-prepared and washed sample were subjected to thermogravimetric measurements. The TGA curves for sample Au-th16 and sample Au-th16_wash are seen in Fig. 3.3.5.
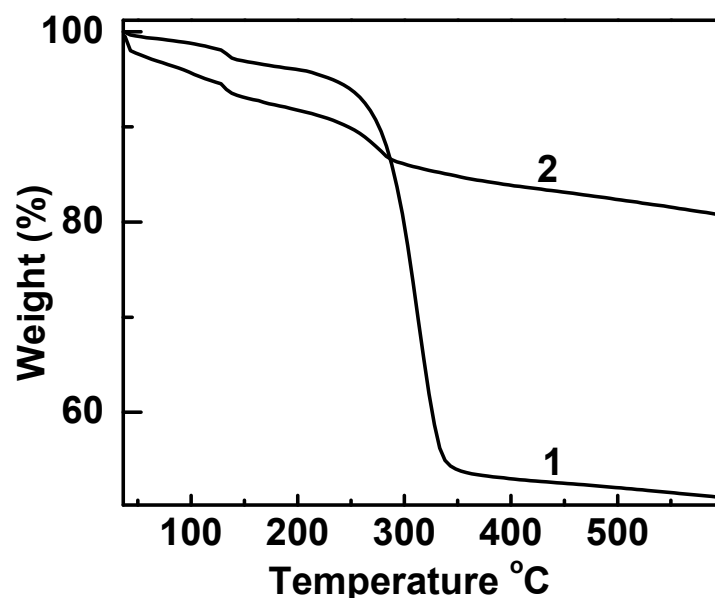
Fig. 3.3.5) *TGA recorded from sample Au-th16 showing weight loss of 50% (curve 1) and sample Au-th16_wash (curve 2) depicting weight loss of ~ 20% which is significantly lower as compared to sample Au-th16.*

The weight-loss for sample Au-th16 is observed to be 50% (curve 1, Fig. 3.3.5), which is very high when judged against the estimated value of thiol fraction if just a monolayer of thiol were present on each nanoparticle, which was calculated (using the footprint area of 21.4 Å^2 [27] to be close to 11%. The details of this calculation for estimating the weight fraction of capping thiol on a gold nanoparticle of size 7 nm are given in Appendix 1. The final value was calculated keeping in mind the reports that thiol coverage on the spherical nanoparticles (3D configuration) is 30% excess than that expected for 2-D film [28]. The weight-loss for Sample Au-th16_wash happens to be 20% (curve 2, Fig. 3.3.5) - a value comparatively closer to that estimated. This indicates that the template for the assemblies constitutes of something other than the monolayer of hexadecanethiol. One possibility for this would be the formation of gold thiolate as a result of extensive refluxing of the gold colloid in the presence of excess alkanethiol.

3.3.2.4 SAXS Measurement

Powders of sample Au-th16 and sample Au-th16_wash were analyzed by Small Angle X-ray Scattering (SAXS) technique. The results are shown in Fig.3.3.6.
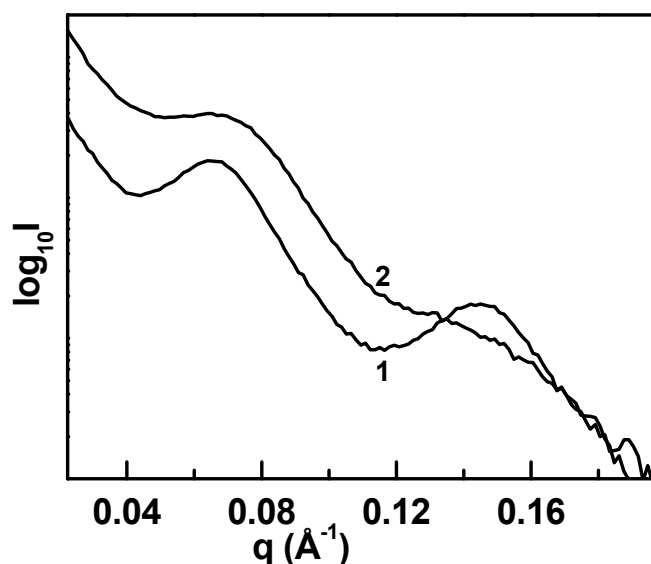

Fig. 3.3.6) *Graph of SAXS plotted as log_{10}Intensity vs. wavevector q. Curve 1 corresponds to sample Au-th16 while curve 2 is recorded from sample Au-th16_wash.*

Curve 1 corresponds to sample Au-th16 and shows two prominent peaks – one at wavevector value ~0.065 Å^{-1} and the other at ~0.135 Å^{-1}. So, the ratio of their wavevectors comes out to be ~1:2. In case of Sample Au-th16_wash (curve 2), the first peak is marginally broadened but appeared at the same position while the second peak has subsided significantly.

3.3.2.5 Hypothesis for the formation of linear assembly

Taking into consideration, all the results discussed above, we propose a hypothesis that the linear assembly is an outcome of nanoparticles held together by a lamellar template.
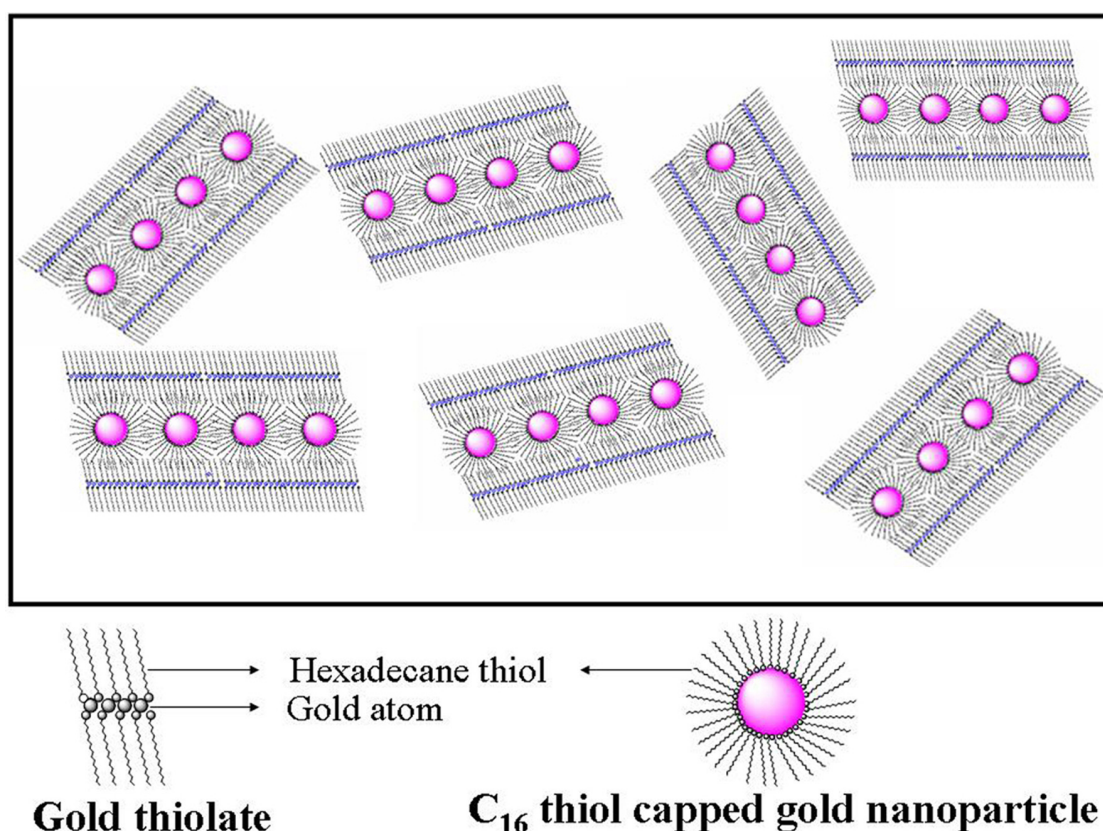
Fig. 3.3.7) *Schematic illustrating the hypothetical mechanism for linear assembly formation of gold nanoparticles. Lamellar nature of gold thiolate is assumed to act as a template forcing the nanoparticles to form short-range linear organizations.*

It is well reported in the literature that the metal and sulfur from the alkanethiol can interact and form alkylthiolates [28, 29]. It is known that alkylthiolates have a lamellar structure [30]. Hence here, gold thiolate could be forming during the digestive ripening process whereby gold nanoparticles were extensively refluxed in the presence of excess hexadecanethiol and in ambient

atmosphere. The nanoparticles would be embedded linearly in these gold thiolate layers as shown in the schematic in Fig 3.3.7.

To support the hypothesis, the following arguments are presented:

1) The TEM images displayed that the linear assemblies were always accompanied by the region of low contrast. The arrangement of nanoparticles was linear and short range. After washing of the sample, the linear organization disappeared along with the surrounding moiety. This indicates the presence of template which is present in the sample and which could be washed off with ethanol and acetone.

2) TGA results are also in accordance with the TEM images. The higher value of weight loss in sample Au-th16 as compared to the estimated value, points at the presence of some moiety which gets washed off and hence the weight loss for the washed sample is seen to decrease to a value closer to the expected value.

3) From the literature, it is known that the metal and sulfur from the alkanethiol can interact and form alkanethiolates and that such thiolates are known to have a lamellar structure. Here, the gold colloid was refluxed along with excess hexadecanethiol as part of the digestive ripening process. Hence, there could be an interaction between the sulfur from alkanethiol and the gold atoms from the nanoparticles to give rise to the gold thiolate formation. Now, as the gold nanoparticles are coated with hexadecanethiol, the alkyl chain can possibly have mutual affinity towards the thiolates due to the van der waal attraction. Due to this, these nanoparticles could get embedded in the lamellar structure of gold-thiolates and hence appear as linear assemblies.

4) In case of SAXS analysis, the peak positions of the wavevectors in the SAXS plot would follow certain patterns depending upon the morphology of the microdomains in the sample [31]. The sequence of peak values should be 1, 2, 3, 4… for lamellar microdomain; 1, $\sqrt{3}$, $\sqrt{4}$, $\sqrt{7}$, ... for cylinders in a hexagonal array and 1, $\sqrt{2}$, $\sqrt{3}$, $\sqrt{4}$, ... for spheres in a body-centered cubic array etc. In our case, the peak value ratio has been ~1:2 which point towards a lamellar microdomain as expected for gold thiolates. The deformation of peaks in case

of the washed sample could be a sign of disappearance of the thiolate templates after washing.

The results described above are in agreement with the hypothesis made. Hence it appears that the linear assembly is a template directed process. The role played by evaporation of solvent to form assembly is not ruled out but the disappearance of assembly in case of washed sample favours the hypothesis.

3.4 Conclusion

Digestive ripening method could be used to prepare monodisperse alkanethiol coated gold nanoparticles in organic medium. These nanoparticle are seen to demonstrate interesting kind of assemblies spontaneously. In case of dodecanethiol capped gold nanoparticles, the assemblies were in the form of superlattices while the hexadecanethiol capped gold nanoparticles organized in a linear formation. The assembly is seen to be a function of synthesis parameters. The capping agent may be playing a greater role than just a 'spectator' or just slowing down the evaporation process. The compactness of the superlattices is seen to vanish after extensive washing, pointing towards loss of binding moiety. To probe this further, the samples were characterized by different techniques. The melting properties of the closed assemblies were also studied. The analysis points towards the role of excess thiol in the assembly formation. Hence, if the proportion of the excess alkanethiol can be tuned, the formation of superlattices could be controlled as per the requirement of their applications. The mechanism of linear assembly formation was studied to perceive whether the construction of assembly was mainly a template directed process. This work will be helpful in understanding the formation and properties of assemblies of gold nanoparticles. Such understanding would further facilitate their use in diverse applications.

3.5 References

1) (a) Hutchings, G. J.; Brust, M.; Schmidbaur, H. *Chem. Soc. Rev*. **2008**, *37*, 1759.

   (b) Daniel, M. C.; Astruc, D. *Chem. Rev.* **2004**, *104*, 293.

   (c) Rosi, N. L.; Mirkin, C. A. *Chem. Rev.* **2005**, *105*, 1547.

   (d) Jain, P. K.; Huang, X.; El-Sayed, I. H.; El-Sayed, M. A. *Acc. Chem. Res.* **2008**, *41*, 1578.

   (e) Hu, M.; Chen, J.; Li, Z. Y.; Au, L.; Hartland, G. V.; Li, X.; Marquez, M.; Xia, Y. *Chem. Soc. Rev.* **2006**, *35*, 1084.

   (f) Murphy, C. J.; Gole, A. M.; Stone, J. W.; Sisco, P. N.; Alkilany, A. M.; Goldsmith, E. C.; Baxter, S. C. *Acc. Chem. Res.* **2008**, *41*, 1721.

   (g) Zhou, J.; Ralston, J.; Sedev, R.; Beattie, D. A. *J. Colloid Interface Sci.* **2009**, *331*, 251.

   (h) Dykman, L. A.; Bogatyrev, V. A. *Russ. Chem. Rev.* **2007**, *76*, 181.

2) (a) Giersig, M.; Mulvaney, P. *Langmuir* **1993**, *9*, 3408.

   (b) Brust, M.; Walker, M.; Bethell, D.; Schiffrin, D. J.; Whyman, R. *J. Chem. Soc., Chem. Commun.* **1994**, 801.

   (c) Zhang, S.; Leem, G.; Srisombat, L. O.; Lee, T. R. *J. Am. Chem. Soc.* **2008**, *130*, 113.

   (d) Schroedter, A.; Weller, H. *Angew. Chem. Int. Ed.* **2002**, *41*, 3218.

   (e) Lin, X. M.; Sorensen, C. M.; Klabunde, K. J. *Chem. Mater.* **1999**, *11*, 198.

   (f) Leff, D. V.; Ohara, P. C.; Heath, J. R.; Gelbart, W. M. *J. Phys. Chem.* **1995**, *99*, 7036.

   (g) Zhang, S.; Leem, G.; Srisombat, L. O.; Lee, T. R. *J. Am. Chem. Soc.* **2008**, *130*, 113.

3) Kelly, K. L.; Coronado, E.; Zhao, L. L.; Schatz, G. C. *J. Phys. Chem. B* **2003**, *107*, 668.

4) (a) Lin, X. M.; Sorensen, C. M.; Klabunde, K. J. *J. Nanopart. Res.* **2000**, *2*, 157.

   (b) Prasad, B. L. V.; Stoeva, S. I.; Sorensen, C. M.; Klabunde, K. J. *Langmuir* **2002**, *18*, 7515.

   (c) Lin, S. T.; Franklin, M. T.; Klabunde, K. J. *Langmuir* **1986**, *2*, 259.

(d) Stoeva, S.; Klabunde, K. J.; Sorensen, C. M.; Dragieva, I. *J. Am. Chem. Soc.* **2002**, *124*, 2305.

(e) Prasad, B. L. V.; Stoeva, S. I.; Sorensen, C. M.; Klabunde, K. J. *Chem. Mater.* **2003**, *15*, 935.

(f) Stoeva, S. I.; Smetana, A. B.; Sorensen, C. M.; Klabunde, K. J. *J. Colloid Interface Sci.* **2007**, *309*, 94.

(g) Smetana, A. B.; Klabunde, K. J.; Sorensen, C. M. *Interface Sci.* **2005**, *284*, 521.

(h) Kim, S. W.; Park, J.; Jang, Y.; Chung, Y.; Hwang, S.; Hyeon, T.; Kim, Y. W. *Nano Lett.* **2003**, *3*, 1289.

(i) Smetana, A. B.; Klabunde, K. J.; Sorensen, C. M.; Ponce, A. A.; Mwale, B. *J. Phys. Chem. B* **2006**, *110*, 2155.

(j) Stoeva, S. I.; Zaikovski, V.; Prasad, B. L. V.; Stoimenov, P. K.; Sorensen, C. M.; Klabunde, K. J. *Langmuir* **2005**, *21*, 10280.

(k) Barnard, A. S.; Lin, X. M.; Curtiss, L. A. *J. Phys. Chem. B* **2005**, *109*, 24465.

5) (a) Lin, X. M.; Sorensen, C. M.; Klabunde, K. J. *Chem. Mater.* **1999**, *11*, 198.

(b) Lin, X. M.; Wang, G. M.; Sorensen, C. M.; Klabunde, K. J. *J. Phys. Chem. B* **1999**, *103*, 5488.

(c) Lin, X. M.; Jaeger, H. M.; Sorensen, C. M.; Klabunde, K. J. *J. Phys. Chem. B* **2001**, *105*, 3353.

(d) Stoeva, S. I.; Prasad, B. L. V.; Uma, S.; Stoimenov, P. K.; Zaikovski, V.; Sorensen, C. M.; Klabunde, K. J. *J. Phys. Chem. B* **2003**, *107*, 7441.

(e) Prasad, B. L. V.; Sorensen, C. M.; Klabunde, K. J. *Chem. Soc. Rev.* **2008**, *37*, 1871.

6) (a) Abecassis, B.; Testard, F.; Spalla, O. *Phys. Rev. Lett.* **2008**, *100*, 115504.

(b) Andres, R. P.; Bielefeld, J. D.; Henderson, J. I.; Janes, D. B.; Kolagunta, V. R.; Kubiak, C. P.; Mahoney, W. J.; Osifchin, R. G. *Science* **1996**, *273*, 1690.

(c) Santhanam, V.; Liu, J.; Agarwal, R.; Andres, R. P. *Langmuir* **2003**, *19*, 7881.

(d) Murray, C. B.; Kagan, C. R.; Bawendi, M. G. *Annu. Rev. Mater. Sci.* **2000**, *30*, 545.

(e) Korgel, B. A.; Zaccheroni, N.; Fitzmaurice, D. *J. Am. Chem. Soc.* **1999,** *121,* 3533.

(f) Dong, T.- Y.; Wu, H.- H.; Lin, M.-C. *Langmuir* **2006**, *22*, 6754.

(g) Shen, C. M.; Hui, C.; Yang, T. Z.; Xiao, C. W.; Tian, J. F.; Bao, L. H.; Chen, S. T.; Ding, H.; Gao, H. J. *Chem. Mater.* **2008**, *20*, 6939.

(h) Zheng, N.; Fan, J.; Stucky, G. D. *J. Am. Chem. Soc.* **2006**, *128*, 6550.

(i) Martin, J. E.; Wilcoxon, J. P.; Odinek, J.; Provencio, P. *J. Phys. Chem. B* **2000**, *104*, 9475.

(j) Wang, Z. L.; Harfenist, S. A.; Vezmar, I.; Whetten, R. L.; Bentley, J.; Evans, N. D.; Alexander, K. B. *Adv. Mater.* **1998**, *10*, 808.

(k) Brown, L. O.; Hutchison, J. E. *J. Phys. Chem. B* **2001**, *105*, 8911.

(l) Kim, Y. H.; Lee, D. K.; Cha, H. G.; Kim, C. W.; Kang, Y. S. *Chem. Mater.* **2007**, *19*, 5049.

(m) Korgel, B. A.; Fullam, S.; Connolly, S.; Fitzmaurice, D. *J. Phys. Chem. B* **1998**, *102*, 8379.

7) (a) Shevchenko, E. V.; Talapin, D. V.; Kotov, N. A.; O'Brien, S.; Murray, C. B. *Nature* **2006**, *439*, 55.

(b) Kiely, C. J.; Fink, J.; Brust, M.; Bethell, D.; Schiffrin, D. J. *Nature* **1998**, *396*, 444.

(c) Saunders, A. E.; Korgel, B. A. *ChemPhysChem* **2005***, 6*, 61.

(d) Cheon, J.; Park, J. I.; Choi, J. S.; Jun, Y. W.; Kim, S.; Kim, M. G.; Kim, Y. M.; Kim, Y. J. *Proc. Natl. Acad. Sci. USA* **2006**, *103*, 3023.

(e) Brust, M.; Kiely, C. J. *Colloids Surf., A* **2002**, *202*, 175.

(f) Rogach, A. L.; Talapin, D. V.; Shevchenko, E. V.; Kornowski, A.; Haase, M.; Weller, H. *Adv. Funct. Mater.* **2002**, *12*, 653.

8) (a) Badia, A.; Cuccia, L.; Demers, L.; Morin, F.; Lennox, R. B. *J. Am. Chem. Soc.* **1997**, *119*, 2682.

(b) Badia, A.; Singh, S.; Demers, L.; Cuccia, L.; Brown, G. R.; Lennox, R. B. *Chem. Eur. J.* **1996**, *2*, 359

(c) Bensebaa, F.; Ellis, T. H.; Badia, A.; Lennox, R. B. *Langmuir* **1998**, *14*, 2361.

9) (a) Sandhyarani, N.; Resmi, M. R.; Unnikrishnan, R.; Vidyasagar, K.; Ma, S.

        G.; Antony, M. P.; Selvam, G. P.; Visalakshi, V.; Chandrakumar, N.;
Pandian, K.; Tao, Y. T.; Pradeep, T. *Chem. Mater.***2000**, *12*, 104.

    (b) Sandhyarani, N.; Antony, M. P.; Selvam, G. P.; Pradeep, T. *J. Chem. Phys.*
2000, *113*, 9794.

    (c) Sandhyarani, N.; Pradeep, T.; Chakrabarti, J.; Yousuf, M.; Sahu, H. K.
Phys. Rev. B **2000**, *62*, R739.

10) Chaki, N. K.; Vijayamohanan, K. P. *J. Phys. Chem. B* **2005**, *109, 2552.*

11) Landman, U.; Luedtke, W. D. *Faraday Discu.* **2004**, *125*, 1.

12) Warner, M. G.; Hutchison, J. E. *Nat. Mater.* **2003**, *2*, 272.

13) Cheng, J. Y.; Zhang, F.; Chuang, V. P.; Mayes, A. M.; Ross, C. A. *Nano
Lett.* **2006**, *6*, 2099.

14) In, I.; Jun, Y. W.; Kim, Y. J.; Kim, S. Y. *Chem. Commun.* **2005**, 800.

15) Wanunu, M. ; Popovitz-Biro, R. ; Cohen, H. ; Vaskevich, A. ; Rubinstein,
I. *J.Am. Chem. Soc*. **2005**, *127,* 9207.

16) Zhang, Y. X.; Zeng, H. C. *J. Phys. Chem. B* **2006**, *110*, 16812.

17) DeVries, G. A.; Brunnbauer, M.; Hu, Y.; Jackson, A. M.; Long, B.;
Neltner, B. T.; Uzun, O.; Wunsch, B. H.; Stellacci, F. *Science* **2007**, *315*,
358.

18) Liao, J. H.; Chen, K. J.; Xu, L. N.; Ge, C. W.; Wang, J.; Huang, L.; Gu,
N. *Appl. Phys. A* **2003***, 76*, 541.

19) Perepichka, D. F.; Rosei, F. *Angew. Chem. Int. Ed.* **2007**, *46*, 6006.

20) Lin, S.; Li, M.; Dujardin, E.; Girard, C.; Mann, S. *Adv. Mater.* **2005**, *17*,
2553.

21) Zhang, H.; Fung, K. H.; Hartmann, J.; Chan, C. T.; Wang, D. Y. *J. Phys.
Chem. C* **2008**, *112*, 16830.

22) Fresco, Z. M.; Fréchet, J. M. J. *J. Am. Chem. Soc.* **2005**, *127*, 8302.

23) Thomas, P. J.; Kulkarni, G. U.; Rao, C. N. R. *J. Phys. Chem. B* **2000**, *104*, 8138.

24) (a) Gelbart, W. M.; Sear, R. P. ; Heath, J. R. ; Chaney, S. *Faraday Discuss.* **1999**, *112*, 299.

   (b) Ohara, P. C.; Heath, J. R. ; Gelbart, W. M. *Angew. Chem. Int. Ed.* **1991**, *36,* 1077.

25) (a) Whetten, R. L. ; Price, R. C. *Science* **2007,** *318*, 407.

   (b) Jadzinsky *Science* **2007,** *318*, 430**.**

   (c) Love, J. C.; Estroff, L. A.; Kriebel, J. K.; Nuzzo, R. G.; Whitesides, G. M. *Chem. Rev.* **2005**, *105*, 1103.

   (d) Araki, K.; Mizuguchi, E.; Tanaka, H.; Ogawa, T. *J. Nanosci. Nanotechnol.* **2006**, *6*, 708.

26) (a) Li, J.; Pendry, J. B. *Phys. Rev. Lett.* **2008**, *101,* 203901.

   (b) Pendry, J. B.; Schurig, D., Smith, D. R. *Science* **2006**, *312*, 1780.

27) Strong, L.; Whitesides, G. M. *Langmuir* **1988**, *4*, 546.

28) Pradeep, T.; Mitra, S.; Sreekumaran Nair, A.; Mukhopadhyay, R. *J. Phys. Chem. B* **2004**, *108*, 7012.

29) Badia, A.; Demers, L.; Dickinson, L.; Morin, F. G.; Lennox, R. B.; Reven, L. *J. Am. Chem. Soc.* **1997**, *119*, 11104.

30) (a) Thomas, P. J.; Lavanya, A.; Sabareesh, V.; Kulkarni, G. U. *Proc. Ind. Acad. Sci.-Chem. Sci.* **2001**, *113*, 611.

   (b) Corbierre, M. K.; Beerens, J.; Lennox, R. B. *Chem. Mater.* **2005**, *17*, 5774.

   (c) Corbierre, M. K.; Lennox, R. B. *Chem. Mater.* **2005**, *17*, 5691.

   (d) Bensebaa, F.; Ellis, T. H.; Badia, A.; Lennox, R. B. *Langmuir* **1998**, *14*, 2361.

   (e) Bensebaa, F.; Ellis, T. H.; Kruus, E.; Voicu, R.; Zhou, Y. *Can. J. Chem.* **1998**, *76*, 1654.

   (f) Bensebaa, F.; Ellis, T. H.; Kruus, E.; Voicu, R.; Zhou, Y. *Langmuir* **1998**, *14*, 6579.

   (g) Fijolek, H. G.; Grohal, J. R.; Sample, J. L.; Natan, M. J. *Inorg. Chem.*

1997, *36,* 622.

31) Chu, B.; Hsiao, B. S. *Chem. Rev.* **2001**, *101*, 1727.

Chapter IV

Photo-responsive Assemblies of Gold Nanoparticles
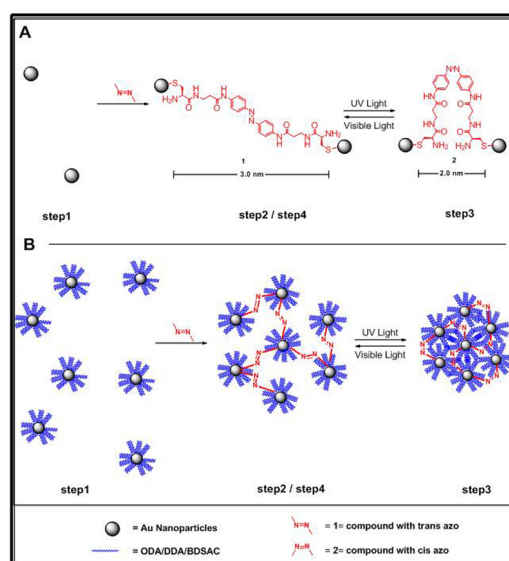
This chapter describes the formation of photo-responsive assembly of ligand capped gold nanoparticles using linker molecules containing azobenzene moiety. The reversible trans-cis isomerization of the azobenzene molecule has been utilized to bring a change in the interparticle spacings of the gold nanoparticles leading to the formation of photo-responsive networks. UV-visible absorbption spectroscopy and transmission electron microscopy techniques have been used to monitor the network formation.

4.1 Introduction

Functional materials have always been an attractive area of research [1]. As evident from the name, these materials are designed to perform a specific function by virtue of their properties. Photochromic materials are one class of functional materials. They demonstrate distinguishing properties when stimulated by light. In nature, photochromic proteins such as bacteriorhodopsin are responsible for light-triggered biological mechanisms like photosynthesis and visual perception [2]. Taking a cue from nature, different kinds of photochromic materials are being produced artificially [3]. These materials undergo a reversible photo-transformation between two forms that show dissimilar physicochemical properties like geometrical structure, absorption spectra, refractive index etc. The variation in properties makes the functional materials promising candidates for applications in the area of photonic devices.

Some desirable qualities for photochromic applications are short response time, clean and tunable energy input, efficient conversion of an optical input into different kinds of output signals or mechanical motion, ability to undergo photo-transformation a multiple number of times etc. Some examples of photochromic materials are spiropyrans [4], fulgides [5], diarylethenes [6, 7] and alkenes like stilbene [8]. Apart from these, azobenzene is an important photochromic molecule showing interesting photo-responsive behaviour.

Azobenzene has been well-known for its use in dyes and pigments. In addition, it has been attracting researchers for decades due to its photo-responsive properties. In 1910, Gortner reported the presence of two steromric forms of azobenzene [9]. Two decades thereafter, Hartley observed the photochemical trans to cis isomerization of azobenzene [10-12]. Robertson analyzed the crystal structures of the photoisomers [13]. Zimmerman *et al.* and Fischer *et al.* studied the photoisomerization of azobenzene in detail [14-16]. Electronic structure and spectra of azobenzene isomers were discussed [17]. Even, kinetics and mechanism for azobenzene formation was analyzed [18]. Several other researchers also gave their contribution to understand the properties of isomers of azobenzene and the process of photoisomerization [19-27]. Photoisomerization of azobenzene is illustrated in Fig. 4.1. As can be seen in the figure, the trans form of azobenzene, upon UV light irradiation, undergoes phototransformation to the less stable cis form, which then

reverts to the trans form when subjected to visible light or thermal energy. The two geometrical isomers – trans and cis can be differentiated on the basis of their optical properties.
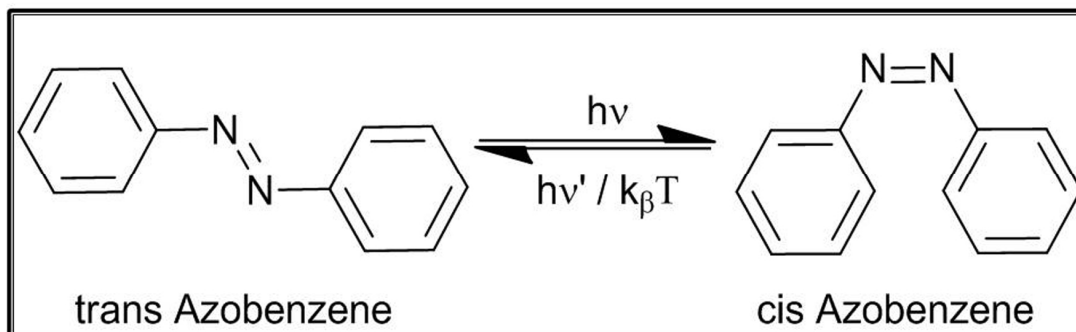

Fig. 4.1 *Schematic depicting the photoisomerization of azobenzene from trans to cis form where hv and hv' correspond to UV and visible radiation respectively while $k_\beta T$ denotes the thermal energy.*

Even now, photoisomerization of azobenzene is being probed [28-35] to facilitate its use in various applications. It has been studied in areas like biological applications [36-46], solar energy [47], optical storage [48], in making photo-responsive dendrimers [49], memories and switches [50, 51] etc. Stoddart and co-workers [52-54], Ikeda and his group [55], Katsonis *et al.* [3] and others [56] have utilized it in the construction of what they term as 'molecular machines'.

Some researchers have coupled azobenzene moieties with nanoparticles and studied their effects. Einaga and co-workers have combined them with iron oxide and Prussian blue nanoparticles to obtain photoswitchable magnetization [57-61]. They prepared iron oxide nanoparticles encapsulated by n-octylamine and an azobenzene compound. Alternate irradiation of UV and visible light led to reversible switching of magnetization values at room temperature. This meant that the magnetic property of the nanoparticles was being controlled optically. The octylamine molecules acted like spacers and made the photoisomerization of azo moiety more efficient. Similarly, composites of Prussian blue and azobenzene were synthesized and were seen to show reversible changes in the magnetization due to photoswitching.

Blending of photo-responsive azobenzene molecule and gold nanoparticles is an interesting topic for research since, photoresponsive behaviour of azobenzene and

optical properties of gold nanoparticles can lead to a synergistic combination of properties [62]. There are a few reports where the combination of azobenzene and gold nanoparticles has been studied. Evans *et al.* have studied the formation of azobenzene-containing mixed monolayers on the surface of gold nanoparticles [63]. Manna *et al.* prepared gold nanoparticles capped by the unsymmetrical azobenzene disulfide and checked their photoisomerization [64]. Photoreactive gold clusters capped by azobenzene derivatives were synthesized by Zhang and co-workers [65]. Yasuda *et al.* observed photoisomerization of azobenzene derivatives grafted on gold and the changes in accompanying conductive characteristics were measured by STM [66].

In the present work, a combination of gold nanoparticles and azobenzene has been used to form networks that can respond to external light stimulus and show tunable optical properties. The optical properties of gold nanoparticles are found to be a function of various parameters like the size, shape, dispersion medium [67]. Similarly, the position of surface plasmon resonance absorption band of gold nanoparticles is found to be a function of their interparticle distance. The fact that the change in interparticle distance can serve as an indicator has been exploited for a variety of applications [68, 69]. In this work, this fact has been utilized to prepare photo-responsive networks of gold nanoparticles connected by azobenzene moiety. The proof of network formation is based on the fact that gold nanoparticles show modulation in their optical spectra with respect to the variation in their interparticle distance. Also, the formation of assembly of gold nanoparticles takes them one step closer towards the potential applications.

4.2 Preparation of gold nanoparticles and their photoresponsive networks

Gold hydrosol was prepared and subsequently phase transferred to obtain ligand capped gold nanoparticles in an organic phase as depicted in Fig. 4.2A. In a typical experiment, 300 mL of 10^{-4} M of aqueous chloroauric acid ($HAuCl_4$) solution was reduced at room temperature using sodium borohydride (0.03 g) as the reducing agent to form gold nanoparticles. Curve 1 from Fig. 4.2B shows the optical spectrum of the ruby red coloured gold nanoparticles in aqueous medium displaying a single peak at around 515 nm as expected [70].
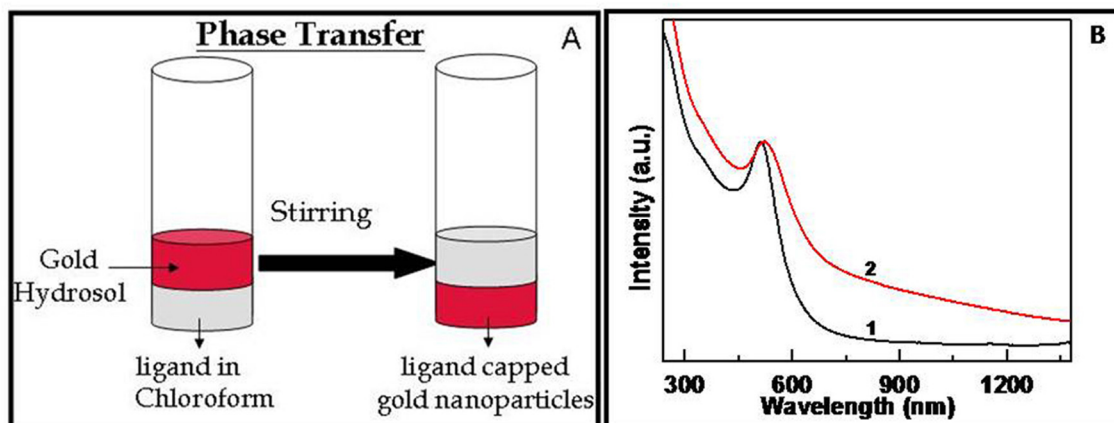
Fig. 4.2 A) *Schematic depicting the phase transfer of gold nanoparticles from aqueous to organic medium by extensive stirring (Figure not to scale)* **B)** *UV-visible absorption spectrum of gold nanoparticles in aqueous phase (curve 1) and after phase transfer to chloroform (curve 2).*

These nanoparticles were then phase transferred to chloroform using three different ligands– one of them being a tetra alkyl ammonium chloride compound namely benzyldimethylstearylammoniumchloride (BDSAC, $C_6H_5CH_2N[(CH_2)_{17}CH_3](CH_3)_2Cl$)) while the other two being alkylamines namely, octadecylamine (ODA, $C_{18}H_{37}NH_2$) and dodecylamine (DDA, $C_{12}H_{25}NH_2$). The ligands not only acted as phase-transferring agents, but also ensured enough free volume to be available in the nanoparticle networks that can facilitate a smooth formation of photoresponsive networks.

300 mL of the gold hydrosol was divided into three equal parts of 100 mL each. To the first part, 100 mL of solution of BDSAC in chloroform (10^{-3} M) was added. 10 mL of a 10^{-2} M solution of ODA in chloroform was added to the second part, while 10 mL of a 10^{-2} M solution of DDA in chloroform was added to the third part. In each case, two immiscible layers were observed. Before the reaction, the colour of the aqueous phases (upper layer) containing gold nanoparticles was red whereas, the organic phase (lower phase) was colorless. The three solutions were then stirred vigorously. This led to the phase transfer of the gold nanoparticles into chloroform rendering the aqueous phase colourless and the organic phase displaying the characteristic red colour of gold nanoparticles. Curve 2 from Figure 4.2B shows a typical UV-vis absorption spectrum of the phase transferred gold nanoparticles. The peak position is seen to shift slightly with respect to the gold hydrosol which can be

attributed to the binding of ligand molecules onto the surface of gold nanoparticles. The aqueous phase from each of the biphasic solutions was discarded and only the organic phases were used for further experiments. Same procedure has been used for all three types of ligand protected gold nanoparticles.

In order to prepare the photo-responsive networks, gold nanoparticles had to be connected to the azobenzene molecule through linker moiety constituting of peptide based ligands with two cysteine end groups (Fig 4.3). These linker molecules have been synthesized by Hotha *et al.* (from National Chemical Laboratory, Pune) and were thoroughly characterized by standard techniques [71]. The choice of spacers was made on the basis of suitability of the functional groups and the convenience of their synthesis.
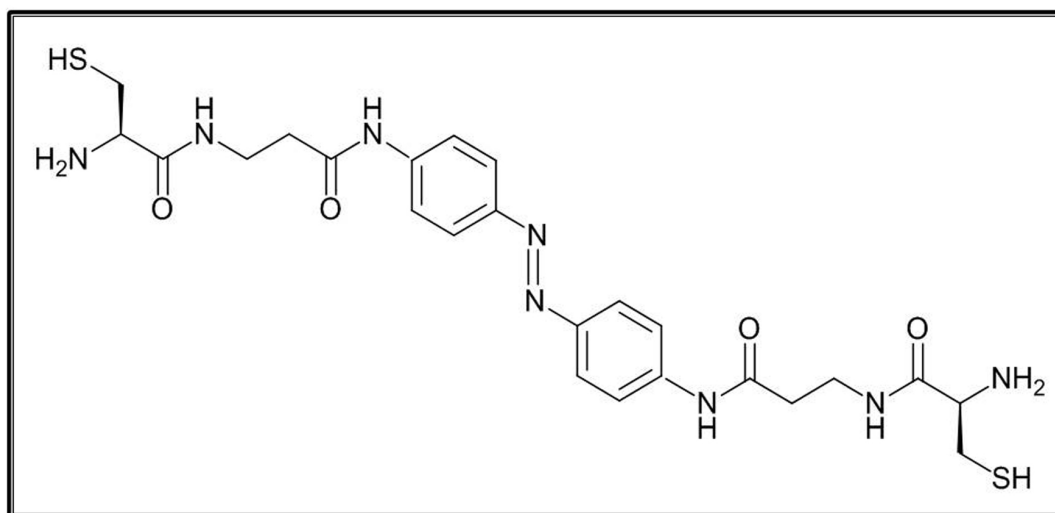
Fig.4.3 *Structure of linker molecule added to the gold nanoparticles with azobenzene in trans isomeric form.*

Chloroform solution of azobenzene compound was added to 10 mL of solution of Au nanoparticles in chloroform. This mixture was then irradiated by UV light for 30 min (Pyrex filter, >280 nm, 450-W Hanovia medium-pressure lamp). This solution was then subjected to irradiation by a normal incandescent lamp (visible light) for 30 min. Usually, irradiation of solution can lead to an increase in the temperature of the solution. To avoid this, the solutions were kept in water baths during irradiation.

The whole experimental procedure to investigate the photo-responsiveness of the system has been summarized in Fig 4.4.

Step 1: Synthesis of Au nanoparticles in aqueous medium and their subsequent phase transfer using ligand

Step 2: Addition of Azobenzene moiety to ligand capped Au nanoparticles

Step 3: Irradiation of this Au-Azo solution by UV light

Step 4: The resultant solution exposed to visible radiation
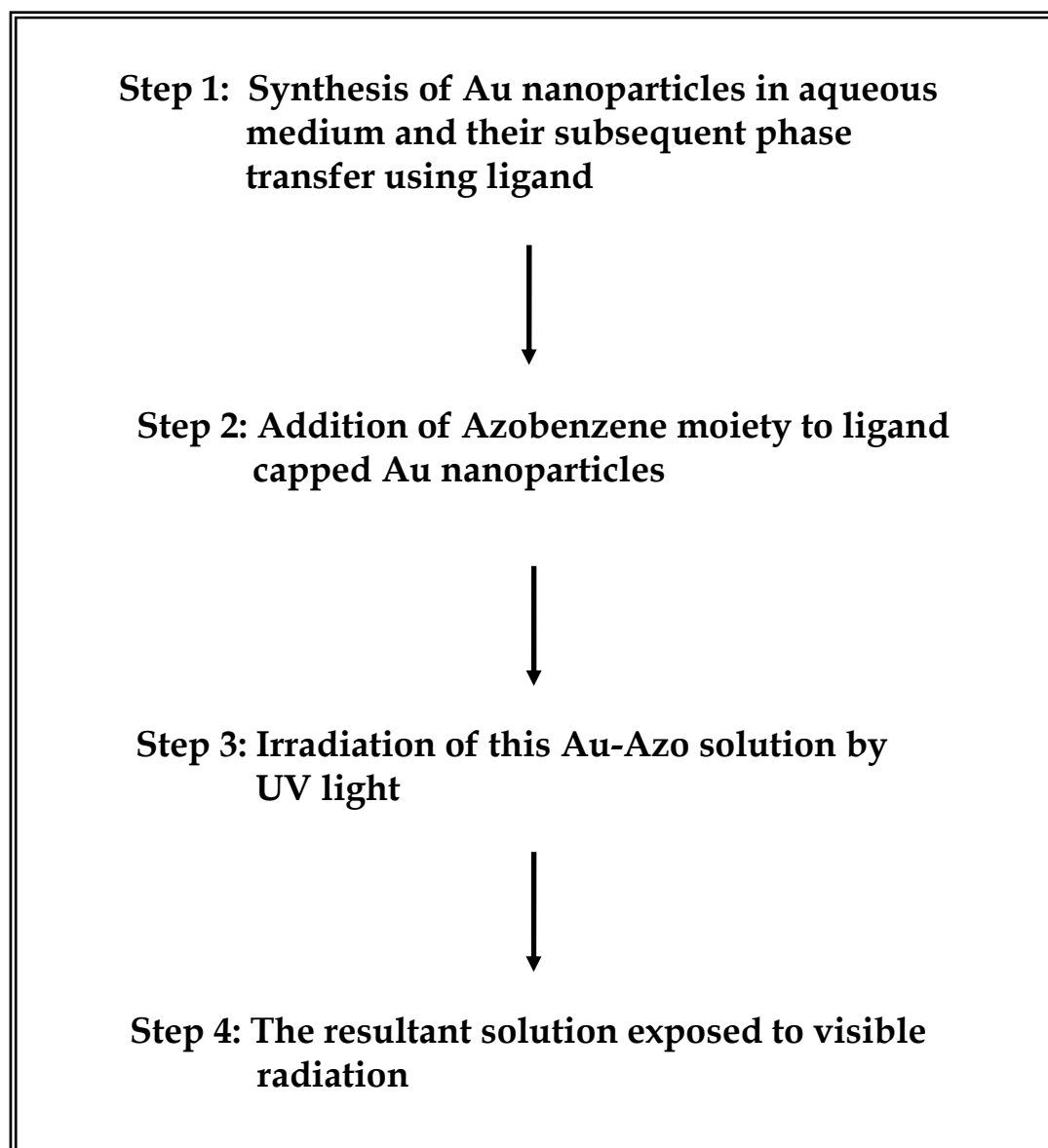
Fig 4.4 *Flow chart showing the procedure for preparation of photo-responsive networks*

The entire experiment was performed in four steps for each of the ligand capped nanoaprticles. After every step, UV-vis absorption of the solution was measured and the solution was drop-coated on a TEM grid for TEM analysis. The results of these analyses have been discussed later in this chapter. Initially, the UV-visible absorption spectroscopic analysis of the 3 samples of ligand capped gold nanoparticles has been given followed by the description of TEM images. The inference from these results has been described taking into account the role played by the capping ligands.

4.3. UV-visible absorption spectroscopy

4.3.1 BDSAC capped gold nanoparticles

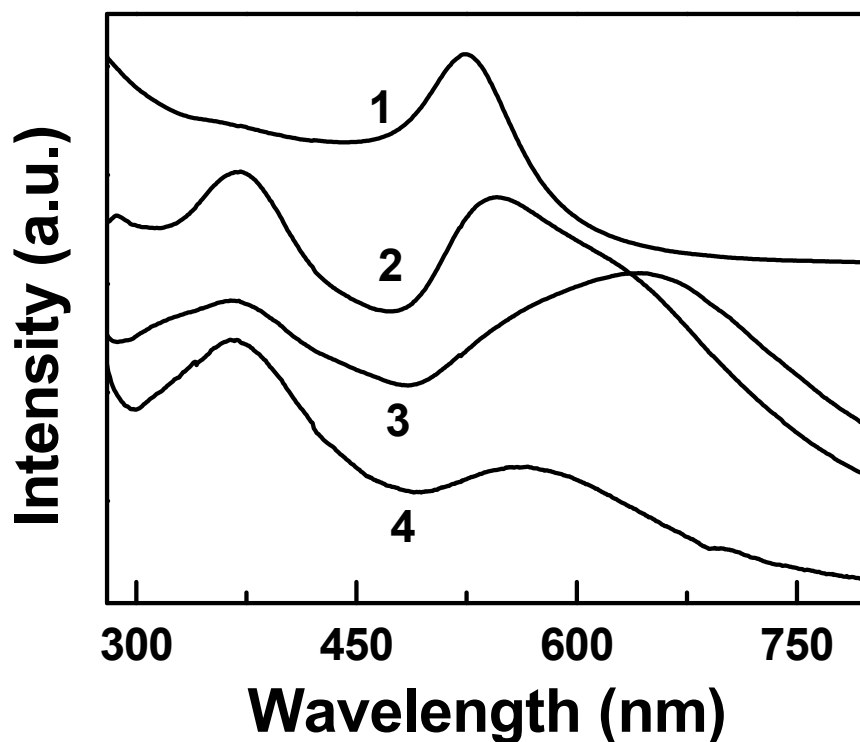Fig. 4.5 shows the UV-visible absorption spectra of the BDSAC capped gold nanoparticles in the four steps.

Fig. 4.5) *UV-visible absorption spectra of BDSAC capped nanoparticles corresponding to different steps. Curve 1: spectrum of BDSAC capped gold nanoparticles. Curve 2: Spectrum recorded after addition of compound containing azobenzene moiety to the gold nanoparticles. Curve 3: spectrum taken after irradiating the resultant solution with UV light. Curve 4: Spectrum recorded after subsequent irradiation with visible light.*

Curve 1 corresponds to the spectrum of the gold nanoparticles immediately after their phase transfer into chloroform that exhibits a peak centered around 520 nm confirming that the gold nanoparticles have been phase transferred in organic medium. The spectrum after the addition of linker molecule with azobenzene moiety to the gold nanoparticle solution is represented by curve 2 where the peak position of the gold nanoparticles is seen to shift to 550 nm and is accompanied by the emergence of an additional peak at around 360 nm corresponding to the azobenzene moiety. Curve 3 is the UV-visible absorption spectrum of the solution after irradiation with UV light and it has two absorption bands like the previous step. The azobenzene peak

is seen to broaden while the SPR band of gold nanoparticles was red shifted to 642 nm. After exposure to visible light (step 4), SPR band appeared around 565 nm (curve 4), similar to the spectra 2 (step 2) and the azobenzene peak width became narrower as seen after step 2. The red shift in the SPR band of gold nanoparticles after irradiation with UV light and the blue shift after illumination by visible light, indicates that particles could have come closer after irradiation with UV lightand this process is reversible by the action of visible light. It is a clear reflection of change in interparticle distance brought about by the geometrical isomerism displayed by the azobenzene linker molecule.

4.3.2 ODA capped gold nanoparticles
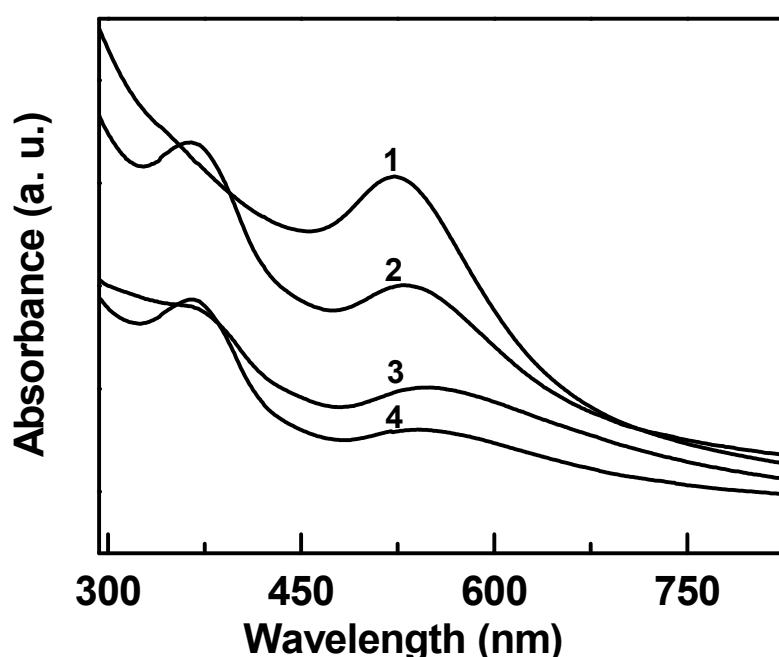
Fig. 4.6 *Spectra recorded from octadecylamine capped nanoparticles at various stages. Curve 1: ODA capped gold nanoparticles. Curve 2: addition of linker molecule with azobenzene moiety. Curve 3: after UV light irradiation. Curve 4: after illumination by visible light.*

The UV-visible absorption spectra for ODA capped gold nanoparticles (Fig. 4.6) show similar trends as that of the BDSAC capped gold nanoparticles but the red shift in the SPR band is less than the earlier case. The SPR band of gold nanoparticles appears at 520 nm as seen in curve 1 which undergoes a small red shift after the addition of azobenzene compound to it. The peak is now observed to occur at 530 nm in curve 2 along with the azobenzene peak at around 360 nm. The spectra taken after

step 3 is represented by curve 3 revealing the shift in peak corresponding to gold nanoparticles to ~550 nm and broadening of the azobenzene peak. The SPR band of gold nanoparticles again reverts to 540 nm with a concomitant sharpening of azobenzene peak after step 4, as evident from curve 4.
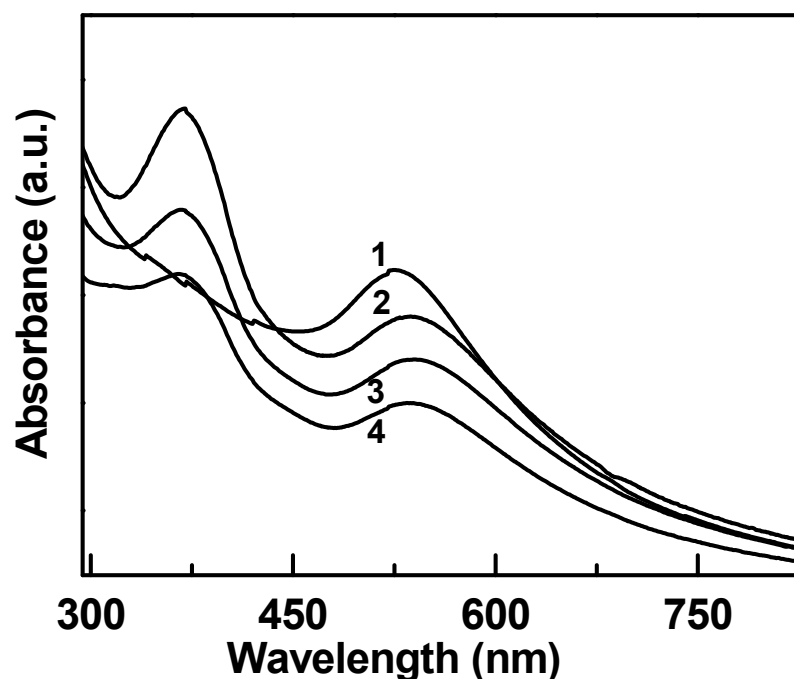
4.3.3 DDA capped gold nanoparticles

Fig. 4.7 *UV-visible absorption spectra of dodecylamine capped nanoparticles at various stages. Curve 1: spectra of phase transferred nanoparticles. Curve 2: Immediately after the addition of azobenzene compound. Curve 3: after irradiating the solution with UV light. Curve 4: after the solution has been subjected to visible light irradiation.*

The case for DDA capped nanoparticles is entirely different from the previous two cases. Fig. 4.7 shows the UV- visible absorbance spectra for this system. Curve 1 corresponds to the DDA capped gold nanoparticles displaying a peak at 525 nm. After addition of azobenzene spacer, the gold peak is positioned at 535 nm (curve 2) and the azobenzene peak appears at ~ 360 nm. But no further change is observed in either the nature or position of the peaks even after subjecting the solution with UV and visible irradiation (steps 3 and 4). Hence, the UV-visible absorption spectra corresponding to DDA capped gold nanoparticles differ from their counterparts in the case of BDSAC and ODA capped molecules. The reasons governing this difference would be discussed further in the chapter.

4.4 TEM analysis

4.4.1 BDSAC capped gold nanoparticles
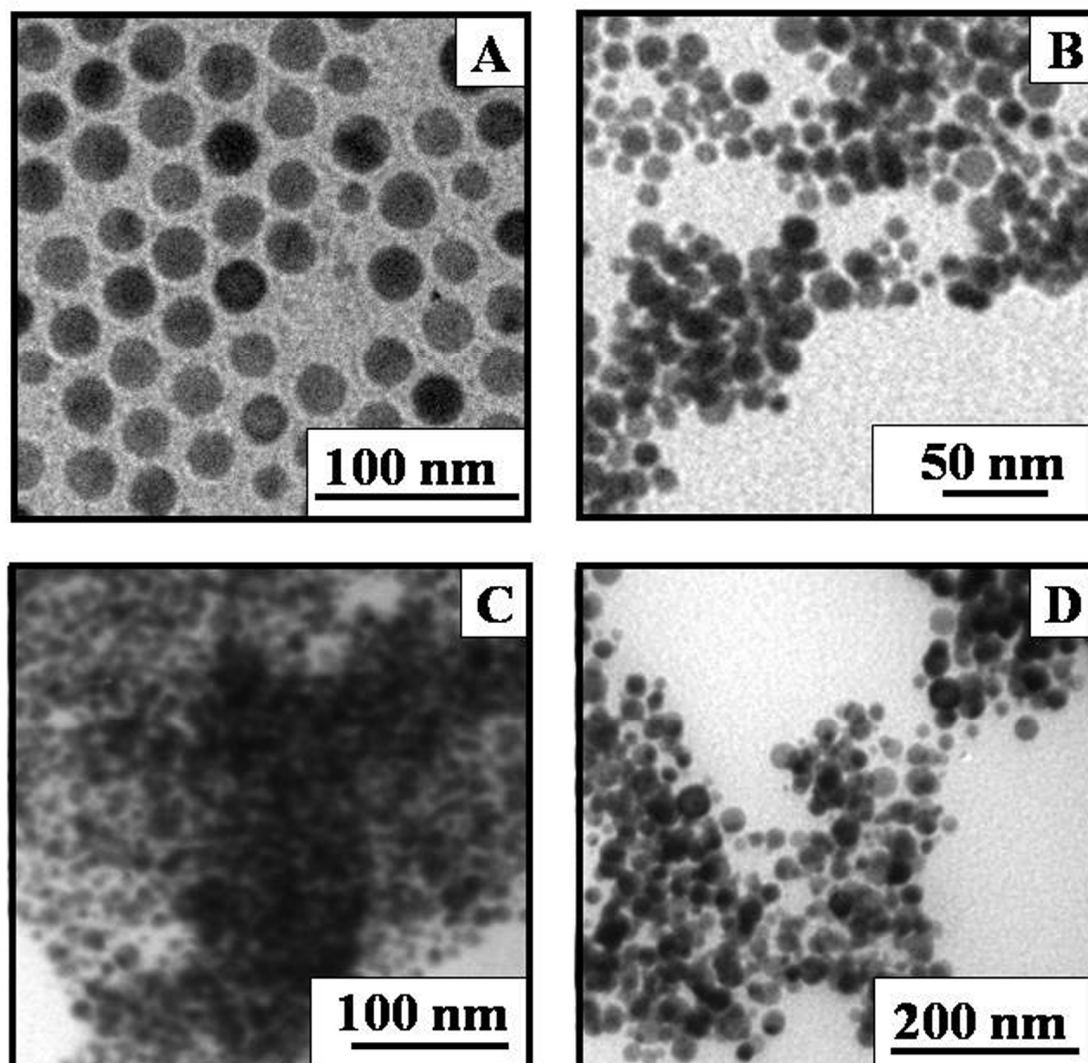
Fig. 4.8 *TEM images displaying BDSAC capped nanoparticles at subsequent stages* ***A)*** *after phase transferring and capping with BDSAC* ***B)*** *after the addition of azobenzene linker* ***C)*** *after exposure to UV light and* ***D)*** *after being subjected to visible light.*

The representative TEM images of the BDSAC capped gold nanoparticles at different stages are shown in Fig 4.8. The nanoparticles just after phase transfer and capping with BDSAC are uniform and isolated in nature as seen in Fig. 4.8 A. The linker molecule containing azobenzene moiety has two terminal thiol groups. As soon as this bifunctional linker molecule is added to the gold nanoparticles, it is expected to join the gold nanoparticles and subsequently bring these nanoparticles closer (Fig. 4.8 B). Further, when these nanoparticles were exposed to UV light, they formed networks as seen in Fig.4.8 C. The opening up of these networks due to visible radiation is observed in Fig. 4.8 D.

4.4.2 ODA capped gold nanoparticles
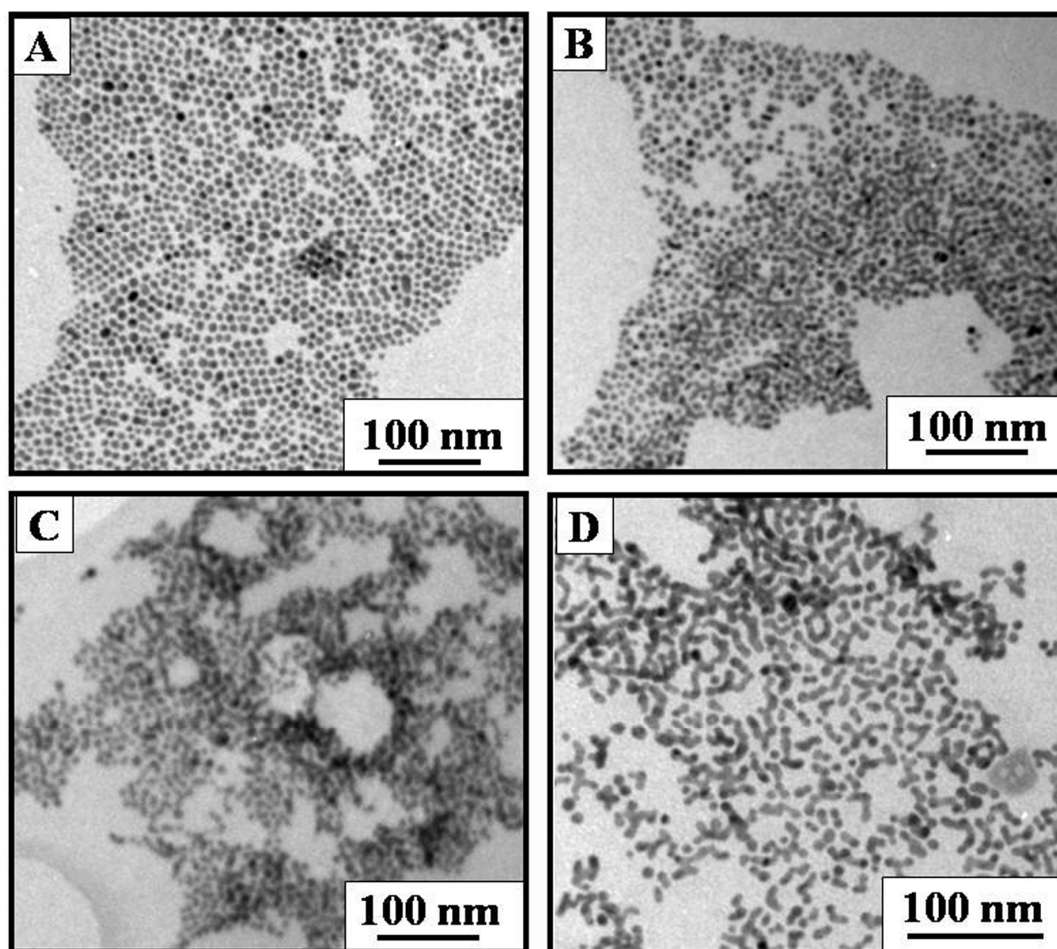
Fig. 4.9 *Representative TEM images of octadecyl amine derivatized nanoparticles **A)** after phase transfer using ODA. **B)** after the addition of linker molecule **C)** after irradiation with UV light and **D)** after being subjected to visible light irradiation.*

Fig. 4.9 depicts the TEM images of the ODA capped gold nanoparticles taken stepwise. After the first step, well-separated ODA capped gold nanoparticles are seen (Fig. 4.9A). The particles tend to come closer after addition of azobenzene moiety (Fig 4.9B). Next, in Fig. 4.9 C, the particles came further closer by forming a dense network. Fig. 4.9 D is the image after the networks in Fig. 4.9 C were exposed to visible light. Here again, separated particles can be seen.

4.4.3 DDA capped gold nanoparticles
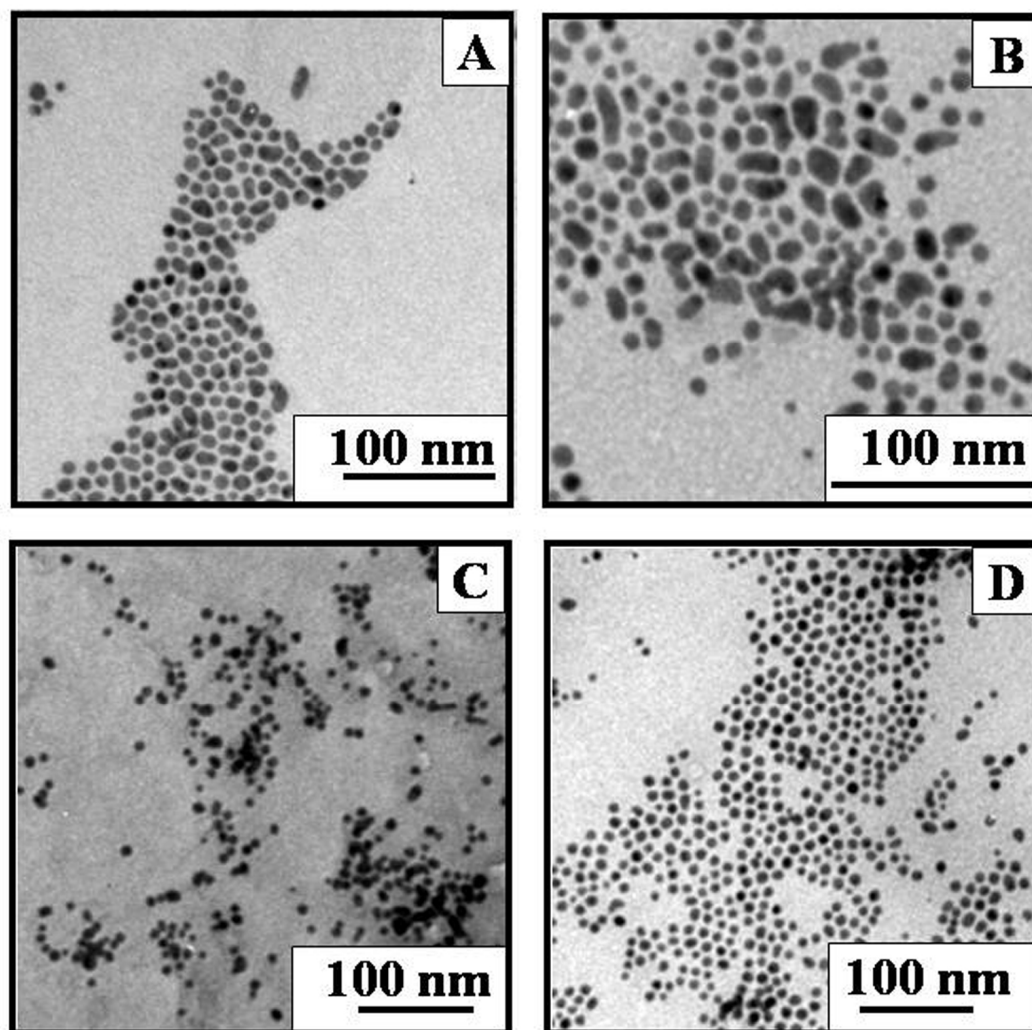
Fig. 4.10 *TEM images of dodecylamine functionalized gold nanoparticles at various stages A) immediately after phase transfer and capping using DDA, B) after adding the azobenzene linker molecule, C) when UV light is incident and D) after irradiating with visible light.*

Unlike the BDSAC capped and ODA capped gold nanoparticles, the DDA capped gold did not show any discernible changes in the TEM images indicating that exposure of the networks to UV light and visible light has not caused any changes in the interparticle distances. This is illustrated in their TEM images (Fig. 4.10 A-D) corresponding to the four steps. The phase transferred nanoparticles (Fig. 4.10 A) retain their distinct nature even after addition of azobenzene followed by the irradiation by UV and visible light respectively.

4.5 Discussion

4.5.1 Formation of photo-responsive network of gold nanoparticles: Interpretation of the UV spectra and TEM images

The sequence of events occurring in the four steps of the experiment and the observed results have been depicted in the schematic (Fig. 4.11). As can be seen, the distinct nanoparticles connect via a linker molecule containing azobenzene moiety. The change in the interparticle distance due to photoisomerization of azobenzene molecule upon irradiation of light has also been displayed. The case of two nanoparticles has been illustrated in Fig. 4.11 A while the network formation by many such linked nanoparticles is shown in Fig. 4.11 B.
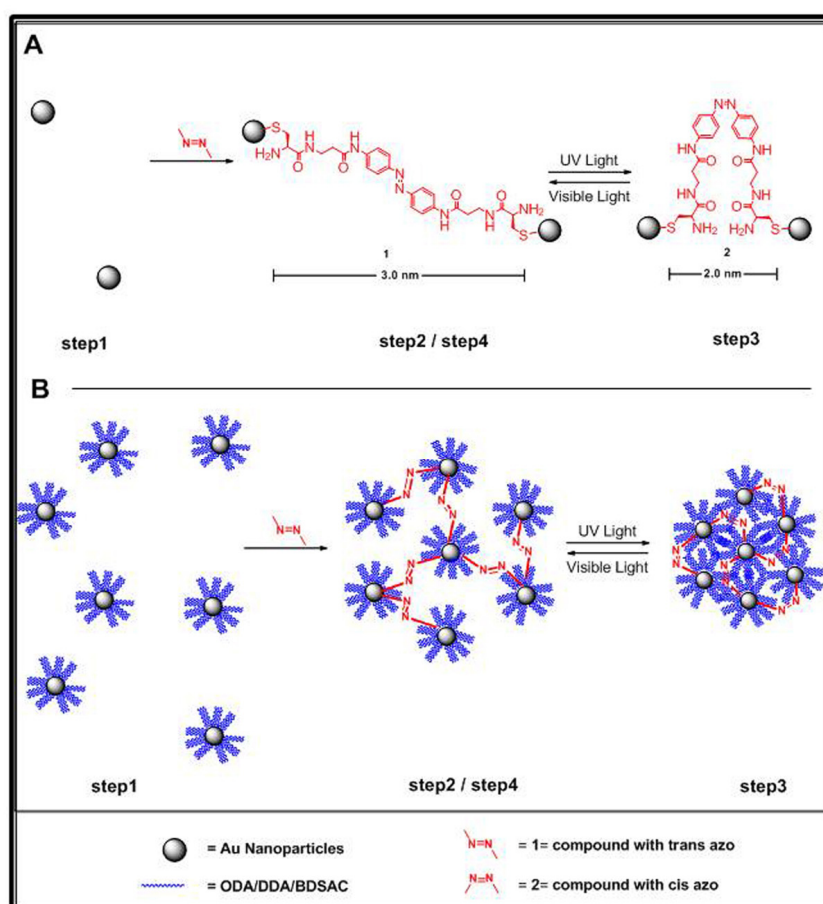

Fig. 4.11 A) *The change in the interparticle spacing of gold nanoparticles connected through linker molecule containing photoisomerizing azobenzene moiety is depicted.* **B)** *The schematic illustrating the photostimulated network formation of the gold nanoparticles. The network closes on UV light irradiation whereas opens up when visible light is incident. [Figure not to scale].*

The results of UV-vis absorption spectrophotometry and TEM measurements for all the three systems are similar in the first step where the synthesis of gold nanoparticles is followed by phase transfer using the capping ligand. The UV-vis absorption spectra (curve 1 of Fig.4.5, Fig.4.6 and Fig.4.7) depict the spherical and distinct nature of the ligand capped gold nanoparticles, which is further confirmed from the corresponding TEM images (Fig.4.8 A, Fig.4.9 A, Fig. 4.10A).

In case of the second step, as the azobenzene derivatives are being added to gold nanoparticles, they are expected to interconnect two gold nanoparticles and eventually, a network of gold nanoparticles will form. As a consequence, emergence of a signatory peak of trans-azobenzene around 360 nm along with a slight shift in the peak for gold nanoparticles is seen in all the three UV- vis absorbance spectra (Curve 2, Fig.4.5, Fig.4.6 and Fig.4.7). The TEM Images (Fig.4.8B, Fig. 4.9B, and Fig. 4.10B) are also in consonance with the UV-visible absorption spectra, with the nanoparticles coming closer to each other as compared to the individual particles seen in Fig. 4.8, 4.9 and 4.10 A.

Next step onwards, only BDSAC and ODA capped gold nanoparticles are seen to show similar results. The findings for BDSAC capped gold nanoparticles are interpreted first. The UV-vis absorption peak of these gold nanoparticles is seen to undergo a huge red-shift (shift towards higher wavelength) with a concomitant flattening of the azobenzene peak. Interestingly, after irradiation with visible light, the peak position of gold nanoparticles is seen to blue-shift with a concomitant sharpening of the azobenzene peak. When all the results are seen together, they point towards a reversible process. The primary reason for the shift in gold SPR is change in interparticle spacing. The SPR is known to shift to the higher wavelength (red-shift) with the decrease in the interparticle distance and shift to the lower wavelength (blue-shift) due to the increase in interparticle spacing [72]. The terminal bi-functional molecules would bind with adjacent nanoparticles and bring them together, when added to nanoparticle solution. It is known that UV irradiation induces the isomerization of trans isomer into cis isomer. End to end distance between the trans isomer linked nanoparticles is longer (~ 3 nm) than the cis isomer linked nanoparticles (~ 2 nm). Due to this fact, interparticle distance between the gold nanoparticles connected through trans azobenzene linker is going to decrease after photoisomerization is induced by UV light and similarly, the interparticle distance

will increase when the cis isomer gets reverted to trans-isomer after irradiation with visible light. After the irradiation of visible light, the cis-isomer will convert back to trans-isomer due to which the linker molecule will regain its length and the gold nanoparticles will go apart. When many such gold nanoparticles are considered, they can be visualized to form a network. As the gold nanoparticles are coming closer and moving apart due to the photostimulation, the whole network will appear to close in or "breathe in" and open out or "breathe out" (see Fig. 4.11). As the photoisomerization is two-way, the process of network formation is also reversible.

These features are further confirmed from TEM images. The well-separated nanoparticles seen in Fig. 4.8 A and Fig. 4.9 A are seen to come closer after addition of azobenzene (Fig. 4.8 B). The densification of the network, after UV light irradiation, is clearly seen in Fig. 4.8 C while the opening up of the network after irradiation of visible light is depicted in Fig. 4.8 D. Hence, the TEM images point towards reversible formation of networks of gold nanoparticles using a photo-responsive azobenzene moiety.

The case of ODA capped gold nanoparticles would now be considered. The UV-visible absorption spectra (Fig. 4.6) of these nanoparticles show the same trend as the BDSAC capped gold nanoparticles indicating the presence of both gold and trans-azobenzene. The changes in the azobenzene peak due to photoisomerization and the shift in the peak position of gold nanoparticles are similar to the BDSAC capped gold nanoparticles. But only the extent of shift is seen to decrease for the ODA capped gold nanoparticles. This demonstrates that the photoresponsiveness is also dependent on the phase transferring agent. The TEM images clearly demonstrate the closing in (Fig. 4.9 C) and opening up (Fig. 4.9 D) of the network of gold nanoparticles.

The results for DDA capped gold nanoparticles would now be interpreted. The UV-visible absorption spectra are shown in Fig. 4.7. Curve 1 shows the peak arising from DDA capped gold nanoparticles. It undergoes a slight shift after the addition of azobenzene linker molecule. But when subjected to irradiation with UV light and visible light, the peak position does not undergo any shift, unlike the previous two cases of capped gold nanoparticles. This is also reflected in the TEM images (Fig. 4.10) where network formation is not observed.

4.5.2 Role of capping ligand in the network formation

The three ligands could be compared to understand the role played by them in the network formation of gold nanoparticles. Fig. 4.12 depicts the structures of the three ligands used for capping and phase transferring the gold nanoparticles.
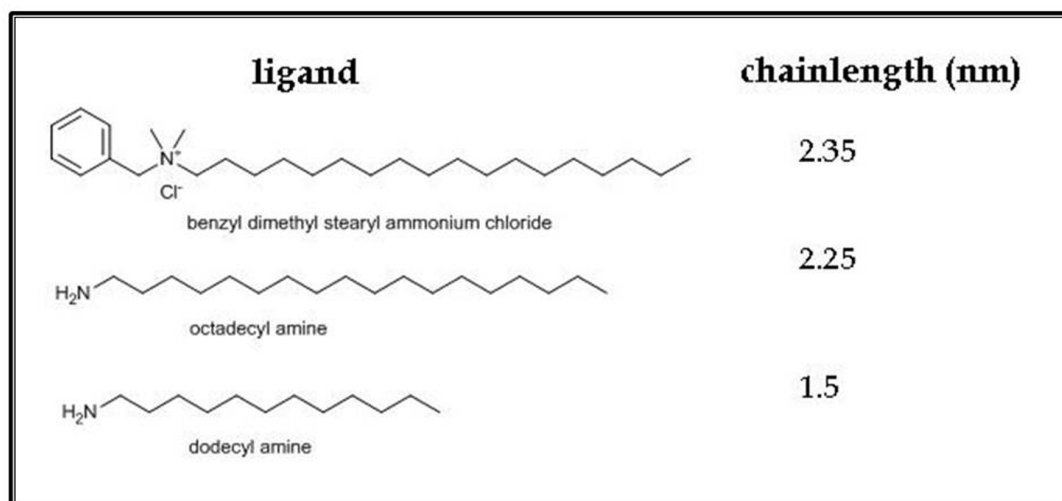

Fig. 4.12 *Structures and chain lengths of the ligands used for capping and phase transferring the gold nanoparticles.*

Based on the structures and their chain length of the capping agents, important observations have been made and are given below:

i) ODA and DDA are alkylamines while BDSAC is a quaternary ammonium salt.

ii) The strength of interaction and hence the attachment of tetra alkyl ammonium group to the gold surface is weaker as compared to alkyl amine interaction.

iii) The chain length corresponding to DDA (~1.5 nm) is lower as compared to BDSAC (~2.35 nm) and ODA (~ 2.25 nm).

Taking into account the above mentioned factors the results can be comprehended in the following way. As the linker molecule is added to the nanoparticle solution, it will get attached to two nanoparticles (step 2, schematic in Fig. 4.11). When UV light is irradiated, the trans-cis isomer conversion will take place bringing the nanoparticles closer (step 3, schematic in Fig. 4.11). Since, the nanoparticles are capped with ligands, as they approach each other, the ligands will have to interdigitate. It can be seen that of the three ligands, greater length of BDSAC

and ODA molecules will facilitate more interdigitation of the capping ligands and therefore the nanoparticles could avail of more space for coming together during the *trans-cis* isomerization of the linker molecules. However, alkylamines like ODA are known to have strong attachment to the gold surfaces [73], but at the same time, they do not facilitate interdigitation as much as other ligands like thiol [74]. BDSAC molecule is longer and bulkier than ODA molecule. Also, tetra alkyl ammonium groups attach weakly to the gold surface. Therefore it may facilitate the nanoparticles to come closer to each other easily as compared to the alkyl amines.

However, in case of DDA, chain-length is the smallest, which would make steric repulsions dominant and hence prohibit the network formation. As the linker molecule is added to the DDA capped gold nanoparticles, the presence of trans-azobenzene is confirmed from its representative peak in the UV-visible absorption spectra. The slight shift in the SPR peak position indicates its binding with the gold nanoparticles. Due to the smaller length of the DDA molecule, there is just enough space for the linker molecule to attach to two nanoparticles capped by DDA ligands. So, if two DDA capped gold nanoparticles have to come closer during *trans-cis* isomerization by UV light exposure, DDA molecules on neighboring nanoparticles have to interdigitate fully, which may not be possible for an alkylamine ligand like DDA [74]. Hence, the *trans-cis* isomerization of the linker molecule could get hindered resulting in unchanged position of surface plasmon resonance peak. The unaltered nature of trans-azobenzene peak further confirms this.

A significant feature of the photo-responsiveness of the network is that it is reversible as well as recyclable a few times i.e. red shift and blue shift are observed consecutively corresponding to the sequential UV and visible light irradiation. But there is a loss in the intensity of the SPR peak which could be attributed to the irreversible aggregation of some nanoparticles during networking. This would be the only constraint in having a large number of cycles.

Uncontrolled aggregation due to thermal effects could have been a possibility for the shift in UV- visible spectra. But, it has been ruled out because in that case, peaks should be shifting in only one direction by both UV and visible light irradiation while in the present work, a reversible peak shift has been achieved.

The results obtained in the present work are significant for the field of photochromic materials, which remains to be a hot topic for many researchers [75-84]. In fact, following the present work about gold nanoparticles, optical switching of silver nanoparticles using azobenzene has also been reported by Schiffrin and co-authors [85].

4.6 Conclusion

The photo-responsive assemblies of gold nanoparticles have been obtained by connecting them with linker molecules containing azobenzene moiety showing photoisomerization. The gold nanoparticles were initially synthesized in aqueous medium and then three different ligands namely BDSAC, ODA and DDA were employed to phase transfer and subsequently cap the nanoparticles. The formation of photo-responsive networks was monitored by UV-visible absorption spectrometry and TEM which revealed that the ligands played an important role in the assembly formation. The photoresponsive networks of gold nanoparticles would be potential candidates for optoelectronic applications.

4.7 References:

1) Aviram, A.; Ratner, M. A. *Chem. Phys. Lett.* **1974**, *29*, 277.

2) Hampp, N. *Chem. Rev.* **2000**, *100*, 1755

3) Katsonis, N.; Lubomska, M.; Pollard, M. M.; Feringa, B. L.; Rudolf, P. *Prog. Sur. Sci.* **2007**, *82*, 407.

4) Berkovic, G.; Krongauz, V.; Weiss, V. *Chem. Rev.* **2000**, *100*, 1741.

5) Yokoyama, Y. *Chem. Rev.* **2000**, *100*, 1717-1740

6) Pu, S.; Fan, C.; Miao, W.; Liu, G. *Tetrahedron* **2008**, *64*, 9464.

7) Jeong, Y.-C.; Park, D. G.; Lee, I. S.; Yang, S. I.; Ahn, K.-H. *J. Mater. Chem.* **2009**, *19*, 97.

8) Jiang, C.; Xie, R.; Li, F.; Allen, R. E. *Chem. Phys. Lett.* **2009**, *474*, 263-267.

9) Gortner, C. V.; Gortner, R. A. *J. Am. Chem. Soc.* **1910**, *32*, 1294.

10) Hartley, G. S. *Nature* **1937**, *140*, 281.

11) Hartley, G. S. *J. Chem. Soc. (Resumed)* **1938**, 633.

12) Hartley, G. S.; Le Fèvre, R. J. W. *J. Chem. Soc. (Resumed)* **1939**, 531.

13) Robertson, J. M. *J. Chem. Soc. (Resumed)* **1939**, 232.

14) Zimmerman, G.; Chow, L.-Y.; Paik, U.- J. *J. Am. Chem. Soc.* **1958**, *80*, 3528.

15) Fischer, E. *J. Am. Chem. Soc.* **1960**, *82*, 3249.

16) Gegiou, D.; Muszkat, K. A.; Fischer, E. *J. Am. Chem. Soc.* **1968**, *90*, 3907.

17) Beveridge, D. L.; Jaffé, H. H. *J. Am. Chem. Soc.* **1966**, *88*, 1948.

18) Yunes, R. A.; Terenzani, A. J.; Amaral, L. D. *J. Am. Chem. Soc.* **1975**, *97*, 368.

19) Shinkai, S.; Nakaji, T.; Nishida, Y.; Ogawa, T.; Manabe, O. *J. Am. Chem. Soc.* **1980**, *102*, 5860.

20) Asano, T.; Okada, T.; Shinkai, S.; Shigematsu, K.; Kusano, Y.; Manabe, O. *J. Am. Chem. Soc.* **1981**, *103*, 5161.

21) Rau, H.; Luddecke, E. *J. Am. Chem. Soc.* **1982**, *104*, 1616-1620.

22) Siampiringue, N.; Guyot, G.; Monti, S.; Bortolus, P. *J. Photochem.* **1987**, *37*, 185.

23) Kumar, G. S.; Neckers, D. C. *Chem. Rev.* **1989**, *89*, 1915-1925.

24) Dias, A. R.; Piedade, M. E. M. D.; Simões, J. A. M.; Simoni, J. A.; Teixeira, C.; Diogo, H. P.; Yang, M. Y.; Pilcher, G. *J. Chem. Thermodynamics* **1992**,

24, 439.

25) Gillberg, G.; Leube, H.; McKenzie, L.; Pruksarnukul, L.; Reeder, L. *J. Appl. Poly. Sci.* **1994**, *53*, 687.

26) Sekkat, Z.; Wood, J.; Knoll, W. *J. Phys. Chem.* **1995**, *99*, 17226.

27) Lednev, I. K.; Ye, T. Q.; Matousek, P.; Towrie, M.; Foggi, P.; Neuwahl, F. V. R.; Umapathy, S.; Hester, R. E.; Moore, J. N. *Chem. Phys. Lett.* **1998**, *290*, 68.

28) Zettsu, N.; Ubukata, T.; Seki, T.; Ichimura, K. *Adv. Mater.* **2001**, *13*, 1693.

29) Biswas, N.; Umapathy, S. *J. Chem. Phys.* **2003**, *118*, 5526.

30) Kamenjicki, M.; Lednev, I. K.; Asher, S. A. *J. Phys. Chem. B* **2004**, *108*, 12637.

31) Henzl, J.; Mehlhorn, M.; Gawronski, H.; Rieder, K. H.; Morgenstern, K. Ang*ew. Chem. Int. Ed.* **2006**, *45*, 603.

32) Han, M. R.; Hashizumeb, D.; Hara, M. *New J. Chem.* **2007**, *31*, 1746.

33) Shirai, Y.; Sasaki, T.; Guerrero, J. M.; Yu, B. C.; Hodge, P.; Tour, J. M. *ACS Nano* **2008**, *2*, 97.

34) Chen, J. I. L.; Ozin, G. A. *Adv. Mater.* **2008**, *20*, 4784.

35) Sauer, P.; Allen, R. E. *Chem. Phys. Lett.* **2008**, *450*, 192.

36) Willner, I.; Rubin, S.; Riklin, A. *J. Am. Chem. Soc.* **1991**, *113*, 3321.

37) Willner, I.; Willner, B. *Adv. Mater.* **1997**, *9*, 351.

38) Ulysse, L.; Cubillos, J.; Chmielewski, J. *J. Am. Chem. Soc.* **1995**, *117*, 8466.

39) Ueno, A.; Takahashi, K.; Anzai, J. I.; Osa, T. *J. Am. Chem. Soc.* **1981**, *103*, 6410.

40) Kumita, J. R.; Smart, O. S.; Woolley, G. A. *Proc. Natl. Acad. Sci. USA* **2000**, *97*, 3803.

41) Flint, D. G.; Kumita, J. R.; Smart, O. S.; Woolley, G. A. *Chem. Bio.* **2002**, *9*, 391.

42) Chen, E.; Kumita, J. R.; Woolley, G. A.; Kliger, D. S. *J. Am. Chem. Soc.* **2003**, *125*, 12443.

43) Sadovski, O.; Beharry, A. A.; Zhang, F. Z.; Woolley, G. A. *Angew. Chem. Int. Ed.* **2009**, *48*, 1484.

44) Asanuma, H.; Takarada, T.; Yoshida, T.; Tamaru, D.; Liang, X. G.; Komiyama, M. *Angew. Chem. Int. Ed.* **2001**, *40*, 2671.

45) Liang, X. G.; Asanuma, H.; Komiyama, M. *J. Am. Chem. Soc.* **2002**, *124*, 1877.

46) Aemissegger, A.; Krutler, V.; van Gunsteren, W. F.; Hilvert, D. *J. Am. Chem. Soc.* **2005**, *127*, 2929.

47) Taoda, H.; Hayakawa, K.; Kawase, K.; Yamakita, H. *J. Chem. Eng. Japan* **1987**, *20*, 265.

48) Natansohn, A.; Rochon, P.; Gosselin, J.; Xie, S. *Macromolecules* **1992**, *25*, 2268.

49) Junge, D. M.; McGrath, D. V. *Chem. Commun.* **1997**, 857.

50) Irie, M. *Chem. Rev.* **2000**, *100*, 1683.

51) Irie, M. *Bull. Chem. Soc. Jpn.* **2008**, *81*, 917

52) Asakawa, M.; Ashton, P. R.; Balzani, V.; Brown, C. L.; Credi, A.; Matthews, O. A.; Newton, S. P.; Raymo, F. M.; Shipway, A. N.; Spencer, N.; Quick, A.; Stoddart, J. F.; White, A. J. P.; Williams, D. J. *Chem. Eur. J.* **1999**, *5*, 860.

53) Brown, C. L.; Jonas, U.; Preece, J. A.; Ringsdorf, H.; Seitz, M.; Stoddart, J. F. *Langmuir* **2000**, *16*, 1924.

54) Balzani, V.; Credi, A.; Marchioni, F.; Stoddart, J. F. *Chem. Comm.* **2001**, 1860.

55) Yamada, M.; Kondo, M.; Mamiya, J. I.; Yu, Y. L.; Kinoshita, M.; Barrett, C. J.; Ikeda, T. *Angew. Chem. Int. Ed.* **2008**, *47*, 4986.

56) Renner, C.; Moroder, L. *ChemBioChem* **2006**, *7*, 869.

57) Einaga, Y. *J. Photochem. Photobio C: Photochem. Rev.* **2006**, *7*, 69.

58) Einaga, Y.; Gu, Z. Z.; Hayami, S.; Fujishima, A.; Sato, O. *Thin Solid Films* **2000**, *374*, 109.

59) Einaga, Y.; Sato, O.; Iyoda, T.; Fujishima, A.; Hashimoto, K. *J. Am. Chem. Soc.* **1999**, *121*, 3745

60) Taguchi, M.; Yamada, K.; Suzuki, K.; Sato, O.; Einaga, Y. *Chem. Mater.* **2005**, *17*, 4554.

61) Mikami, R.; Taguchi, M.; Yamada, K.; Suzuki, K.; Sato, O.; Einaga, Y. *Angew. Chem. Int. Ed.* **2004**, *43*, 6135

62) Eustis, S.; El-Sayed, M. A. *Chem. Soc. Rev.* **2006**, *35*, 209.

63) Evans, S. D.; Johnson, S. R.; Ringsdorf, H.; Williams, L. M.; Wolf, H.

Langmuir **1998**, *14*, 6436.

64) Manna, A.; Chen, P. L.; Akiyama, H.; Wei, T. X.; Tamada, K.; Knoll, W. C*hem. Mater.* **2003**, *15*, 20.

65) Zhang, J.; Whitesell, J. K.; Fox, M. A. *Chem. Mater.* **2001**, *13*, 2323.

66) Yasuda, S.; Nakamura, T.; Matsumoto, M.; Shigekawa, H. *J. Am. Chem. Soc.* **2003**, *125*, 16430.

67) Link, S., El-Sayed, M. A. *Int. Rev. Phys. Chem.* **2000**, *19*, 409.

68) Rosi, N. L. ; Mirkin, C. A. *Chem. Rev.* **2005,** *105*, 1547

69) (a) Wilson, R. *Chem. Soc. Rev.* **2008**, *37*, 2028**.**
    (b) Ghosh, S. K.; Pal, T. *Chem. Rev.* **2007**, *107*, 4797

70) Kelly, K. L.; Coronado, E.; Zhao, L. L.; Schatz, G. C. *J. Phys. Chem. B* **2003**, *107*, 668.

71) Sidhaye, D. S.; Kashyap, S.; Sastry, M.; Hotha, S.; Prasad, B. L. V. *Langmuir* **2005**, *21*, 7979.

72) Jin, R. C.; Wu, G. S.; Li, Z.; Mirkin, C. A.; Schatz, G. C. *J. Am. Chem. Soc.* **2003**, *125*, 1643

73) Brown, L. O.; Hutchison, J. E. *J. Phys. Chem. B* **2001**, *105*, 8911.

74) Prasad, B. L. V.; Stoeva, S. I.; Sorensen, C. M.; Klabunde, K. J. *Chem Mater.* **2003**, *15*, 935.

75) Callari, F.; Petralia, S.; Sortino, S. *Chem. Comm.* **2006**, 1009.

76) Hirose, T.; Matsuda, K.; Irie, M. *J. Org. Chem.* **2006**, *71*, 7499.

77) Russell, L. E.; Pompano, R. R.; Kittredge, K. W.; Leopold, M. C. *J. Mater. Sci.* **2007**, *42*, 7100.

78) Juluri, B. K.; Zheng, Y. B.; Ahmed, D.; Jensen, L.; Huang, T. J. *J. Phys. Chem. C* **2008**, *112*, 7309.

79) Nishi, H.; Kobatake, S. *Macromolecules* **2008**, *41*, 3995.

80) Zhou, J.; Sedev, R.; Beattie, D.; Ralston, J. *Langmuir* **2008**, *24*, 4506.

81) Liu, L.; Zhang, D. Q.; Zheng, X. P.; Wang, Z.; Zhu, D. B. *J. Nanosci. Nanotech.* **2009**, *9*, 3975.

82) Osaki, M.; Takashima, Y.; Yamaguchi, H.; Harada, A. *Org. Bio. Chem.* **2009**, *7*, 1646.

83) Zhou, J.; Ralston, J.; Sedev, R.; Beattie, D. A. *J. Col. Int. Sci.* **2009**, *331*, 251.

84) (a) Browne, W. R.; Feringa, B. L. *Annu. Rev. Phys. Chem.* **2009**, *60*, 407.

(b) Browne, W. R.; Feringa, B. L. *Nature Nanotech.* **2006**, *1*, 25.

85) Ahonen, P.; Schiffrin, D. J.; Paprotny, J.; Kontturi, K. *Phys. Chem. Chem. Phy.* **2007**, *9*, 651.

Chapter V

Conclusion

This chapter contains a summary and concluding remarks for the work described in this thesis and then lays out the future scope pertaining to this work.

5.1 Summary of the thesis:

The work encompassed in this thesis pertains to two crucial steps towards realization of the application potential of nanomaterials – synthesis of nanoparticles followed by their assembly. The work considers metal nanoparticles. Out of synthesis and assembly, the synthetic aspect is taken first. Realizing that an aqueous medium based simple reduction method for the synthesis of monodisperse cobalt and nickel nanoparticles is still a daunting task, this issue was addressed first. The efforts in this direction resulted in a new protocol. This protocol is based on commonly available metal salts and their reduction in the presence of stabilizing agents with optimum concentration. The importance of this protocol arises from its ability to yield stable solutions of monodisperse nanoparticles in aqueous medium and at ambient conditions. A further advantage is the spontaneous assembly of the nanoparticles.

While dealing with the assemblies of nanoparticles, two types were considered – assemblies held together with an in-situ formed template and assemblies that respond to external stimuli. In the former study, the simple digestive ripening method (normally used for preparing monodisperse metal nanoparticles) has been extended and shown to yield interesting one dimensional assemblies of gold nanoparticles under appropriate conditions. The mechanism of formation of these assemblies has been probed by utilizing various techniques like TGA, DSC and SAXS.

Taking the scope of assemblies of nanoparticles little further, the possibility of forming photoresponsive networks of gold nanoparticles connected by azobenzene moiety bearing linker molecules was unveiled. Azobenzene has been known to undergo isomerization from trans to cis form and vice-a-versa on irradiation with UV light and visible light respectively. Here, it was a constituent of the linker molecules connecting gold nanoparticles. So, its light induced isomerization resulted in the reversible modulation of interparticle distance between gold nanoparticles. This led to formation of photoresponsive networks. The nature of networks formed was also seen to be a function of capping ligand used.

As the application potential of any such assemblies is mainly governed by their thermal stability, the melting characteristics of 3-dimensional assemblies of dodecanethiol capped gold nanoparticles were probed. Interestingly, it was seen that the formation as well as the melting characteristics of these 3D assemblies are greatly

influenced by the presence of excess thiol. This finding could have important bearing in realizing the preparation of highly captivating meta-materials based on self-assembly of nanoparticles.

5.2 Scope for future work:

The individual nanoparticles of cobalt and nickel have been analyzed in this thesis. The extension of this work would be investigation of their assemblies to gain knowledge about their collective properties especially their magnetic interactions. The nanoparticles were seen to assemble spontaneously. The mechanism of formation of these assemblies can be probed via techniques like DLS and neutron scattering. Catalytic activity of the nickel and cobalt nanoparticle can also be studied for reactions like hydrogenation. The synthesis protocol developed here can be extended to other metal nanoparticle systems like silver.

The collective optoelectronic properties of organization of gold nanoparticles can be measured. The digestive ripening method involves breaking up of anisotropic nanoparticles into spherical nanoparticles upon ligand addition. This can be probed in-situ. The measurements of changes in the conductivity in the photoresponsive networks can be carried out. The assemblies can be prepared using different photoresponsive molecules like stilbene and comparative studies could also be done.

The magnetic and optical properties can be combined in bimetallic systems like core-shell nanoparticles. A bi-functional system with cobalt or nickel nanoparticles as core that is coated by a silver or gold shell can be designed, synthesized and probed for its applications. Some preliminary studies in this direction led to highly anisotropic nanostructures absorbing infra-red light of frequencies corresponding to the biologically permissible optical window. Such a system can be a potential candidate for biological applications like hyperthermia and targeted drug delivery.

Appendix I

First the number of thiol molecules on the nanoparticle surface is determined.

$$T = \frac{A}{F}$$

Where, T = No. of thiol molecules surrounding one gold nanoparticle,

A = Surface area of one gold nanoparticle

F = Footprint Area of single thiol molecule (taken to be 21.4 Å^2)

After that, the weight corresponding to such monolayer is calculated.

$$W_1 = \frac{(T \times MW)}{N}$$

Where, W_1 = Weight of thiol molecules,

MW = Molecular weight of thiol

N = Avogadro's No.

Then, the weight of gold nanoparticle is calculated

W_2 = (V x ρ) Where, W_2 = Weight of gold nanoparticle

V = volume of gold nanoparticle for a given diameter

ρ = density of gold nanoparticles

From the above two the thiol weight fraction can be obtained as:

$$\textbf{thiol weight fraction (\%)} = \frac{W_1}{(W_1 + W_2)} \times 100$$

After the evaluation of thiol fraction for nanoparticles, the values have been plotted (Fig. A1) as a function of diameter of nanoparticle. As here the size of nanoparticles is 7 nm, the corresponding thiol fraction is found to be 11%.
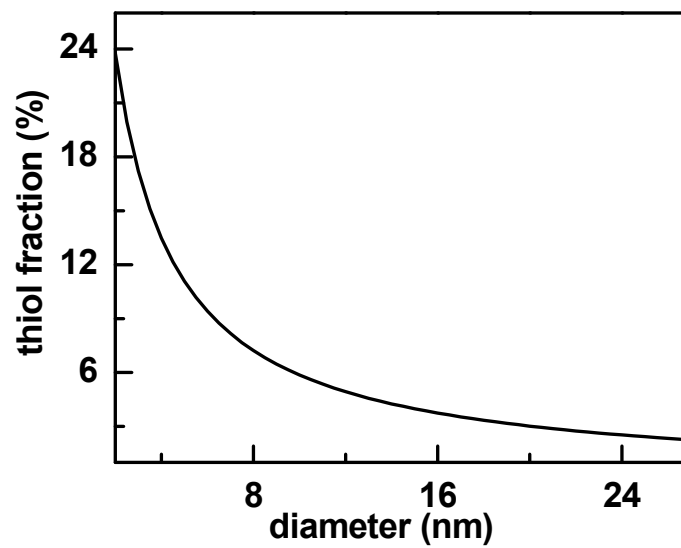
Fig. A1 *Graph plotted to determine the estimated thiol weight fraction (in percentage) when the gold nanoparticles are assumed to be coated with a monolayer of hexadecanethiol.*

Appendix II

Instrument details

➢ **Ultraviolet-visible (UV-vis) absorption spectrophotometry:**

UV- vis absorption measurements were carried out on a JASCO model V-570 dual-beam spectrophotometer operated at a resolution of 2 nm.

➢ **Fourier Transform Infra Red (FTIR) spectrophotometry:**

FTIR spectra were recorded on a Perkin Elmer Spectrum One FTIR spectrophotometer in diffuse reflectance mode, operating at a resolution of 4 cm^{-1}.

➢ **Transmission electron microscope (TEM):**

TEM measurements were performed on a JEOL Model 1200EX instrument operated at an accelerating voltage of 80 kV. TEM samples were prepared by placing drops of dispersed samples over carbon coated copper grids and allowing the solvent to evaporate.

➢ **High Resolution Transmission Electron Microscope (HRTEM):**

HRTEM imaging and electron diffraction analysis of the samples drop-casted on the carbon coated copper grids was done on TECHNAI G2 F30 S-TWIN instrument (Operated at an acceleration voltage of 300 kV with a lattice resolution of 0.14 nm and a point image resolution of 0.20 nm).

➢ **X-ray diffraction (XRD):**

The diffractograms were recorded on a PANalytical X'pert pro machine using a CuKα source and operating conditions of 40 mA and 30 kV at a scan rate of 4.66 theta/min. samples were prepared by drop-casting samples over glass slide and allowing the solvent to evaporate.

➢ **Thermo gravimetric analysis (TGA):**

TGA was carried out on (i) Mettler Toledo TGA Instrument (TGA/SDTA 851e) controlled by STARe software (Mettler Toledo GmbH, Switzerland); rate = 10º/ min. (ii) TA instrument SDT Q600 analyzer ; rate = 10º/ min. The samples were in powder form.

> ➤ **Magnetic measurements:**

The magnetic measurements were performed on sample powders using a commercial Physical Property Measurement System (PPMS) by Quantum Design. Variation of magnetization of samples with respect to external magnetic field and temperature [field cooled (FC) and zero field cooled (ZFC) mode] was studied.

> ➤ **Differential Scanning Caloriemetry (DSC):**

Melting characteristics of powdered samples were studied using Mettler -Toledo DSC 821^e (Mettler–Toledo, Switzerland) equipped with intracooler. Indium/Zinc standards were used to calibrate DSC temperature and enthalpy scale. The samples were weighed and hermetically sealed in aluminum pans and heated and cooled at a constant rate of 5 °C/min, over a temperature of (i) 25-200 °C (ii) 25-300 °C. Inert atmosphere was maintained by purging nitrogen gas (flow rate, 50 ml/min).

> ➤ **Small Angle X-ray Scattering (SAXS) measurements:**

The samples (in powder form) were characterized using Bruker Nanostar 2D SAXS Instrument with rotating anode generator, Cu Kα radiation and 2D Multitime HiStar$^®$ detector.

Appendix III

List of abbreviations

1D: one-dimensional

2D: two-dimensional

3D: three-dimensional

AOT: sodium bis-(2-ethylhexyl) sulfosuccinate

BDSAC: benzyldimethylstearylammonium chloride

CMC: Critical Micelle Concentration

CTAB: cetyltrimethylammonium bromide

CVD: Chemical Vapour Deposition

DDA: dodecylamine

DDAB: didodecyldimethylammonium bromide

DNA: Deoxyribonucleic acid

DSC: Differential Scanning Calorimetry

FC: field cooled

FCC/ fcc: Face Centered Cubic

FTIR: Fourier Transform Infra-Red

HCP/ hcp: Hexagonal Closed Packing

HDA: hexadecylamine

HRTEM: High Resolution Transmission Electron Microscope/microscopy

LASER: Light Amplification by Stimulated Emission of Radiation

LB: Langmuir-Blodgett

MEMS: MicroElectroMechanical Systems

NEMS: NanoElectroMechanical Systems

NIR: Near Infra-Red

ODA: octadecylamine

PVD: Physical Vapour Deposition

PVP: polyvinylpyrrolidone

Rpm: rotations per minute

RT: Room Temperature

SAED: Selected Area Electron Diffraction

SAM: Self Assembled Monolayer

SAXS: Small Angle X-ray Scattering

SDS: Sodium Dodecyl Sulfate

SERS: Surface Enhanced Raman Spectroscopy

SMAD: Solvated Metal Atom Deposition

SPR: Surface Plasmon Resonance

TBP: tributylphosphine

TEM: Transmission Electron Microscope/microscopy

TGA: Thermo Gravimetric Analysis

THF: tetrahydrofuran

TOP: trioctylphosphine

TOPO: trioctylphosphine oxide

UV: Ultra-violet

XRD: X-Ray Diffraction

ZFC: zero-field cooled

<u>Appendix IV</u>

<u>List of publications</u>

1) **Gold Nanoparticle Networks with Photo-Responsive Interparticle Spacings**

<u>Deepti S. Sidhaye</u>, S. Kashyap, M. Sastry, S. Hotha, B. L. V. Prasad

Langmuir **2005,** *21,* 7979-7984.

2) **Linear Assembly of Hexadecanethiol Coated Gold Nanoparticles**

<u>Deepti S. Sidhaye</u>, B.L.V. Prasad

Chem. Phys. Lett. **2008**, *454,* 345–349.

3) **Static and Dynamic Magnetic Properties of Co Nanoparticles**

S. Srinath, P. Poddar, <u>Deepti S. Sidhaye</u>, B. L. V. Prasad, J. Gass, H. Srikanth *J. Nanosci. Nanotechnol.* **2008**, *8,* 4086-4091.

4) **Preparation of Nearly Monodisperse Nickel Nanoparticles by a Facile Solution Based Methodology and Their Ordered Assemblies**

<u>Deepti S. Sidhaye</u>, T. Bala, S. Srinath, H. Srikanth, P. Poddar, M. Sastry, B. L. V. Prasad *J. Phys. Chem. C* **2009**, 113, 3426-3429.

5) **Melting Characteristics of Superlattices of Alkanethiol Capped Gold Nanoparticles: The "Excluded" Story of Excess Thiol**

<u>Deepti S. Sidhaye</u> and B. L. V. Prasad (Communicated)

Conference Proceedings:

1) **Synthesis of Anisotropic Core-shell nanostructures**

<u>Deepti S. Sidhaye,</u> B. L. V. Prasad, M. Sastry

Nano 2005 Proc. Int. Conf. Nanomat.*,* **2005**, 489-494.